Development of High Performance NTC Thermistors

A THESIS
SUBMITTED TO THE
GOA UNIVERSITY
FOR THE DEGREE OF

DOCTOR OF PHILOSOPHY

IN

ELECTRONICS

BY

RAJANISH K. KAMAT

ELECTRONICS PROGRAMME
DEPARTMENT OF PHYSICS
GOA UNIVERSITY
TALEIGAO PLATEAU
GOA - 403 206

AUGUST 2002

Certified that all corrections have been incorporated.
Guide

Certified that all corrections/suggestions indicated by the referees have been incorporated.

Dr S. Asokan
Indian Inst of Science
Bangalore 560012
17/2/03

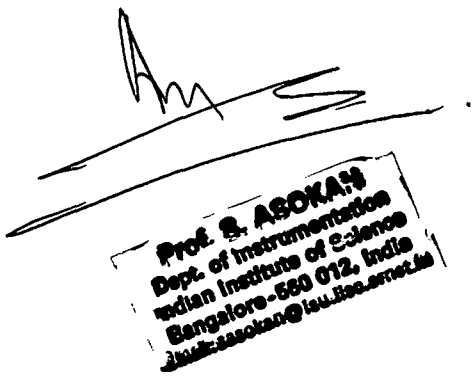

DEDICATED TO .....

My Parents

STATEMENT

I hereby state that this thesis for the Ph.D. degree on "Development of High Performance NTC Thermistors" is my original work and that it has not previously formed the basis for the award of any degree, diploma, associateship and fellowship or any other similar title to the best of my knowledge and information.

Rajanish K. Kamat
(Candidate)

CERTIFICATE

As required under the University ordinance, I certify that the thesis entitled "Development of High Performance NTC Thermistors" submitted by Mr. Rajanish K. Kamat for the award of Doctor of Philosophy in Electronics is a record of research done by the candidate during the period of study under my guidance and that it has not previously formed the basis for the award to the candidate of any degree, diploma, associateship, fellowship or other similar titles.

Date : 15th August 2002

Dr. Gourish M. Naik,
Research Guide
Electronics Programme,
Department of Physics,
Goa University.

ACKNOWLEDGMENTS

It gives me a great pleasure to express my deep sense of gratitude towards my research guide Dr. Gourish M. Naik, Head, Instrumentation Department, Goa University, whose able guidance and constant inspiration enabled me to complete my thesis. It is my great privilege that I have had an opportunity of working with him.

Thanks are due to Professor S.R. Sawant, Head, Department of Electronics, Shivaji University who has stimulated my interests in the field of sensors and was very gracious to provide laboratory facilities whenever required. I am fortunate to have published a good number of research papers on various aspects of materials which has really served as a platform for the present research work.

I am very grateful to Professor Jayant Budkuley, former Head, Department of Chemistry, for allowing me to use various facilities in the Chemistry Department and Dr. V. M. S. Verenkar for helping me in the materials preparation work and interpretation. I offer my special thanks to Professor K.R. Pai, Head, Electronics Department, PCC College, Verna for advising me from time to time as a FRC member during my research work. I am deeply indebted to Professor G.G. Tengshe, Head, R&D, D.Y.Patil Engineering College, Kolhapur and Mr. Rajendra Gad, Instrumentation Centre, Goa University for their untiring support.

I thank Professor P.R. Sarode, Head, Physics Department for his help and support throughout this work. My sincere thanks are due to my colleagues in the Department of Physics, Dr. J.A.E. Desa, Professor R.B. Prabhu, Dr. R.B. Tangsali, and others for their co-operation and constructive criticism.

I would like to place on record my thanks to the Sensors Fraternity of University of Pune for giving me an opportunity to discuss various technical aspects presented in this thesis.

I want to thank Dr. V.R. Indolkar of ACD Machine Control Tools, Mumabi, Dr. S. Lotake, Mr. Deorukhkar, Mr. Sachin Kalas and Mr. Anil Mohitae, Common facility Center, Shivaji University, Kolhapur for their help at various stages of experimentation. I also wish to appreciate the help received from Dr. Sandeep Garg, Goa University, Late Professor S.A. Patil, Shivaji University, as well as Mr. J.P. Kamat, Mr. Dayanand, Mr. Lopis and Mr. Ankush.

I will be failing in my duties, if I do not mention the support received from my M.Sc. Electronics students during the course of this work. I am also grateful to many of my friends and relatives for encouraging me throughout this work. Notable among them are Shri Shashikant Desai, Manager, Intel Waste Chemicals Project, CA, Shri Vimalanand Prabhu, University of North Carolina, Chapel Hill, my brother Durgaprasad Kamat, Kale Consulatancy, Captain R.W. Khanolkar and Shri Dada Walawalkar.

I appreciate my wife Rucha for her support and assistance during the course of my research work. Special thanks are due to my in-laws for encouragement and moral support.

CONTENTS

LIST OF FIGURES

Chapter 3

Chapter 4

Appendix I

2. TG/DTA Spectra are in the following order

List of Tables

Chapter 1

Chapter 2

CHAPTER 1

Introduction

1.1 Temperature Sensing in New Technology Regime:

Sensors control machines which support man more than ever before and free him from superfluous work. The operation of today's industrialised world depends to a great extent on the ability to measure and control a variety of physical parameters. Sensors are electronic devices that gather information from the environment and act as transducers, converting the energy form associated with the information that is sought into a form in which it can be easily processed. The energy forms typically involved, in sensing processes, include chemical, electrical, magnetic, mechanical, radiant, and thermal. There is a continuous need for the development of rugged and reliable sensors capable of making measurements in harsh industrial environments found in the steel, heat treating, metal casting, glass, ceramic, pulp and paper, automotive, aerospace, utility and power industries. The application of sensor and measurement technology has resulted in many benefits including improved energy efficiency, better quality, lower scrap or off-specification products, and reduced emissions [72]. The automotive industry is an excellent example, where increased use of electronics technology in sensor and measurement has led to improvements in engine performance, higher energy efficiency and reduced pollutant emissions [76]. Environmental concerns, health and safety regulations have necessitated an increased use of sensors, from industrial plant settings to automobiles, to the workplace, and even to homes [172]. Wherever sensor technology has been applied, it has proven

to be very beneficial in improving energy efficiency, service, product quality and reducing emissions.

Temperature was one of the first physical parameters to be measured in the process field and has been sensed in just about every way imaginable over the years. At one time or another, just about every physical property that changes with respect to temperature has been used as a basis for this measurement. It is estimated that, over 50% of all measurements of important variables in industrial and related fields are measurements of temperature [73]. Discussions on precision temperature sensing and electronic acquisition have been occurring since the beginning of modern industrialisation. The amount of study, experiments, and effort that have been applied to the measurement of temperature is perhaps far greater than, that devoted to any other field of industrial instrumentation. Over the years, an enormous amount of research and development efforts have been devoted to improve temperature sensor characteristics [20,69-76119,120,123]. This is coupled with the developments in improvement of the signal conditioning circuits to reliably transform the temperature sensor output signal into a useful, electrical form [9, 23, 32, 43, 47, 48, 52, 54, 59, 67, 95]. It would make sense that this market has matured to the point where further work would just belabour the subject, seemingly, all of the concepts surrounding these sensors and electronics are all too well understood. This is far from being true. The subject of temperature sensing is kept alive with innovations in sensor manufacturing and enhancements

to sensor interfaces[71]. Over the last few years, the development of low cost, micro controllers and associated electronics circuitry has allowed the cost effective measurement and control of temperature, that was not possible before [44,89,92,96,99105]., Today's microprocessors and microcontrollers are powerful and yet affordable, and they have really revitalised the thermal instrumentation world. This impact has resulted into the fast calibration methods which has almost eliminated the huge look up tables required for error correction. So in a nutshell, to say, "Enough is enough" as regards to the research and development work of temperature sensors and circuit design may be a little premature in light of the continuing improvements, and therefore, the changing scene prompts a re-visit to the basics of temperature sensing.

1.2 Basics of Thermal Sensing Technology: A Review

As a leading sensors of ambient conditions, temperature sensors act as important sensing devices which are essential in a large variety of products. Variety of temperature sensors are available in the market, to meet specific application needs. The most common of them include thermocouple, resistive temperature detector (RTD), thermistor and silicon based sensors. The classification of temperature sensors is shown in figure 1.1. The comparison of all these sensors reveal some interesting facts. Thermocouples are the most ancient, popular, rugged, temperature sensors available in a wide temperature range. However their output is too small typically in micro-volts per change in degree centigrade and therefore

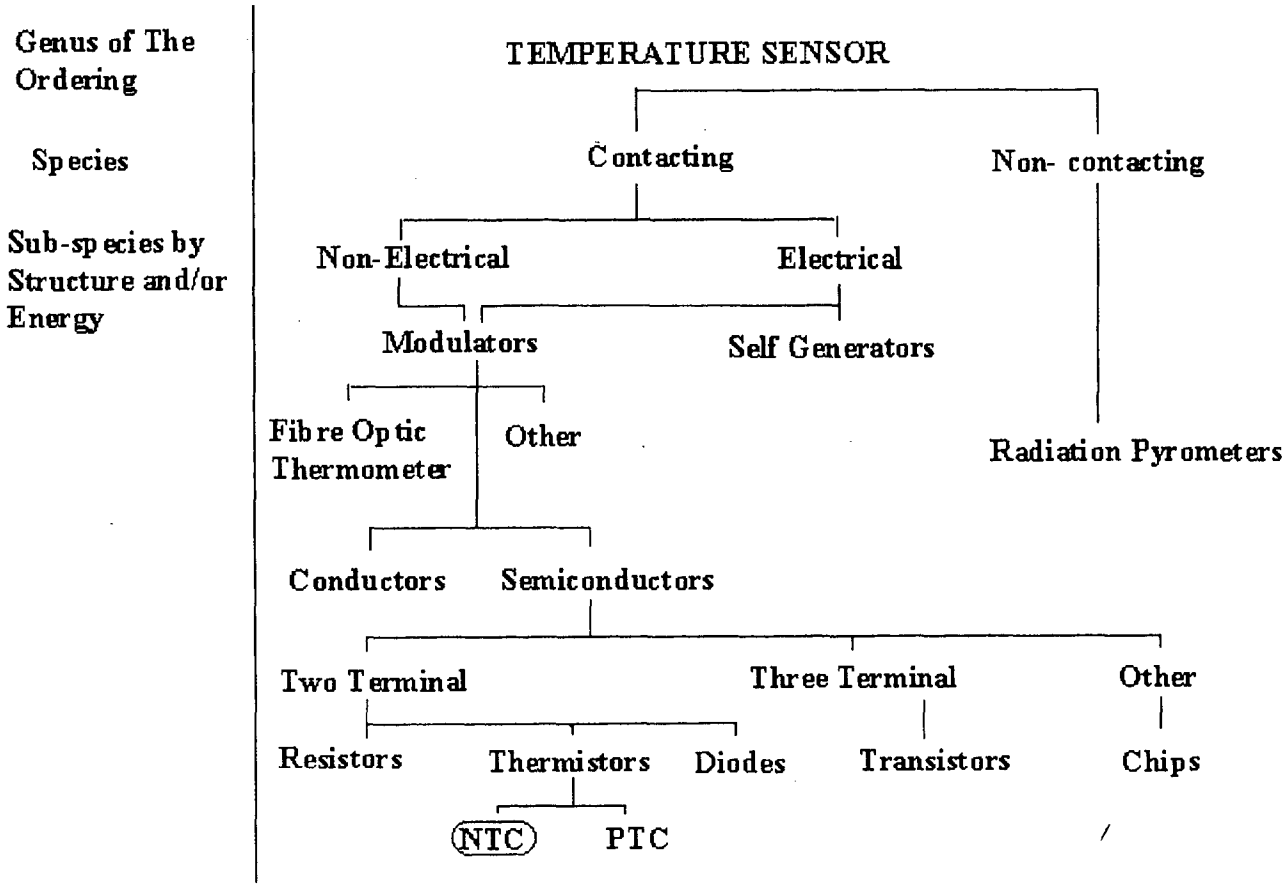

Figure 1.1: Holistic Taxonomy of Temperature Sensors by McGhee et. Al. [77]

to get adequate resolution a low noise, high gain amplification (mostly chopper based) is a must. Further for absolute temperature measurement an additional reference cold junction compensation is required. It is worth notable that for high precision linearised temperature measurement, with a K type thermocouple, a full measurement range required an 11 x 14 sized linearisation matrix [173]. Therefore, wherever accuracy is the main concern, there is nothing like using RTD as a temperature sensor. Materials for RTDs can be gold, silver, copper or platinum. Platinum, however, has become the most-used metal for RTDs. A thin film of platinum or a thin platinum wire is deposited on a flat ceramic material and sealed. Platinum has a nearly linear temperature versus resistance relationship. The Callendar-Van Dusen equation approximates the RTD curve:

$$R_T = R_0 + R_0\alpha\,[\,T - \delta(T/100-1)(T/100) - \beta\,(T/100-1)\,(T^3/100)] \quad \text{------[1.1]}$$

In the above equation R_T is the resistance of RTD at temperature T, R_0 resistance at 0°C, α the temperature coefficient at T=0°C, δ is a constant =1.49 for Platinum and β is also a constant equal to zero when the temperature is above 0°C. RTD provides high accuracy [173] between boiling point of oxygen (-82.96°C) and the boiling point of antimony (630.74°C), with a useful measurement range from -240°C to 750 °C. A typical comparison of accuracy of RTD with other sensors is as follows: thermocouple 0.5°C to 5°C; RTD 0.01°C to 0.1°C and thermistor 0.1°C to 1°C. However current excitation is the main requirement and a trade of

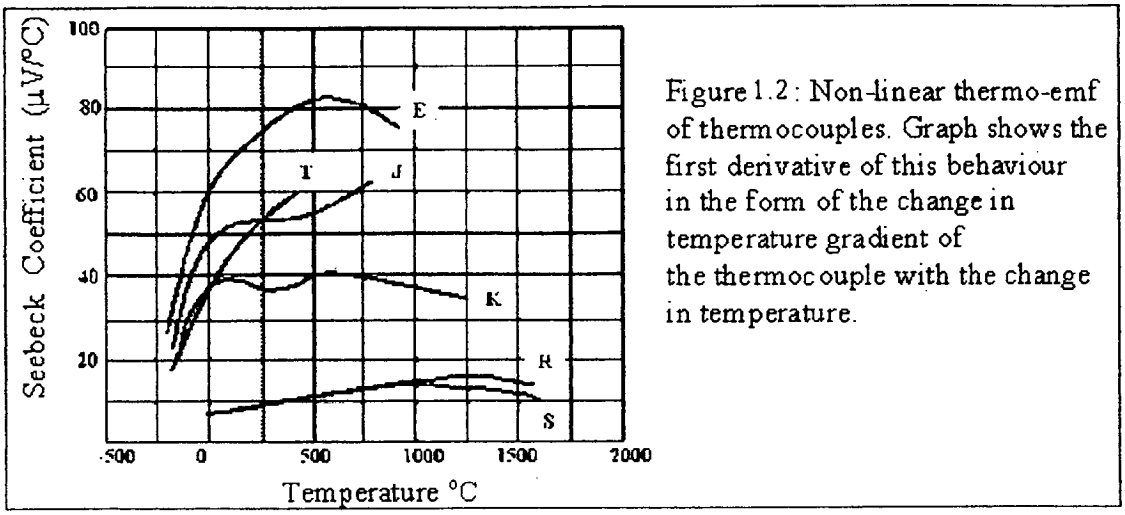

Figure 1.2 : Non-linear thermo-emf of thermocouples. Graph shows the first derivative of this behaviour in the form of the change in temperature gradient of the thermocouple with the change in temperature.

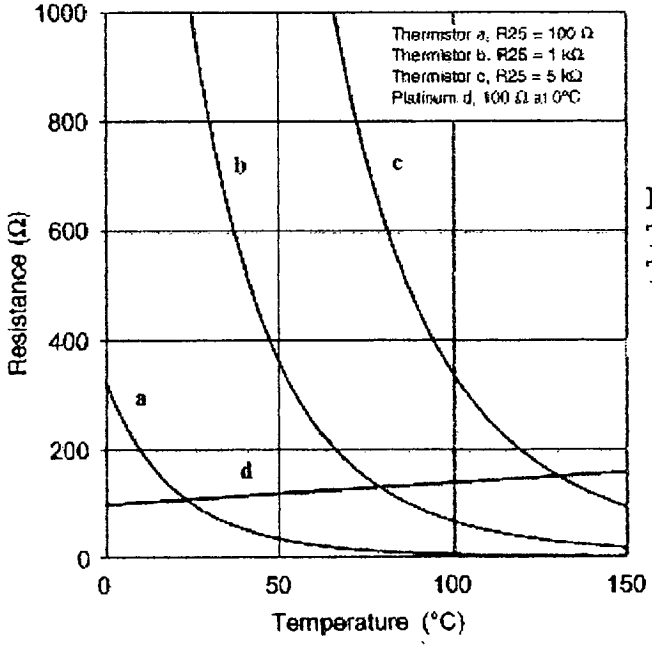

Figure 1.2: Comparative Resistance-Temperature Characteristics of Thermistor Vs RTD

exists while deciding the value of current. With higher current levels the RTD goes into the self heating region causing measurement error, while with lower current levels yield a low output susceptible to noise. Further three / four wire connection schemes has to be implemented to avoid the measurement errors due to leads. Although IC sensors have more advantages in terms of high level linear output which almost does not require further conditioning, their range is restricted. So out of all the above mentioned temperature sensors, the discussion of thermistor looking at their wide use for temperature monitoring, control and compensation, in almost every conceivable fields like home appliances, manufacturing industries, biomedical, transportation and security. NTC thermistors offer designers, many advantages over other type of sensing technologies including the highest sensitivity to temperature changes, high signal to noise ratio, simple operation as well as low cost. Just to give an idea, have a look at these comparative figures of sensitivity viz. Thermocouple: 6 $\mu V/^{o}C$, RTD: 0.4 $\Omega/^{o}C$ and thermistor: 400 $W/^{o}C$. Unlike RTD, lead compensation is not at all required in thermistors making them the most suitable choice for remote sensing applications. The latest comparative figures of cost, in US$, for all these sensors are, thermocouple: $1/foot, RTD $20 to $100/piece and thermistor: $10 to $100/piece (depending on configuration and other specifications). Though the thermocouple appears to be cheaper, considering the signal conditioning required, the most cost effective sensor is thermistor.

However despite of all these positive points that makes thermistor a widely used sensor, there are few misapprehensions like non-linearity, ageing, stability, cracking, batch-to-batch tolerance, time consuming manufacturing process etc. Formerly, the non-linear resistance versus temperature characteristic was problematic in analog sensing circuits. Today, however, with the advent of digital electronic controls, the translation is handled via equations in software or lookup tables. This thesis presents research work to minimise most of the drawbacks mentioned above and to improve the technical specifications of thermistors.

Table 1.1 : Comparison of Widely Used Temperature Sensing Technologies:

SENSOR TYPE	NTC THERM-ISTOR	RTD	THERMO-COUPLE	I.C. SENSOR
PARAMETER	Resistance vs. Temperature	Resistance vs. Temperature	Voltage vs. Temperature	Voltage or Current vs. Temperature
Advantages	Large Change in Resistance vs. Temperature, Fast Time Response, High Resistance Eliminates the Need for Four Wire Measurement, Small Size, Inexpensive, High Stability.	Linear, High Stability, Wide Operating Temperature Range, Inter-changeable Over Wide Temperature Range.	Wide Operating Temperature Range, Simple, Inexpensive, Rugged, No External Power Supply Required.	Linear, High Output vs. Temperature, Inexpensive
Drawbacks	Non-Linear, Operating Temperature Limited to Approximately -60 to +300 Degrees Celsius, Inter - changeable Over Relatively Narrow Temperature Ranges, Current Source Required.	Small Change in Resistance vs. Temperature, Relatively Slow Time Response, Low Resistance Requires Three or Four Wire Measurement, Sensitive to Shock and Vibration, Current Source Required, Expensive.	Non-Linear, Relatively Low Stability, Low Sensitivity, Low Voltage Output Can Be Affected By RFI and EMI, Reference Junction Compensation Required.	Limited Operating Temperature Range , Current Source Required, Subject to Self-Heating, Limited Configuration.

1.3 Historical Note on the Thermistors:

Michael Faraday (1791-1867), the British chemist and physicist, is best known for his work in electromagnetic induction and electrochemistry. Less familiar is his 1833 report on the semiconducting behaviour of Ag_2S (silver sulfide), which can be considered as the first recorded NTC thermistor [197]. Because the early thermistors were difficult to produce and applications for the technology were limited, commercial manufacture and use of thermistors did not begin until 100 years later. Around 1930 thermistors based on CuO were developed as an immediate need of World War II. After another two years they were developed as commercial product based on Urodox (UO_2) by Osram in Germany. Philips also started making thermistors initially in the year 1936 based on silicon/ferrosilicon sintered together with inorganic binder with a trade name 'startotube' and later based on Iron Oxide with different valences. During the early 1940s, Bell Telephone Laboratories developed techniques to improve the consistency and repeatability of the manufacturing process. Some of the first commercial thermistors were the disc type, and by today's standards, their tolerances were quite broad. These devices were used primarily for regulation, protection, and temperature compensation of electronic circuits. In the 1950s and 1960s, the expanding aerospace industry's requirement for more accurate and stable devices led to several improvements in the materials used to manufacture glass bead and disc thermistors [199]. During the 1960s and 1970s, the demand for tight-tolerance devices in high

volumes at a lower cost led to the development of the chip thermistor [199]. As the reliability of these devices improved during the 1980s, the use of electronic thermometers in the health care industry increased. The rising costs of sterilisation and concerns about cross-infection among patients led to the demand for low-cost disposable temperature probes, for which chip thermistors were well suited. Throughout the 1980s and 1990s, the use of NTC thermistors has continued to grow in the automotive, food processing, medical, HVAC, and telecommunications markets [70].

1.4 NTC Thermistor Theory:

Although the word thermistor is derived from THERMally sensitive resISTOR, the NTC thermistor can be more accurately classified as a ceramic semiconductor. They are the temperature sensitive passive semiconductors exhibiting a large change in electrical resistance when subjected to a relatively minute change in body temperature. Negative Temperature Coefficient (NTC) thermistors decrease in resistance when subjected to an increase in body temperature. They are usually made of a semiconducting transition metal oxide. By controlling the chemical composition and the geometrical parameters of the NTC-thermistors, it is possible to construct devices having electrical resistance in the range of about 1 Ω to 1 MΩ at room temperature. Their extreme sensitivity to minute temperature changes enables them to perform many unique functions heretofore impossible with standard electronic components [75]. The

theoretical aspects of NTC thermistors are discussed in depth in the literature [1,12,14,20,22,26,52,53121].

1.4.1 Thermistor Materials, From Stones to Ceramic Sensors:

Typical commercial NTC thermistors are realised using ceramic technology. These functional ceramics are stone-like materials that are made by adding various chemical raw materials, separated and purified at atomic level, to a ceramic base which is hardened by firing. By adding trace quantities of doping materials and changing firing conditions or atmospheric conditions, these "wonder stones" [135] can vary with a wide variety of electrical characteristics. Long standing involvement with these "wonder stones", or functional ceramics, has borne fruit in the form of a rich variety of innovative electronic components like soft ferrites, varistors, PZT and thermistors. These High-technology ceramics are now playing an important role in the future of electronics, processing and manufacturing systems automation, and in the automotive, utility, and fabrication industries The ceramics technology is growing increasingly important as a key driving force in the creation of a new electronics revolution for the 21st century.

The popular NTC thermistor materials, for the temperature range from room temperature to 300°C specially useful for domestic and industrial fields consists of ceramics composed of oxides of transition metals (manganese, cobalt, copper and nickel) which can form a new crystal phase known as spinel. Although oxides of rare earth elements (e.g., Sm and Tb) have been considered for use at higher temperatures, reliable

thermistors for applications near and above 1000° C are yet to be developed. Materials like ZrO_2, Y_2O_3 and ThO_2 are also been used for making high temperature thermistors for the temperature range 300°C to 1000°C [124].

1.4.2 Raw Material Selection and Synthesis of Powder:

NTC thermistor makers have a very broad choice of chemical precursors (raw material sources). The unit processes are defined and checked for compatibility with the raw materials selection. The precursor choice is firmly established after an initial development trial and extensive processing of ground rules. The major concern during this process are consistency upon processing, cost, precursor chemistry, impurity levels, reactivity, synthesis approach, physical parameters, size, packing efficiency and mixing ease or mix homogeneity. Traditionally two synthesis approaches have been used for synthesising thermistors viz. Reactive sintering of oxide mixture compacts and sintering of synthesised powder compacts. In the former approach the oxide raw materials are usually selected for chemical purity, particle size and batch to batch consistency which are then weighed, intimately mixed, compacted into desired shape and subjected to time-temperature-atmosphere sintering cycle to form the thermistors. In the later approach, intimate powder mixtures of NTC formulations in fluid suspension are consolidated, dried, granulated and calcined typically for two to eight hours at temperature below the normal sintering conditions. This pre-sintering partially reacts the precursor mixture

to form oxide agglomerate that approximates the final NTC chemistry and crystal structure. The first method gives better chemical uniformity and good mechanical properties for the finished product. The later method allows broad range of chemical precursor as inputs and the calcination results in significant shrinkage of the precursor mix and chemical homogenisation yielding a high quality, close tolerance NTC sensors. In the present work, we have used carboxylate and oxalic methods to obtain the raw precursor and after extensive trials finalised the manufacturing schedule.

1.4.3 Thermistor Configurations:

Thermistors are available in number of configurations that includes beads, disks, wafers, SMTs, flakes, rods, and washers [197]. Non-bead thermistors are also known as surface electrode thermistors and their manufacturing process has many similarities to the construction of ceramic capacitors. First, powdered metal oxides are combined with a plastic binder and additives that enhance stability. The mixture is then formed into sheets that are cut to component size or formed into pellets and pressed into disks. The bodies are then sintered at temperatures in excess of 1,000°C that forms the final polycrystalline NTC thermistor body. The sides are then silvered, leads attached, sealed, varnished, marked and marketed.

Manufacturing of bead thermistor starts with platinum or copper alloy wires and slurry of the metal oxide with suitable binder. Drops of the slurry are dabbed onto the wires. The surface tension pulls the drops into small

Table 1.2 : Comparison of various thermistor designs:

Thermistor Configuration	Prime Forming Method	Typical Specifications	Pros and Cons
Bead	Slurry cast on wires	Dimensions: 0.01 in. to 0.06 in. (0.25 mm to 1.5 mm) in dia., Dissipation Constant 0.05-0.30 mW/K, time constant 0.2-3.0 Sec.	excellent long-term stability and reliability for operation at temperatures up to 300°C, quick response to temperature changes, small size devices hard to handle during assembly and have the effect of limiting their power dissipation, more difficult and more expensive to produce glass beads with close tolerances and interchangeability
Disk	Uniaxial Compaction	Dimensions: uncoated (0.05 in. to 0.10 in. (1.3 mm to 2.5 mm) in dia., coated disc 0.10 in. to 0.15 in. (2.5 mm to 3.8 mm) in dia. Dissipation Constant ≈15 mW/K, Time Constant ≈ 100 Sec.	Chip and Disk: tight tolerances and interchangeability at a relatively low cost compared to bead thermistors, size permits power dissipation higher than that of beads, disc thermistors normally have larger coated diameters and higher power dissipation capabilities than chip thermistors, chip thermistors typically can be produced to smaller coated diameters and are better suited for applications requiring smaller size and faster response times
Chip	Slurry Tape Casting	Dimensions: 0.04 in. by 0.04 in. (1 mm by 1 mm) to 0.10 in. by 0.10 in. (2.5 mm by 2.5 mm) in square or rectangular shapes,	
Rod	Dough Extrusion	Dimensions: Dia.:0.5-1.5 cm, Length: 0.5-4.0 cm., A/L: 0.2-0.3 cm.	Uniform Temperature Profile, Good Accuracy

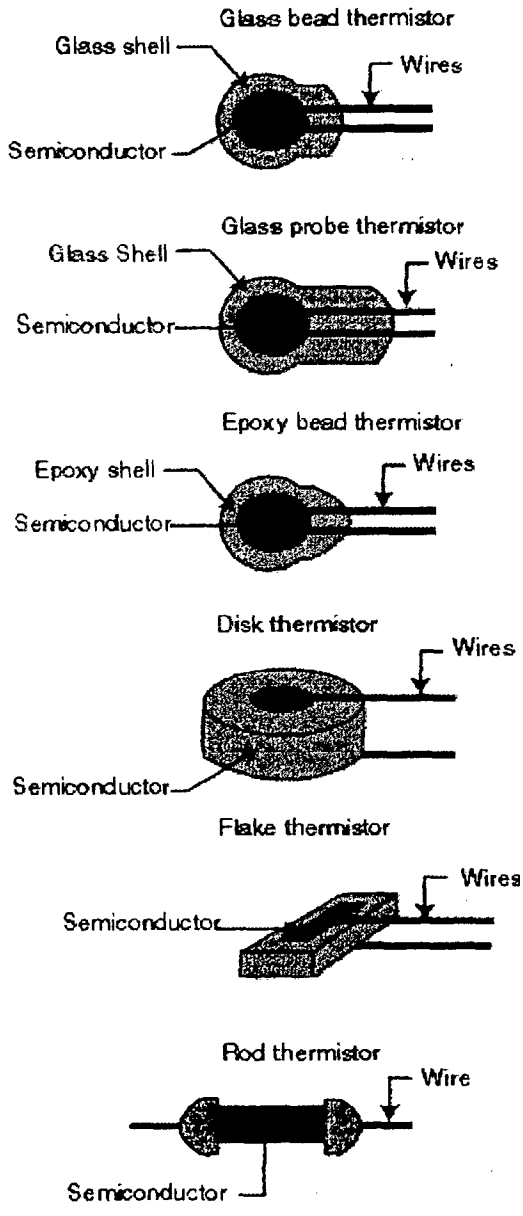

Figure 1.4 : various thermistor Designs

elliptical beads. The string of beads is then allowed to dry and then sintered at high temperature. During sintering the beads shrink and form an excellent electrical connection with the wires. Later, the wires are cut to form the individual thermistors. Finally, the thermistors are coated and most often hermetically sealed with glass.

Rod extrusion employs a dough of different binder and higher oxide content than that of the slurries of bead thermistor. The stiff dough is dried and placed in an auger or plunger press. Long rods of thermistor dough are extruded through a die orifice and supported on grooved board. After slow evaporation of the solvent, rods of desired size are cut from the extrusion and processed for sintering.

Disc and washer thermistors are made by preparing the various metal oxide powders, blending them with a suitable binder, and then compressing small amounts of the mixture in a die under several tons of pressure. The discs are then fired at high temperatures to form solid ceramic bodies. A thick film electrode material, typically silver, is applied to the opposite sides of the disc to provide the contacts for the attachment of lead wires. A coating of epoxy, phenolic, or glass is applied to each device to provide protection from mechanical and environmental stresses.

Chip thermistors are manufactured by tape casting, a more recent technique borrowed from the ceramic chip capacitor and ceramic substrate industries. An oxide-binder slurry similar to that used in making bead thermistors is poured into a fixture, which allows a very tightly controlled

thickness of material, to be cast onto a belt (or movable) carrier. The cast material is allowed to dry into a flexible ceramic tape, which is cut into smaller sections and sintered at high temperatures into wafers 0.01 in. to 0.03 in. (0.25 mm to 0.80 mm) thick. After a thick film electrode material is applied, the wafers are diced into chips. The chips can be used as surface mount devices or made into discrete units by attaching leads and applying a protective coating of epoxy, phenolic, or glass. Various thermistor designs are shown in figure 1.4.

1.4.4 Thermistor Nomenclature:

a. Zero Power Condition : When current flows through the NTC thermistor it heats itself and this changes the resistance. When self-heating is negligible, it is called the zero-power condition. It is essential to know how small does the power dissipation have to be, in order to be considered as "zero-power"? Paraphrasing the MIL specification on this issue: "the power is negligible when a further decrease in power will not result in a resistance change more than 0.1%".

b. Zero Power Resistance (R_T) : The zero power resistance is the dc resistance of a thermistor at a specified temperature with power dissipated by the thermistor low enough that any further decrease in power will result in no more than 0.1% (or one tenth of the specified measurement tolerance, whichever is smaller) change in resistance.

c. Resistance Ratio Characteristics : The resistance ratio is the ratio of the zero-power resistance of thermistor measured at two specified

reference temperatures. The most popular forms of specifying resistance ratio are either (R_0/R_{50}) or (R_{25}/R_{85}) or (R_{25}/R_{125}).

d. Zero Power Temperature Coefficient of Resistance (α) : The ratio at a specified temperature(T), of the rate of change of zero power resistance with temperature to the zero power resistance of the thermistor. For Negative Temperature Coefficient (NTC) Thermistors, typical values of alpha are in the range -3%/°C to -6%/°C. The temperature coefficient is a basic concept in thermistor calculations. Because the resistance of NTC thermistors is a non-linear function of temperature, the alpha value of a particular thermistor material is also non-linear across the relevant temperature range.

$$\alpha = (1/R_T) \times (dR/dT) \times 100\% \quad (\%/^{o}C) \text{ ---------- (1.2)}$$

Where RT is the resistance of the component at the relevant temperature T (°C), dR/dt is the gradient of the Resistance Vs Temperature curve at that temperature point, and α is expressed in units of "percentage change per degree Centigrade".

e. Maximum Operating Temperature: It is the maximum body temperature at which the thermistor will operate for an extended period of time with acceptable stability of its characteristics. This temperature can be the result of internal or external heating, or both, and should not exceed the maximum safe value specified.

f. Maximum Power Rating : It is the maximum power, which a thermistor will dissipate for an extended period of time with acceptable stability in its characteristics.

g. Dissipation Constant : It is the ratio, (expressed in milli-watts per degree C) at a specified ambient temperature, of a change in power dissipation in a thermistor due to the resultant body temperature change.

h. Thermal Time Constant : It is the time required for the thermistor to change 63.2% of the total difference between its initial and final body temperature when subjected to a step function change in temperature under zero-power conditions.

i. Resistance-Temperature Characteristics : The resistance temperature characteristics is the relationship between the zero-power resistance of a thermistor and its body temperature. The Steinhart and Hart equation is an empirical expression which best models the thermistor characteristics.

j. Temperature - Wattage Characteristics : It is the relationship at a specified ambient temperature between a thermistor temperature and the applied steady-state wattage.

k. Current-Time characteristics: It is the relationship at a specified ambient temperature between the current through a thermistor and time, upon application (or interruption) of applied voltage.

l. Stability : The stability of a thermistor is its ability to retain specified characteristics after being subjected to designated environmental or electrical test conditions.

m. Materials Constant (β) : The materials constant of a thermistor β, is derived form thermistor resistance measurements obtained at 0°C and 50°C.

n. Maximum Steady State Current (I_{max}): For power thermistors, the maximum continuous steady state current, either DC or RMS AC, which the device is capable of passing.

1.4.5 Thermistor in the Context of Modern Instrumentation :

In the present era of inexpensive, compact microcontrollers, display modules and versatile electronic instrumentation, the scope of potential applications has grown enormously [28,32,90,114]. Inexpensive NTC thermistor elements are being utilised extensively as sensors, probes and components in complex circuits in a variety of applications. NTC Thermistor devices are extremely versatile components in electronic circuits. They offer distinct advantages in terms of matching impedance levels to available instrumentation or compensation circuit needs. The thermistor material composition, for example, can be adjusted and customised to achieve a desired resistivity-temperature response, within certain constraints, for a sensing device.

Precision NTC thermistors offer designers the greatest sensitivity to temperature of any electronic temperature sensing component. They

exhibit a negative temperature coefficient of resistance in the region of -3%/°C to -5%/°C at 25°C. This is roughly an order of magnitude higher than the sensitivity of positive temperature coefficient (PTC) metal resistors or thermocouple sensor elements. This provides some distinct advantages in system designs where sensitivity, circuit simplicity and overall system cost are important.

Drawbacks of NTC Thermistor devices include a non-linear resistance versus temperature characteristic and the fact that small bead and chip element devices have limited power handling capability. These disadvantages, however, are often overcome with innovative circuit designs. Presently, NTC thermistors are the preferred sensing element for many applications where precise measurement and control are required. Inexpensive microprocessor and display components are now being coupled with NTC thermistors and hybrid circuits. Such designs dominate industrial applications and can offer high performance temperature measurement and control capabilities for very reasonable overall system cost.

1.5 NTC Thermistor Manufacturing, A Global Scenario :

The temperature sensor market, in general, is mature but fragmented, typically characterised by moderate growth and narrow margins [134]. Individual thermistor manufacturers target their strengths at particular market segments. Numerous temperature sensor suppliers provide thermistor and RTD (resistance temperature detector) components,

as well as offer a complete temperature probe assemblies to OEMs who produce monitoring and control products that use temperature as a critical system parameter. The latest trend of thermistor manufacturing has been discussed at a good number of websites [129-174, 197]

1.5.1 State of the Art :

NTC thermistor is a such an vital sensor that its production in Asia has not been affected by the world wide economic recession. A market research report by Trade Media Holdings Ltd. UK[158] predicts that both local and overseas demand for thermistors is expected to remain steady, with a little hope to increase from last year's figure. Even this is evident from the annual report of Shibaura Electronics Co. Ltd., a manufacturer of NTC glass sealed thermistors and glass sealed thermistor sensors, head quartered at Saitama-City, Japan, a leading company not only in Japan but also in the world, in this field. Shibaura ranks one in the global thermistor market and supplies over 200 Million thermistors a year[201]. In fiscal 2000, Shibaura has posted ordinary profit 660 Million Japanese Yen on a turnover of 10,700 Million Japanese Yen. As on May 31, 2001, Shibaura had employed more than 1700 people world-wide including their affiliated companies in China, Hong Kong, and Thailand. Recently the company has signed an agreement with EPCOS, a equally strong company (In fiscal 2000, EPCOS posted net profit of Euro 240 million on sales of Euro 1.86 billion. As of September 30, 2000, the company employed more than 13 000 people world-wide), for manufacturing electronic components, for

technological co-operation in NTC glass-sealed thermistors. Using each other's sales networks, Shibaura and EPCOS plan to strengthen their market positions in Europe and Japan respectively and promote establishment of NTC glass-sealed thermistors as a world-wide standard.

As per the predictions of the Japan Electronic Materials Manufacturers Association, the production of thermistors is expected to rise to some six percent in monetary value to $388 million and 17 percent in number of units to 2.5 billion pieces in the fiscal year 2001 (April 2001 to March 2002). Japanese companies are leading in the forefront of new product releases mostly focusing on surface-mount, compact thermistors for popular applications such as mobile phones. Manufacturers also reported the prices on a downtrend in the past few years. A 10- to 20-percent drop was estimated last year. Further cuts of up to 10 percent are likely until year-end 2002. Recent reports also indicate a slight glut in thermistor supply, industry analysts however hope that the situation is likely to be a temporary one, as demand is expected to rebound in no time.

1.5.2 Growth Economics :

In order to appreciate the present market figures let us compare them with the past. In 1992, Ceramic Industry Magazine[202] reported a market of $9000 million for electronic components. At that time it was predicted the scenario to be continued for ten to fifteen more years which now seems to come true. The Indian market[68] at that time was nearly 75 million dollars which was nearly 7% of the South Korea market and 1% of

the world market. For the development period of 1986-1992, approximate cost of finished thermistors was 100 Rs/Kg for the high end products. The successful commercialisation reported in 1995, is mostly for PTC thermistors. The notable among them is the PTC thermistor developed by Bharat Electronics, Bangalore for the colour picture tube degaussing. They have been successful in developing know-how for doping ppm levels of dopants in the ceramics homogeneously, while maintaining the purity, reproducibly and cost effectiveness by using inexpensive sintering technology. The other two notable thermistor manufacturers in this period were Translektra Domestic Products, Mumbai (PTC thermistors for mosquito repellent heater), Thakarsons, Pune (NTC thermistors).

1.5.3 Revival of Thermistors and the Latest Releases :

Mobile phones are reportedly one of the biggest and most important applications of thermistors, because the market for them has grown huge over the past few years [168]. Several thermistors are usually employed in one mobile phone unit. Thus, brisk mobile phone sales have greatly contributed to the upward movement of thermistor demand. In terms of product trends, makers have been coming forth with compact models. A few years ago, 1005 NTC thermistors for TCXOs, for instance, represented a greater percentage of the total production. Smaller models have been catching on lately, and this trend is expected to continue in the near future as well. Along this line, surface-mount models have also been growing popular. In addition, some makers have begun releasing lead-free

thermistors from the standpoint of environmental protection. It has also been reported that despite the reported lack of advanced technology in most countries, new manufacturers are constantly entering the line and optimistic of grabbing a share of the market. It is also observed that the new thermistor releases are mostly targeting telecommunication applications. Besides, booming demand for DVD players and other portable communication appliances have also pushed up the popularity of NTC thermistors. From the conventional device types like rod, bead, disk, new kind of forms like SMD, lead-less are also seen to be evolving. Both DIP and surface mount types are being heavily manufactured, although the former are more popular due to their high flexibility in applications while later forms the ideal solution where temperature sensing within a constraint area is needed. Due to growing share of high precision products there is a demand for small resistance tolerance units. Chip thermistors can be made with tight tolerances of the order of $\pm$ 0.05°C, eliminating the costly calibration process required by other temperature sensors like RTD, thermocouple etc. Number of developments are also taking place for linearising the thermistor characteristics by developing look up tables and time efficient software routines.

In general thermistor manufacturers are seem to be busy in extensive activities to develop customised sensors, to diminish product sizes, improve precision, accelerate response speed, expand the range of temperatures they cover and to establish standards to simplify mounting.

Efforts are being directed to increase of productivity by improved production technology. The main objective of present research and development is to explore further reductions in price and improvement in specifications along with the formation of thermistor based smart sensor.

1.6 Thermistor Applications :

Inexpensive NTC thermistor elements are being utilised extensively as sensors, probes and components in complex circuits in a variety of applications [70,74]. NTC Thermistor devices are extremely versatile components in electronic circuits . They offer distinct advantages in terms of matching impedance levels to available instrumentation or compensation circuit needs [54]. The thermistor material composition, for example, can be adjusted and customised to achieve a desired resistivity-temperature response, within certain constraints, for a sensing device. Precision NTC thermistors offer designers the greatest sensitivity [75] when compared to any electronic temperature sensing component. They exhibit a negative temperature coefficient of resistance in the region of -3%/°C to -5%/°C at 25°C. This is roughly an order of magnitude higher than the sensitivity of positive temperature coefficient (PTC) metal resistors or thermocouple sensor elements. This provides some distinct advantages in system designs where sensitivity, circuit simplicity and overall system cost are important.

Drawbacks of NTC Thermistor [71] devices include a non-linear resistivity and the fact that small bead and chip element devices have

limited power handling capability. These disadvantages, however, are often overcome with innovative circuit designs. Presently, NTC thermistors are the preferred sensing elements for many applications, where precise measurement and control are required. Inexpensive microprocessor and display components are now being coupled with NTC thermistors and hybrid circuits. Such designs dominate industrial applications and can offer high performance temperature measurement and control capabilities for very reasonable overall system cost.

Thermistor applications make use of the basic thermistor features, such as Resistance versus Temperature characteristics, zero-power characteristics, self heating effects and thermal characteristics like heat capacity and dissipation constant [44,45,49,50,51,56-59,66]. A knowledge of these factors is important in understanding the principles of thermistor applications.

1.6.1 Domestic Applications :

It has been reported that at present 90% of all temperature sensors employed in house hold electrical products are thermistors [76]. One can locate them in microwave ovens, electrical cookers, refrigerators, petroleum fan heater, liquid warmers, potato chip fryer etc. One of the main reasons for such a wide usage of thermistors is their small power dissipation and low cost. They need not be too accurate but should have low price, reliability, less ageing, stability, long service life etc.

1.6.2 Applications in Consumer Electronics :

Thermistors have been used in plain paper copiers (PPC) to control the surface temperature of the image fixing rollers [73]. In this application the sensor requirements are accuracy and rapid response. Accuracy decides the quality of the copied picture and response decides the time per copy. Another application of thermistors is in maintaining the vertical linearity of the picture which changes with temperature. This is achieved either by inserting thermistor in the tube plate circuit or by embedding it into one of the coils in series to compensate the increase in resistance of the coil. Another very popular application is controlling the temperature during rapid recharging of the Ni-Cd or Ni-H_2 batteries. This greatly enhances the service life of the battery. High temperature thermistor compositions based on ZrO_2, ThO_2 and CeO_2 doped with trivalent rare earth oxides have a good potential in automobile electronics. They can be used for maintaining the optimal temperature range of catalytic exhaust converter to reduce the unburned fuel and minimise air pollution. They are also found useful for detecting various important parameters for engine performance control.

1.6.3 Thermistor for Metrology :

Since 1957, thermistor rods were used in radio sondes of the United State Weather Services for temperature measurement as well as gradient of air pressure and velocity to make weather maps. It was found that the

sluggishness and self heating of the sensors poses a bottleneck which was corrected by replacing the rod with the aluminised dot thermistor[70].

1.6.4 Other Applications :

It is not practically feasible to describe in depth each and every application of NTC thermistors in this thesis. A good amount of research papers and technical articles [3,5,9,11,28,32,37,42,43,44,45] discuss various applications of NTC thermistors. The objective of the present work is development of NTC thermistor for the temperature range from room temperature to 150°C, as this is the range required in most of the applications. Varieties of applications of thermistor are listed at 1.6.5

1.6.5 Thermistor Applications:

[I] Consumer Electronics:
Air Conditioners
Audio Amplifiers
Cellular Telephones
Cloths Dryers
Computer Power Supplies
Dish Washers
Electric Blanket Controllers
Electric Water Heaters
Electronic Thermometers
Fire Detectors
Home Weather Stations
Oven Temperature Control
Pool and Spa Control
Rechargeable Battery Packs
Refrigerator and Freezer
Temperature Control
Small Appliance Control
Solar Collector Controls
Thermostats
Toasters
Washing Machines
Audio Amplifiers

[II] Automotive
Automatic Climate Control
Coolant Sensors
Electric Coolant fan
Temperature control
Emission Controls
Engine Block Temperature Sensors
Engine Oils Temperature Sensors
Oil Level Sensors
Outside Air Temperature Sensors
Transmission Oil Temperature Sensors
Water Level Sensors

[III] Medical Electronics
Blood Analysis Equipment
Blood Dialysis Equipment
Blood Oxygenate Equipment
Clinical Fever Thermometers
Oesophageal Tubes
Infant Incubators
Internal Body Temperature Monitors
Internal Temperature Sensors
Intravenous Injection Temperature Regulators
Myocardial Probes
Respiration rate Measurement Equipment
Skin Temperature Monitor
Thermodilution Catheter Probes

[IV] Industrial Electronics
Commercial Vending Machines
Crystal Ovens
Fluid Flow Measurement
Gas Flow Indicators
HVAC Equipment
Industrial Process Controls
Liquid Level Indicators
Microwave Power Measurements
Photographic Processing Equipment
Plastic Laminating Equipment
Solar Energy Equipment
Thermal Conductivity Measurements (Diamond Tester etc.)
Thermocouple Compensation
Thermoplastic Moulding Equipment
Thermostats
Water Purification Equipment
Welding Equipment

[V] Military and Aerospace
Aircraft Temperature
Bathythermography
Bomb Fuses
Fire Control Equipment
Missiles and Spacecraft
Temperatures Oscillator Compensation
Psychological Monitoring Satellites

[VI] Food Handling and Processing
Coffee Makers
Deep Fryers
Fast Food Processing
Perishable Shipping Temperature
Controlled Food Storage Systems
Thermometers for use in food preparation

[VII] Communication and Instrumen tation:
Amplifier overtemperature Sensing
Cellular Telephones
Copper Coil Winding
Rechargeable Battery Packs
Transistor Gain Stabiliser
Transistor Temperature Compensation

[VIII] Computer

Power Supplies (Inrush Current Limiting)
Uninterruptable Power Supplies (Over Temperature Sensing)
CPU Temperature monitoring.

1.7 Philosophy of the Research Work:

1.7.1 Conventional Approach: trial and error

There are several factors that determine the feasibility of a sensor technology, such as the magnitude of sensitivity to the measured property, the response rate, and the cost of the final product. Sensing devices have been traditionally developed using trial-and-error techniques rather than following an insightful scientific approach. Many of the existing technologies utilise complex mixtures of several different materials, yet the functionality of each component is not known or well understood. Furthermore, the degradation mechanisms leading to the ageing behaviour of a sensor are not fully understood in most of the cases. Basic knowledge of the sensing mechanisms and their degradation behaviour is necessary for the exploitation of the full potential of existing materials and methods to obtain advanced, reliable, affordable, and novel technologies.

1.7.2 Over-specifications by Manufacturer :

One of the problems the thermistor industry has faced over the years is that some manufacturers have claimed their particular style or configuration of thermistor is better than other configurations proposed by their competitors, without regard to other, more pertinent factors. These thermistor "politics," more harmful than beneficial to the industry, can confuse engineers and purchasing agents who are looking for reliable information to help them to choose the appropriate product for their application. Although some thermistor qualities or capabilities, including

interchangeability, repeatability, size, responsiveness, and stability, can either be enhanced or limited by style or geometry, these characteristics are much more dependent on a manufacturer's ability to understand the ceramics technology being used and to maintain control of the manufacturing process.

1.7.3 Development and Optimisation of Sensor Materials :

Fundamental understanding of the materials characteristics is vital in selecting the appropriate combination of sensing elements to achieve selectivity in complex sensor array structures. Therefore, essential sensor performance parameters (e.g., stability, sensitivity, and selectivity) need to be improved, even in commercially available products. e.g. in even the thermistors available in the market, are found to lack unit-to-unit consistency which is often due to poor control over raw materials and fabrication conditions including forming, firing and electrode attachment. In this way most of the sensor specifications depend largely on the physical and chemical characteristics of the materials used to build the sensing devices. One factor having a tremendous impact on the sensor's characteristics is the processing route followed to prepare the material. Sensing devices are often bulk structures. The configuration that is most commonly employed involves either sintered powders in the form of a dense pressed pellet or porous thick films deposited on a tube or a planar substrate.

Different fabrication methods are known to result in a variety of microstructures and varying response characteristics for a particular sensor; there have been no systematic studies to identify an optimal processing technique. In large measure, this is because detailed characterisation of the materials characteristics, including the relationships between microstructure and properties, is still lacking.

The characterisation of the morphological, structural, and chemical features of sensor materials has rarely been reported in the literature. There have been several publications on the structural characteristics of very common electronic ceramic sensor materials (SnO_2, TiO_2, and perovskites), and Nickel manganite (the one which has been selected for the investigation in the present work), however these have not been directly related to sensor performance. Furthermore, in sensor-related publications, several problems that could have been analysed in a straightforward manner in a short time frame, using characterisation techniques. Instead, such problems are approached by alternative routes, typically laborious and time-consuming, often yielding ambiguous results.

1.7.4 Revolution by Materials and Evolution by Signal Processing :

Although several specifications of the sensor could be improved by materials processing, there is a limit to all this. Through study of the thermistor theory reveals that some specifications like non-linearity, lag, and even correction for ageing could be best tackled through application of mathematical modelling through software. Here the digitisation of the

sensor plays a key role. Once the digitized sensor data are ready, the rest of the signal processing is basically a question of the intelligent application of mathematical algorithms.

1.7.5 Combined Approach :

In our opinion, the improvement in thermistor specifications can not be achieved solely by materials way or by the signal processing, however a combined approach will lead in the improvement in the performance. In the course of research work, we have applied different preparation method like carboxylate precursor route to improve the unit to unit tolerance. A good number of materials characterisation tools like X-ray diffraction, TGA/DTA, have been applied to the precursor and its sintered products to confirm the completion of solid state reaction and to study the decomposition process. Efforts have been done to optimise the forming conditions like sintering temperature, which directly affects the densification, grain size distribution and dormant resistivity of the product [198-199]. Fully automated set-up have been developed to characterise the thermistors with respect to their various specifications and effect of environmental factors like moisture.

1.8 Aim and Objectives :

The present thesis reports work on development of high performance Nickel Manganite based NTC thermistors and addresses a few of their important drawbacks mentioned so far. The main objective of the research is all round performance improvement of the NTC thermistor

which requires following important parameters to be studied in detail.

- Optimisation of thermistor characteristics for domestic applications
- improving interchangeability
- improving figure of merit

While concentrating on above parameters it is also necessary to look into following aspects:

- reducing ageing effect
- better resolution
- low power dissipation
- high speed
- application of Thermistor in smart sensors

The methodology adopted and work plan undertaken is as follows.

1.9 Methodology and Work Plan:

It was decided to meet the objectives by combined approach, i.e. improved materials synthesis supported by instrumentation techniques as described at 1.7 (Philosophy of research work). Looking at the multidisciplinary nature of the work, a through literature survey [1-204] was undertaken in various aspects of thermistors like materials preparation methods, materials characterisation techniques, instrumentation development, smart sensors etc. The catalogues of good number of thermistor manufacturers were refereed to get the details of latest products. Several webpages were also referred to get the latest know-how on the subject.

To fulfil the first objective, i.e. sensor development for domestic applications, it was necessary to identify a stable material for the temperature range below 200°C. Several transition metal oxides having mixed metal ions, containing two or more cations have been reported to exhibit semiconducting property. The material Nickel Manganite ($NiMn_2O_4$) was chosen for investigation since it is stable due to less difference in valances of octahedral and tetrahedral ions and their sizes. After selection of the material, the next important thing was to finalise the synthesis route. Based on the investigator's past experience on similar materials [207-212], carboxylate precursors and oxalic precursor methods were finalised. The formation of materials was confirmed by applying characterisation techniques like XRD. The reasons behind ageing and lack of interchangeability were found to be due to poor geometry control of thermistor and their leads and less densification. In order to improve these aspects the lead attachment jig was modified. The power consumption of the thermistor is a direct function of its dormant or room temperature resistance. In order to optimise the power dissipation, the room temperature resistance was varied by changing the stoichiometry in $Ni_{1-X}Mn_{2+x}O_4$.

The need of automated instrumentation systems was felt to characterise and mark the specifications of the thermistors. Various test and characterisation set-ups were conceptualised and executed for this purpose. Finally, in order to achieve the best compatibility of the fabricated

thermistors with digital systems three architectures of smart sensors were proposed.

Thus, work plan was as follows:

- Synthesis and characterisation of materials
- Device Fabrication
- Development of Instrumentation
- Proposing smart sensor architecture

The thesis is organised in five chapters. A brief outline of each chapter is as follows.

Chapter 2 has three subparts. Part I presents the synthesis of nickel manganite required for making the device by using carboxylate precursor method. The preparation methods used are fumarate, succinate, oxalate, tartarate and malonate. Part II covers the details regarding the controlled conditions for fabricating the device with emphasis on management in the range of domestic applications. This part deals with the oxalic precursor route for synthesis of thermistor having composition $Ni_{1-x}Mn_{2+x}O_4$ with x = 0, 0.05, 0.10, 0.20, 0.30, 0.40, 0.45, 0.50, 0.55 and 0.60. The details regarding the chemistry aspects of all the above mentioned techniques is given in the appendix I at the end of the thesis. The last part, presents details of a novel manufacturing set-up for fabricating disc type thermistors. The thermistors fabricated using this set-up have been found to have better interchangeability, minimal ageing, moderate materials constant and

improved resolution. This is evident from the values of resistance ratio, materials constant and its tolerance.

Chapter 3 presents the details of instrumentation for test and characterisation of the thermistors fabricated using the above mentioned techniques. A versatile computer controlled measuring system is described here, used for characterisation of the samples in terms of resistance Vs temperature and current Vs voltage. The set-up comprises of PC based ADD-ON cards having on-board analogue to digital converter and digital to analog converter. A driver software package has been developed to enable the precise acquisition of resistance Vs temperature and current Vs voltage characteristics in relatively short duration of experiments, preventing the damage to the sensor as observed in conventional characterisation set-ups. A complete software package comprising of various 'C' programs, developed for this purpose is listed at the end of the chapter. The striking feature of this set-up is accelerated testing of the thermistor in compressed test time. The chapter also presents the instrumentation set-up developed for finding the time constant of the thermistors. Thermistors are known for their immunity to moisture. In the course of characterisation some anomaly was observed which is attributed to the presence of moisture. In order to characterise the effects of moisture, a probe based on capacitive principle is developed. The probe acts as a capacitor in an oscillator wherein the frequency of the oscillator changes due to change in dielectric constant. The presence of moisture on thermistor is found to affect the dielectric

constant of the probe and hence the change in frequency of the oscillator. This chapter also includes the design of furnace, instrumentation amplifier and temperature controller.

The modest suitability of conventional thermistors is becoming a bottleneck in microprocessor -based data-acquisition systems. This problem is being overcome by the development of smart sensors that are compatible with the microprocessor. Chapter 4 presents the design of thermistor based smart sensors in accordance with one of our objective. It has three subparts. Part I presents smart sensor architecture based on modified Schmitt trigger with in which the thermistor is embedded. The built in programmable hystersis gives a good noise immunity to the sensor, making it useful for applications like over-under temperature switches and biomedical measurements. Part II propose a non-linear ADC (NADC) for thermistor interfacing to digital systems. Presently used linear ADC technology poses various limitations in digitising the output of highly non-linear sensors like thermistors. The architecture proposed here uses a novel modified PWM technique to cancel the non-linearity of the thermistor in the process of digitisation. The last part presents an architecture of low voltage application specific integrated circuit (ASIC) for biomedical applications.

Summary, results, conclusions and scope for the future extension has been presented in Chapter 6.

CHAPTER 2

Materials and Device Fabrication

2.1 Introduction :

In general semiconductors exhibit a negative temperature coefficient of resistance, of magnitude several orders higher than that of metals. The temperature coefficient of resistance of semiconductor generally lies in between -1 and -5 % per K, as against a value of around +0.4% per K for copper and platinum. However, the electronic grade semiconductors (germanium and silicon) needs a high purity and can be obtained only through special processing. No doubt, such semiconductor possess a large value of resistance-temperature coefficient, their conductivity at ordinary temperatures is however too low, for practical thermistor applications. Commercial NTC thermistors are therefore made up of compound semiconductors, which are basically mixed metal oxides of Cobalt, Copper, Manganese, Nickel, Tin, Titanium etc.[154] These mixed metal oxides especially spinels exhibit interesting structural, electrical and magnetic properties. The R-T characteristics is similar to that of intrinsic Germanium or Silicon, in addition to large number of charge carriers due to different phenomenon involving oxygen ions. Since spinel structure is dominating in NTC thermistors, it is worthwhile to take a review of the same.

The Spinel group of minerals is a group of oxides that have very similar structures. The structure is based on the structure of diamond, which has the same high symmetry, 4/m bar 3 2/m [149]. In spinels, the position of the A (tetrahedral) ions is nearly identical to the positions occupied by carbon atoms in the diamond structure. This could explain the

relatively high hardness and high density typical of this group[149]. The arrangement of the other ions in the structure conform to the symmetry of the diamond structure. But, they disrupt the cleavage as there is no cleavage directions in any member of this group. The arrangement of the ions also favours the octahedral crystal habit which is the predominant crystal form and is in fact the trademark of the spinels. All members of this group that share the spinel structure show the same type of twinning that is named after spinel, called the 'Spinel Law'. This group contains over twenty members, but only a few are commonly used [147]. The formula is given as AB_2O_4, where A can be a Group IIA (+2) metal or transition metal in the +2 oxidation state, and B is a Group IIIA (+3) metal or transition metal in the +3 oxidation state [148]. The oxide ions form a close-packed cubic lattice with eight tetrahedral holes and four octahedral holes per AB_2O_4 unit. In a normal spinel, the ions of the Group IIA (+2) metal or transition metal in the +2 oxidation state occupy one-eighth of the tetrahedral holes and the ions of the Group IIIA (3) metal or transition metal in the +3 oxidation state occupy one-half of the available octahedral holes. For example, in the case of $MgAl_2O_4$, the Mg^{2+} ions occupy one-eighth of the tetrahedral holes and the Al^{3+} ions occupy one-half of the octahedral holes. It is convenient to describe the structure of spinels by the parameter λ, which is defined as the fraction of B ions in tetrahedral holes. The values of λ range from zero for normal spinels to 0.50 for inverse spinels. In case of random spinels λ values are intermediate (such as $\lambda = 1/3$), and therefore

it need not be necessarily constant for a given spinel, as it can be altered by appropriate heat treatment. Sintering conditions, therefore play an important role in thermistor characteristics. Values of λ can be determined through X-ray, neutron diffraction, measurements of saturation magnetisation, and IR measurements [148]. The details regarding materials aspects of thermistor are discussed in depth in literature [2,4,6,7,8,10,13,15,16,17, 18-21, 80-86].

2.2 Nickel Manganite based Thermistors:

The present chapter reports synthesis of NTC thermistors based on Nickel Manganite ($NiMn_2O_4$) synthesised by using carboxylate precursor route. The material has been chosen after extensive literature survey [2, 5-8, 13-22, 80-86, 148-150, 161] along with through theoretical analysis. For making high performance NTC thermistors chemical stability and higher activation energy materials are necessary. The type of transition metal oxides required for this purpose should have minimum oxygen absorption during cooling as well as heating cycles. It may be noted here that a thermistor undergoes a large number of heat cycles during fabrication and also during application. The ferrites, which well exhibit the above said property, have been investigated previously for use in NTC thermistors, particularly MFe_2O_4 (M = Mn, Mg, Zn), but these materials tend to have lower β values than nickel manganites [185-189]. On the other hand the Mn and Ni oxides, (separate or compound and also in pure or slightly doped form), show less oxygen reabsorption and also moderate β values.

Moreover this oxide system is useful for the temperature range of domestic applications, which is one of the objectives of the present work. In these compounds the electrical conductivity is due to a model of conduction called as "hopping". It is a form of Ionic conductivity where ions (oxygen ions) "hop" between point defect sites in a spinel crystal structure. The transfer of electrons takes place (hopping) between the Mn^{3+} and Mn^{4+} ions in an octahedral sublattice of the spinel structure[161]. The probability of point defects in the crystal lattice increases as temperature increases, hence the "hopping" is more likely to occur and so material resistivity decreases as temperature increases.

Considerable efforts have been devoted in the past to understand the physical properties of Nickel Manganite. It is a ferrimagnetic material at low temperature. The conditions determining the valency and the lattice site preference of the two cations have been broadly discussed in the literature [2, 4, 15, 17, 21, 81-86, 123], but still they remain uncertain. Experiments have shown that the stoichiometry may strongly depend on the methods of preparation and forming conditions like sintering temperature. A number of investigations have been reported on the measurement of electrical conductivity [2,11-14], seebeck coefficient [2, 12-14], magnetic properties [2, 12, 15], neutron diffraction [16] and x-ray Auger and microstructural studies [17-18]. It was found that the material exhibits poor stability at high temperatures. Some investigators [18] have also reported difficulty in obtaining single phase $NiMn_2O_4$. Researchers

have used several methods to synthesise the material. Some of them are cryo-chemical and spray drying [19], oxalate precursor [20], co-precipitation using hydrogen peroxide [21,22] etc. In nutshell, the most important factor having a tremendous impact on the sensor's characteristics is the processing route followed to prepare the material. Sensing devices are often bulk structures. The configuration that is most commonly employed involves either sintered powders in the form of a dense pressed pellet or porous thick films deposited on a tube or a planar substrate. The present chapter describes the synthesis of thermistor material by using carboxylate precursor method, (a fairly popular synthesis route used for ferrites), for fabrication and characterisation of disc type thermistors. A brief review of the methods of synthesis of the mixed metal oxide precursors has been presented in Section 2.3.

2.3 Materials and Techniques :

The preparation methods for synthesis of oxide materials may be broadly categorised into following :

2.3.1 Ceramic Method : This is one of the most extensively used method in which high purity oxides of desired composition are mixed together in a liquid suspension (water, alcohol, acetone) in a stoichiometric amount and wet milled with steel balls for few hours. After the slurry is filtered and dried, the dried powder mixture is transferred to ceramic crucible and preheated in air or oxygen. In order to have better homogenisation of the product, more grinding is usually done on the preheated products in steel ball mills.

The second grinding not only reduces the diffusion distances but also decreases grain size of the product as well as grain size distribution. Organic binders like Polyvinyl alcohol (PVA) are often added to the preheated samples and then milled and then cold pressed into required shape by using hydraulic press. The pressure applied is generally 5-25 x 10^6 Kg m^{-2}. The pellets thus formed are sintered at high temperature in air or oxygen atmosphere till the completion of solid state reaction. The oxides used must posses high reactivity so as to get a homogeneous composition after mixing and calcination [190].

2.3.2 Precursor Technique : A precursor method involves preparation of an easily decomposible compound of metals which yield the desired oxides on heating. The required stoichiometry for oxides can be fixed at the time of precipitation of the constituent elements from solution using suitable precipitants. By this, one can control the impurity levels in the oxide systems. These precursors can be decomposed to oxides at lower temperatures and then a proper sintering process would give a dense ceramic oxide required in devices at relatively lower sintering temperature. The precursor method has been extensively discussed in literature [191] from ferrites point of view. It can be divided into following types:

(a) Hydroxide Precursors : In this technique a concentrated colloidal sol of the hydroxides is formed and converted into a semirigid gel. The gel is then dried and calcined to form the ferrite. However, the disadvantage of the coprecipitation methods is segregation and

inability to compact easily to high density. This method eliminates the need for the lengthy milling process reported in the earlier methods. However, this requires the knowledge of the solubility of the products. This method has shown good results in case of rare earth garnets.

(b) Oxalate Precursors : The advantage with this method is the usage of ammonium oxalates for precipitation which does not leave any residue after heating. Most of the metal oxalates have very similar crystal structure so that precipitation tends to produce mixed crystals which contain the metallic cations in exactly the same proportions in which they were present in the solution. This achieves the mixing on a molecular scale and the correct stoichiometry. The method is preferred for synthesis of ferrites, due to low solubility and low decomposition temperatures of oxalate precursors.

(c) Hydrazinate Precursors : These precursors have been reported to undergo autocatalytic decomposition, i.e., once ignited the combustion is self sustained. The low temperature synthesis is due to the release of energy accompanied in hydrazine oxidation during the decomposition of the complex.

2.3.3 Wet Chemical Method : Preparation of mixed metal oxides from solutions of water soluble salts of the corresponding metals fall under wet chemical category. This technique is reported to yield ferrite powders having molecular level homogeneity, smaller grain size, low

porosity and larger surface area[192]. The various methods under this category include spray techniques, freeze drying and hydrothermal oxidation.

2.3.4 Decomposition Method : In this method, salts like carbonates, nitrates and oxalates are used. They are mixed in the required stoichiometry and preheated usually in air to form oxides. The oxides thus formed have ability to undergo solid state reaction. Rest of the processing steps are similar to the ceramic method.

2.3.5 Other Methods : The other techniques reported in the literature are [191] explosion method, supercritical drying process, bubbling ozone method, isostatic pressing method and modified hot pressing technique.

2.4 Part I : Carboxylate Precursor Route :

The entire preparation technique (synthesis, characterisation and device fabrication) used in this chapter has been summarised in the flow chart given in figure 2.1. There are four basic steps involved in the fabrication of thermistors as follows:

(i) Preparation of material of desired composition through precursor route.

(ii) Presintering.

(iii) Transforming the presintered material into fine powder and pressing it to desired shape.

(iv) Final sintering to form the dense end product.

2.4.1 Synthesis of Materials:

We have used here a precursor synthesis route to achieve high quality, minimum tolerance NTC thermistors. Various precipitating agents were used to obtain the raw precursor.

- Experimental:

The following carboxylate precursors of nickel manganite were prepared by using salts of carboxylic acid and the respective metal chlorides:

(i) Thermistor Fumarate (TF)

(ii) Thermistor Succinate (TS)

(iii) Thermistor Oxalate (TO)

(iv) Thermistor Tartarate (TT)

(v) Thermistor Malonate (TM)

The details of synthesis procedure is as follows:

2.4.2 Preparation of Metal Chloride Solution :

Stoichiometric amount of $NiCl_2.6H_2O$ (0.25 M) and $MnCl_2.4H_2O$ (0.5 M) were weighed accurately on a Mettler balance. The $NiCl_2.6H_2O$ and $MnCl_2.4H_2O$ were dissolved separately in acidified distilled water. The acidified water was used to prevent formation of hydroxide. Both the salt solutions were then mixed together to make the volume to 100 ml in standard volumetric flask. The solution thus formed was then used for the preparation of the various carboxylate precursors of nickel manganite.

2.4.3 Preparation of the precursor of Thermistor Fumarate (TF) :

Stoichiometric amount of Sodium Fumarate (1M) was dissolved in distilled water to make a solution of 100ml. The solution was then heated upto boiling. The metal chloride solution was also heated. The heated metal chloride solution was then added dropwise to hot sodium fumarate solution with a constant stirring. The precipitate of nickel manganese fumarate was formed. This precipitate was then filtered using buchner funnel. The precipitate was washed with distilled water, until it was free from chloride ions. It was then dried in air and stored in a desiccator.

2.4.4 Preparation of Other Precursors :

Similarly, nickel manganese succinate (TS), oxalate (TO), tartarate (TT) and malonate (TM) precursors were prepared.

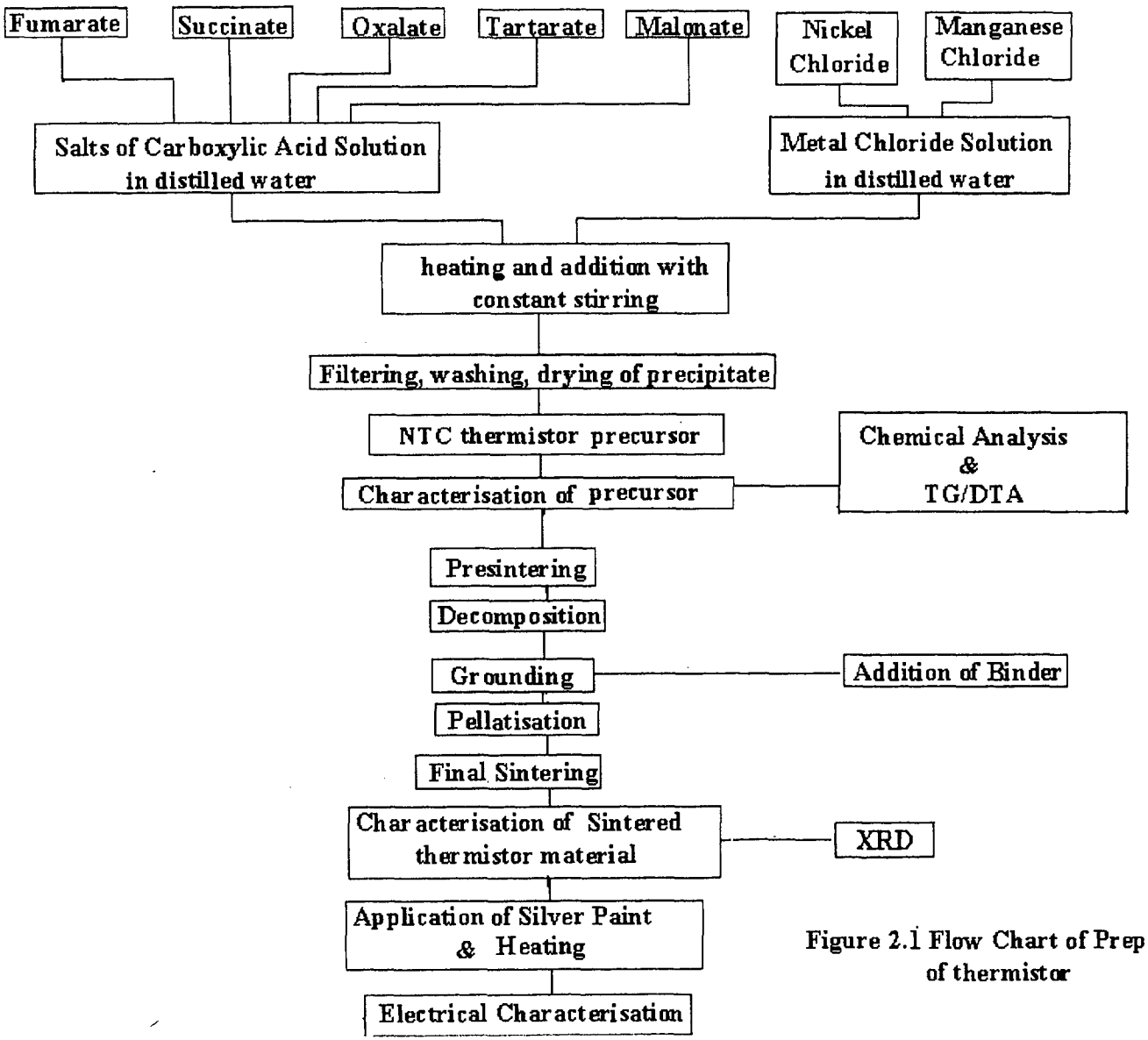

Figure 2.1 Flow Chart of Preparation of thermistor

2.5 Thermal Analysis of Precursors and Decomposed Material:

All the precursors were decomposed by heating at 500°C to get the raw nickel manganite powder. The temperature of decomposition was fixed after doing the TG/DTA analysis of the precursors in air/oxygen atmosphere. The TG/DTA spectra of the precursors are given in Appendix I. The chemical analysis of the nickel manganite powder was done using Atomic Absorption Spectrophotometer, model PE3030, in order to estimate the percentage of nickel and manganese in it.

2.6 Sintering:

sintering the material at elevated temperatures is the most important process in thermistor fabrication. The sintering is carried out in a furnace developed for this purpose. The details are given in Chapter 3. Sintering is carried out in two steps: presintering; and the final sintering.

2.6.1 Presintering :

The purpose of presintering [193] is to decompose carbonates and higher oxides (which reduce with the evolution of gas in final sintering), to assist in homogenising the material and efficiently control the shrinkage of the material. During the presintering phase the raw material partly reacts to form the final product and the extent of reaction depends on the reactivity of the components and the presintering temperature.

The raw thermistor powder, synthesised using carboxylate precursor route, was transferred to silica crucibles and presintered at 800°C for four hours (the details of the furnace and temperature monitoring circuitry are

presented in chapter 3). The furnace was then allowed to cool slowly. The presintered powder was then milled in agate mortar along with an organic binder, polyvinyl alcohol (PVA). The grounding reduces the particle size and promotes mixing of any unreacted oxides.

2.6.2 Pellet Formation :

The dry powder was transferred into dies of various sizes (1 cm to 2 cm diameter). Some thick pellets were also formed to have measurable time constant specifications. The pellets were then pressed in a hydraulic press with the pressure 6 tonnes per square inch for 3 minutes. After removing the load, pellets were carefully taken out from the die.

2.6.3 Final Sintering :

The pellets were placed in a crucible and fired at 1000°C for five hours. The furnace was allowed to cool slowly in order to avoid the formation of micro-cracks on the pellets. The final sintering at elevated temperature increases the density and decreases the porosity of the material.

2.7 Characterisation of the Sintered Product:

The X-ray diffraction of the sintered thermistor material was done. The details are covered in Appendix- I.

2.8 Resistance Vs Temperature Characteristics:

2.8.1 Conduction Mechanism :

The thermistor materials are referred to as valence controlled semiconductors. Conduction occurs when ions having multiple valence

states occupy equivalent crystallographic sites. It must be the same element and differ in valence by one unit and occupy B sites[160]. The conduction mechanism is a thermally activated electron hopping process, in which the electrons hop from one cation (Mn^{3+}) to another (Mn^{4+}) in the B lattice sites under the influence of a potential gradient across the material.

The conductivity is a product of charge density and mobility. The number of charge carriers, the density of B sites, and the probability of a B site being active determine charge density. The mobility is determined by the distance between nearest neighbour B sites, the activation energy (needed for the electron to move from one site to another), and a frequency factor (how often it tries to jump). Charge carries are also produced by other defects such as non-stoichiometry and grain boundaries.

By considering the effects of all the above factors, an expression for conductivity is derived as follows:

$$\sigma = \sigma_{\infty} \exp(-q/kT) \quad \text{----------} \quad (2.1)$$

where σ_{∞} is the infinite temperature conductivity (which includes consideration of charge density and mobility), -q is the activation energy, k is Boltzmann's constant, and T the absolute temperature. For the thermistors, the resistivity ρ (and hence resistance) is of more interest. By replacing resistivity with resistance values and combining the activation energy and Boltzmann's constant terms, the familiar thermistor expression is obtained

$$R = A \exp(\beta / T) \text{ ---------- } (2.2)$$

where A includes dimensional factors and infinite temperature resistance, β is the material constant and T is the absolute temperature.

2.8.2 Experimental :

The experimental set-up for resistance Vs temperature characteristics is described in Chapter 3. Good electrical contacts were ensured by applying a silver paint and annealing at 300°C for 15 minutes. Measurements were made by using two probe method, by mounting the pellet in a sample holder consisting of two brass rods. A photograph of the two probe sample holder is as shown in a photograph at figure 2.2. The pellet can be sandwiched tightly with the help of screws. The resistance Vs temperature tables for a set of samples are presented in tables 2.1 to 2.5.

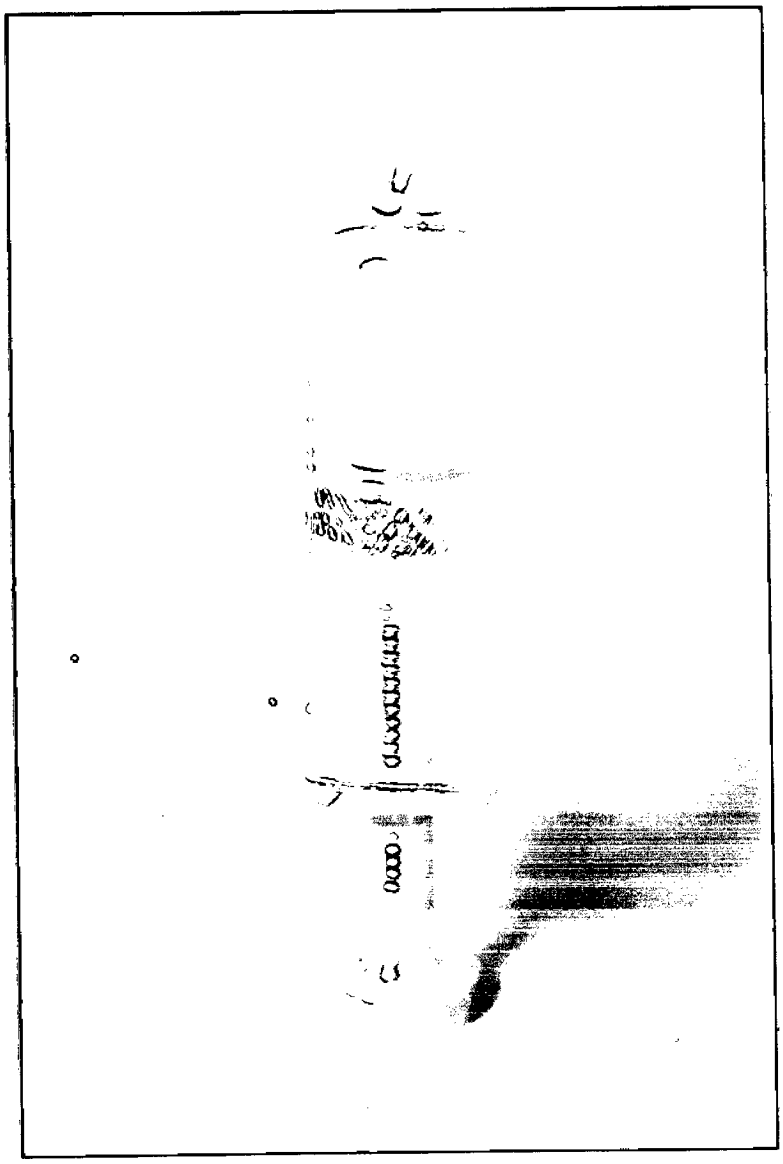

Figure 2.2 : Photograph of the two probe sample holder

Table 2.1: Resistance Vs Temperature Table for TF

Temperature. °C	Resistance KΩ
27	50.2741
28	49.1815
29	48.1196
30	47.0874
31	46.084
32	45.1083
33	44.1594
34	43.2364
35	42.3386
36	41.465
37	40.6149
38	39.7876
39	38.9822
40	38.1981
41	37.4347
42	36.6911
43	35.967
44	35.2615
45	34.5742
46	33.9045
47	33.2518
48	32.6156
49	31.9955
50	31.3908
51	30.8012
52	30.2262
53	29.6654
54	29.1183
55	28.5845
56	28.0637
57	27.5554
58	27.0594
59	26.5751
60	26.1024
61	25.6408
62	25.1901
63	24.7499
64	24.3199
65	23.8999
66	23.4895
67	23.0886
68	22.6968
69	22.3138
70	21.9395
71	21.5736
72	21.2159
73	20.8661
74	20.5241
75	20.1896
76	19.8624
77	19.5423
78	19.2291
79	18.9228
80	18.6229
81	18.3295
82	18.0424
83	17.7613
84	17.4861
85	17.2167
86	16.9529
87	16.6945
88	16.4416
89	16.1938
90	15.951
91	15.7133
92	15.4803
93	15.252
94	15.0283
95	14.8091
96	14.5943
97	14.3837
98	14.1772
99	13.9748
100	13.7764
101	13.5818
102	13.3909
103	13.2038
104	13.0202
105	12.8401
106	12.6635
107	12.4902
108	12.3202
109	12.1533
110	11.9896
111	11.8289
112	11.6711
113	11.5163
114	11.3643
115	11.2151
116	11.0686
117	10.9247
118	10.7835
119	10.6447
120	10.5085
121	10.3747
122	10.2432
123	10.1141
124	9.9872
125	9.8625
126	9.74
127	9.6197
128	9.5014
129	9.3851
130	9.2708
131	9.1585
132	9.0481
133	8.9395
134	8.8328
135	8.7279
136	8.6247
137	8.5232
138	8.4234
139	8.3252
140	8.2287
141	8.1337
142	8.0403
143	7.9484
144	7.858
145	7.769
146	7.6815
147	7.5953
148	7.5106
149	7.4271
150	7.345
151	7.2642
152	7.1846
153	7.1063
154	7.0292
155	6.9532
156	6.8785
157	6.8049
158	6.7324
159	6.661
160	6.5907
161	6.5214
162	6.4532
163	6.3861
164	6.3199
165	6.2547
166	6.1905
167	6.1272
168	6.0648
169	6.0034
170	5.9428

Table 2.2: Resistance Vs Temperature Table for TS

Temp °C	Resistance KΩ	55	27.6645	85	16.4757	115	10.6306	145	7.3043
		56	27.1493	86	16.2177	116	10.4887	146	7.2201
27	49.2708	57	26.6468	87	15.9651	117	10.3494	147	7.1374
28	48.1764	58	26.1565	88	15.7179	118	10.2126	148	7.056
29	47.1134	59	25.6781	89	15.4758	119	10.0783	149	6.9758
30	46.0806	60	25.2113	90	15.2387	120	9.9464	150	6.897
31	45.0769	61	24.7556	91	15.0065	121	9.817	151	6.8194
32	44.1016	62	24.3109	92	14.7791	122	9.6898	152	6.7431
33	43.1534	63	23.8767	93	14.5564	123	9.565	153	6.6679
34	42.2317	64	23.4527	94	14.3382	124	9.4423	154	6.594
35	41.3354	65	23.0388	95	14.1244	125	9.3219	155	6.5212
36	40.4638	66	22.6345	96	13.915	126	9.2035	156	6.4495
37	39.616	67	22.2396	97	13.7097	127	9.0873	157	6.379
38	38.7912	68	21.8539	98	13.5086	128	8.9731	158	6.3095
39	37.9887	69	21.477	99	13.3115	129	8.8608	159	6.2411
40	37.2078	70	21.1088	100	13.1183	130	8.7506	160	6.1738
41	36.4478	71	20.749	101	12.9289	131	8.6422	161	6.1075
42	35.7079	72	20.3974	102	12.7432	132	8.5357	162	6.0422
43	34.9876	73	20.0537	103	12.5612	133	8.431	163	5.9779
44	34.2863	74	19.7177	104	12.3827	134	8.3281	164	5.9146
45	33.6033	75	19.3892	105	12.2077	135	8.227	165	5.8522
46	32.938	76	19.0681	106	12.036	136	8.1276	166	5.7908
47	32.29	77	18.754	107	11.8677	137	8.0299	167	5.7303
48	31.6586	78	18.4469	108	11.7025	138	7.9338	168	5.6707
49	31.0434	79	18.1465	109	11.5405	139	7.8393	169	5.612
50	30.4438	80	17.8526	110	11.3816	140	7.7463	170	5.5541
51	29.8594	81	17.5651	111	11.2257	141	7.655		
52	29.2897	82	17.2839	112	11.0727	142	7.5651		
53	28.7343	83	17.0087	113	10.9226	143	7.4767		
54	28.1927	84	16.7393	114	10.7752	144	7.3898		

Table 2.3 : Resistance Vs Temperature Characteristics of TO

Temp °C	Resistance KΩ
27	51.0858
28	50.0055
29	48.9549
30	47.9331
31	46.9391
32	45.9721
33	45.0311
34	44.1153
35	43.2239
36	42.3561
37	41.5112
38	40.6884
39	39.887
40	39.1063
41	38.3458
42	37.6047
43	36.8825
44	36.1786
45	35.4925
46	34.8235
47	34.1712
48	33.5351
49	32.9146
50	32.3094
51	31.7189
52	31.1428
53	30.5805
54	30.0318
55	29.4961
56	28.9732
57	28.4626
58	27.9641
59	27.4771
60	27.0016
61	26.537
62	26.0831
63	25.6396
64	25.2062
65	24.7826
66	24.3686
67	23.9639
68	23.5682
69	23.1813
70	22.803
71	22.4329
72	22.071
73	21.717
74	21.3706
75	21.0317
76	20.7
77	20.3755
78	20.0578
79	19.7468
80	19.4424
81	19.1444
82	18.8526
83	18.5668
84	18.2869
85	18.0128
86	17.7442
87	17.4811
88	17.2234
89	16.9708
90	16.7233
91	16.4808
92	16.2431
93	16.01
94	15.7816
95	15.5576
96	15.338
97	15.1226
98	14.9114
99	14.7043
100	14.5011
101	14.3019
102	14.1063
103	13.9145
104	13.7263
105	13.5416
106	13.3603
107	13.1825
108	13.0078
109	12.8364
110	12.6682
111	12.503
112	12.3408
113	12.1815
114	12.0251
115	11.8714
116	11.7206
117	11.5724
118	11.4268
119	11.2837
120	11.1432
121	11.0052
122	10.8695
123	10.7361
124	10.6051
125	10.4763
126	10.3497
127	10.2253
128	10.1029
129	9.9827
130	9.8644
131	9.7481
132	9.6338
133	9.5213
134	9.4107
135	9.302
136	9.195
137	9.0897
138	8.9862
139	8.8843
140	8.784
141	8.6854
142	8.5884
143	8.4929
144	8.3989
145	8.3063
146	8.2153
147	8.1256
148	8.0374
149	7.9505
150	7.865
151	7.7808
152	7.6979
153	7.6162
154	7.5358
155	7.4566
156	7.3786
157	7.3018
158	7.2261
159	7.1516
160	7.0781
161	7.0058
162	6.9345
163	6.8643
164	6.7951
165	6.7269
166	6.6597
167	6.5934
168	6.5281
169	6.4638
170	6.4004

Table 2.4 : Resistance vs. Temperature Characteristics or TT

Temp oC	Resistance KΩ
27	47.2948
28	46.1803
29	45.0991
30	44.0502
31	43.0323
32	42.0443
33	41.0853
34	40.1542
35	39.25
36	38.3719
37	37.5188
38	36.6901
39	35.8847
40	35.1021
41	34.3413
42	33.6016
43	32.8825
44	32.1831
45	31.5028
46	30.8411
47	30.1973
48	29.5708
49	28.961
50	28.3675
51	27.7897
52	27.2271
53	26.6793
54	26.1457
55	25.6259
56	25.1196
57	24.6262
58	24.1454
59	23.6768
60	23.2201
61	22.7748
62	22.3406
63	21.9172
64	21.5043
65	21.1015
66	20.7086
67	20.3252
68	19.9511
69	19.5861
70	19.2297
71	18.8819
72	18.5424
73	18.2108
74	17.887
75	17.5709
76	17.262
77	16.9603
78	16.6656
79	16.3776
80	16.0961
81	15.8211
82	15.5523
83	15.2895
84	15.0325
85	14.7813
86	14.5357
87	14.2955
88	14.0605
89	13.8306
90	13.6058
91	13.3858
92	13.1706
93	12.9599
94	12.7538
95	12.552
96	12.3545
97	12.1611
98	11.9718
99	11.7864
100	11.6048
101	11.427
102	11.2529
103	11.0823
104	10.9152
105	10.7515
106	10.591
107	10.4338
108	10.2797
109	10.1287
110	9.9807
111	9.8356
112	9.6933
113	9.5538
114	9.4171
115	9.283
116	9.1514
117	9.0224
118	8.8959
119	8.7717
120	8.6499
121	8.5304
122	8.4132
123	8.2981
124	8.1852
125	8.0744
126	7.9656
127	7.8588
128	7.754
129	7.6511
130	7.55
131	7.4508
132	7.3533
133	7.2577
134	7.1637
135	7.0713
136	6.9806
137	6.8915
138	6.804
139	6.718
140	6.6335
141	6.5505
142	6.4688
143	6.3886
144	6.3098
145	6.2323
146	6.1561
147	6.0812
148	6.0076
149	5.9352
150	5.864
151	5.794
152	5.7251
153	5.6574
154	5.5908
155	5.5253
156	5.4609
157	5.3975
158	5.3351
159	5.2737
160	5.2134
161	5.1539
162	5.0955
163	5.0379
164	4.9813
165	4.9255
166	4.8707
167	4.8166
168	4.7635
169	4.7111
170	4.6596

Table 2.5 : Resistance vs. Temperature for TM

Temp °C	Resistance KΩ
27	47.1804
28	46.0528
29	44.9595
30	43.899
31	42.8703
32	41.8722
33	40.9036
34	39.9635
35	39.0509
36	38.1649
37	37.3045
38	36.4688
39	35.6571
40	34.8684
41	34.102
42	33.3571
43	32.6331
44	31.9292
45	31.2448
46	30.5792
47	29.9318
48	29.302
49	28.6893
50	28.0931
51	27.5128
52	26.9479
53	26.398
54	25.8626
55	25.3412
56	24.8334
57	24.3387
58	23.8568
59	23.3873
60	22.9298
61	22.4838
62	22.0491
63	21.6253
64	21.2121
65	20.8092
66	20.4163
67	20.033
68	19.6591
69	19.2942
70	18.9383
71	18.5909
72	18.2518
73	17.9208
74	17.5977
75	17.2822
76	16.9742
77	16.6733
78	16.3794
79	16.0924
80	15.8119
81	15.5379
82	15.2702
83	15.0085
84	14.7527
85	14.5027
86	14.2583
87	14.0193
88	13.7856
89	13.5571
90	13.3335
91	13.1149
92	12.901
93	12.6918
94	12.487
95	12.2867
96	12.0906
97	11.8987
98	11.7108
99	11.5269
100	11.3468
101	11.1705
102	10.9979
103	10.8288
104	10.6632
105	10.5009
106	10.342
107	10.1863
108	10.0338
109	9.8843
110	9.7378
111	9.5942
112	9.4535
113	9.3155
114	9.1803
115	9.0477
116	8.9176
117	8.7902
118	8.6651
119	8.5425
120	8.4222
121	8.3042
122	8.1884
123	8.0749
124	7.9634
125	7.8541
126	7.7468
127	7.6414
128	7.5381
129	7.4366
130	7.337
131	7.2392
132	7.1432
133	7.0489
134	6.9563
135	6.8654
136	6.7761
137	6.6884
138	6.6022
139	6.5176
140	6.4344
141	6.3527
142	6.2724
143	6.1936
144	6.1161
145	6.0399
146	5.965
147	5.8914
148	5.819
149	5.7479
150	5.678
151	5.6093
152	5.5417
153	5.4752
154	5.4098
155	5.3455
156	5.2823
157	5.2201
158	5.1589
159	5.0987
160	5.0395
161	4.9813
162	4.924
163	4.8676
164	4.8121
165	4.7574
166	4.7037
167	4.6508
168	4.5987
169	4.5475
170	4.497

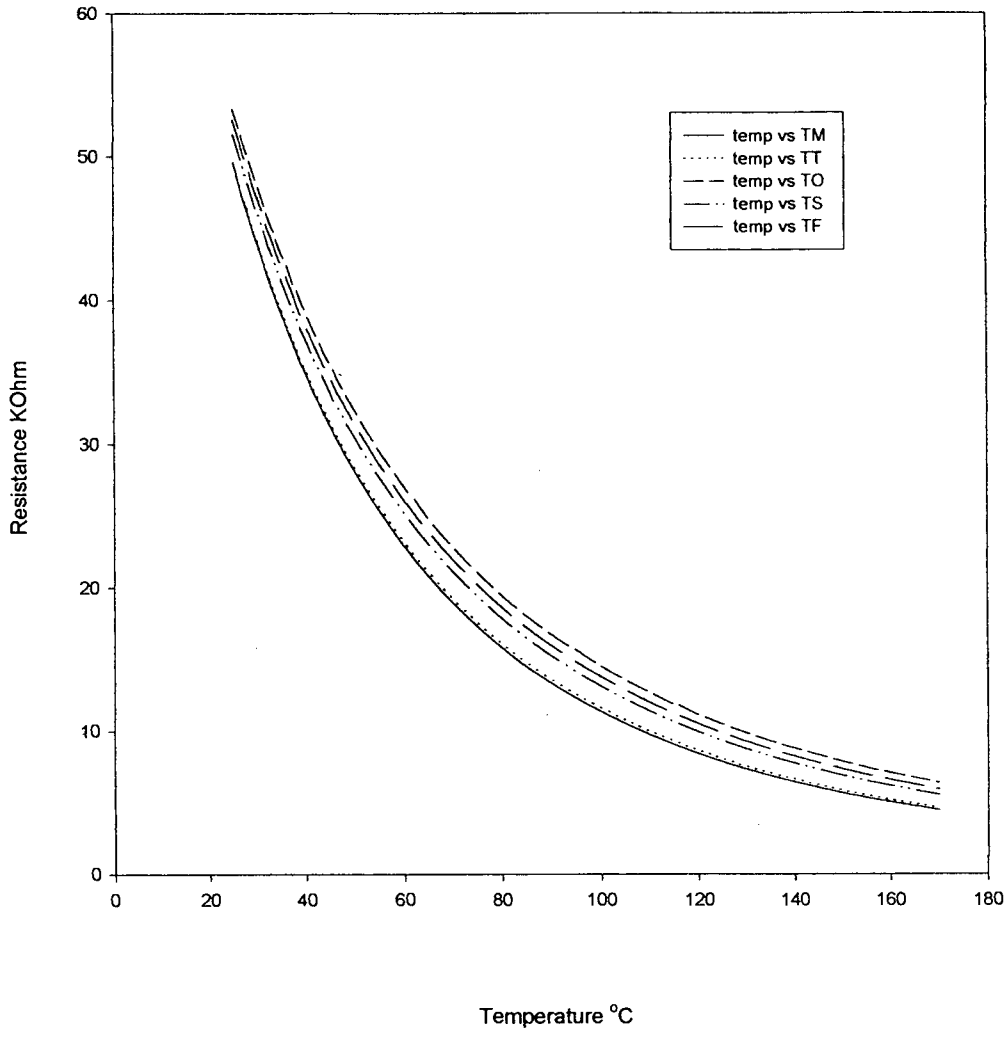

Figure 2.3 : Resistance Vs Temperature Characteristics of thermistors synthesised using carboxylate precursor route.

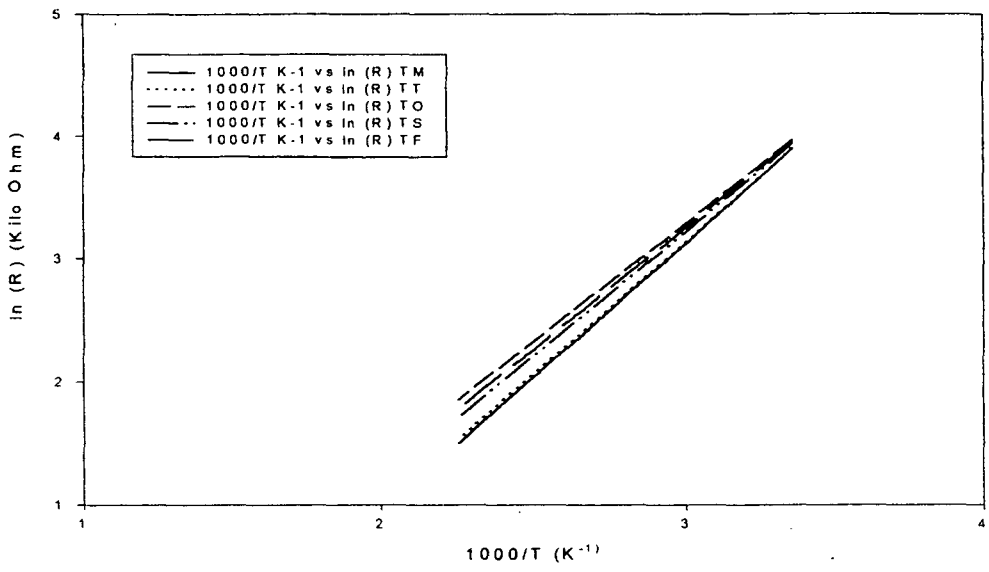

Figure 2.4 : Graph of ln (R) Vs 1000/T of thermistors synthesised using Carboxylate route

Table 2.6 : Beta, resistance ration and beta tolerance of thermistors (Carboxylate method)

Thermistor	β (K)	β Tolerance	Resistance Ratio	α (K^{-1})
TF	1986.161	± 0.003%	5.38	0.01506
TS	2030.118	± 0.005%	5.53	0.01439
TO	1932.06	± 0.006%	5.09	0.01665
TT	2155.59	± 0.009%	6.14	0.01501
TM	2186.376	± 0.004%	6.31	0.01496

2.9 Part II : Oxalic Precursor Route

In industrial applications, power dissipation of the thermistor plays an important role on the temperature range of measurement. By varying the stoichiometry, it is possible to optimise the room temperature resistance of the thermistor. This section presents synthesis and characterisation of nickel manganite thermistors $Ni_{1-x}Mn_{2+x}O_4$ with $0 \lesssim x \lesssim 0.6$ by Oxalic precursor route.

2.9.1 Synthesis of Precursor :

The precursor is obtained by using oxalic precursor method. This preparation method, which is largely described in the literature[194] for synthesis of ferrites, reported to yield extremely pure powders and thus consequently improves the reproducibility (batch to batch tolerance) of the devices. It may be recalled that, optimisation of room temperature resistance and improvement in reproducibility are two important objectives of the present investigations.

The basic series of stoichiometry chosen for the investigation is $Ni_{1-x}Mn_{2+x}O_4$ where, x = 0.0, 0.05, 0.10,0.15, 0.20, 0.25, 0.30, 0.35, 0.40, 0.45, 0.50, 0.55 and 0.60. The details of the amount of nickel acetate, manganese acetate and oxalic acid required for all the thirteen compositions has been presented in Table 2.7.

Table 2.7 : Calculation of Materials for Synthesis of $Ni_{1-x}Mn_{2+x}O_4$ series

Sample Nomenclature	Compostition	Nickel Acetate gms	Manganse Acetate gms	Oxalic Acid
TA1	$NiMn_2O_4$	12.442	24.509	22.0622
TA2	$Ni_{0.95}Mn_{2.05}O_4$	11.8199	25.1217	22.0622
TA3	$Ni_{0.9}Mn_{2.1}O_4$	11.1978	25.7344	22.0622
TA4	$Ni_{0.85}Mn_{2.15}O_4$	10.5757	26.4971	22.0622
TA5	$Ni_{0.8}Mn_{2.2}O_4$	9.9536	26.9599	22.0622
TA6	$Ni_{0.75}Mn_{2.25}O_4$	9.3315	27.5726	22.0622
TA7	$Ni_{0.7}Mn_{2.3}O_4$	8.7094	28.1853	22.0622
TA8	$Ni_{0.65}Mn_{2.35}O_4$	8.0873	28.7890	22.0622
TA9	$Ni_{0.6}Mn_{2.4}O_4$	7.4652	29.4108	22.0622
TA10	$Ni_{0.55}Mn_{2.45}O_4$	6.8431	30.0235	22.0622
TA11	$Ni_{0.5}Mn_{2.5}O_4$	6.221	30.6362	22.0622
TA12	$Ni_{0.45}Mn_{2.55}O_4$	5.5989	31.2489	22.0622
TA13	$Ni_{0.4}Mn_{2.6}O_4$	4.9766	31.8617	22.0622

Around 0.4 M solutions of Nickel and Manganese Acteates were taken in the desired stoichiometry (as given in table 2.7) and seperately dissolved in distilled water and heated subsequently. The hot acetate solutions were then added slowly with constant stirring to hot oxalic acid solution (quantity taken as per the calculation given in table 2.7) using two seperating funnels. The precipitate of the desired stoichiometry was obtained, which was then filtered, washed with distilled water and dried.

2.9.2 Thermal Analysis of Precursors and decomposed material :

The thermal decomposition of some of all the oxalate precursors was done by heating at 400°C. The TG/DTA analysis of all the samples was done to fix the thermal decomposition temperature. The TG/DTA traces of few oxalate samples are enclosed in Appendix-I. XRD Studies

were also conducted on the preheated precursor at different temperature. The XRD patterns are enclosed in appendix -I. The metal analysis of he decomposed powder was done using A.A.S., model PE3030.

2.9.3 Sintering:

The precursor was presintered at 800°C for four hours, then allowed to cool slowly. The presintered powder was then milled in agate mortar for 2 hours.

2.9.4 Pellet Formation:

The dry powder was transferred into dies of various sizes (1cm to 2cm diameter). The pellets were pressed in a hydraulic press with the pressure of 6 tonnes per square inch for 3 minutes. After removing the load, pellets were carefully taken out from the die.

2.9.5 Final Sintering:

The pellets were placed in a crucible and fired in a furnace with a microprocessor based temperature controller. The sintering cycle is shown in the figure 2.5

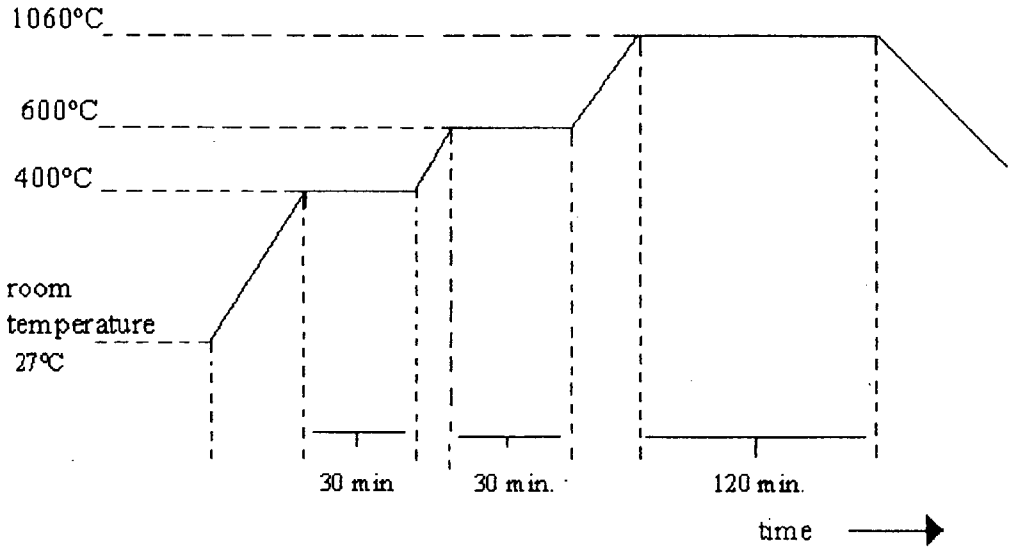

Figure 2. 5 : Sintering Cycle for oxalate precursors

2.9.6 Resistance Vs Temperature Characterisation :

The resistance Vs temperature characteristics was recorded for all the samples. The same is enclosed in the tables 2.8 to 2.12. The variation in room temperature resistance with Nickel content is shown in table 2.13.

Table 2.8 : Resistance Vs Temperature Data for the Composition $NiMn_2O_4$ (TA1)

Temp °C	Resistance KΩ
27	53.1749
28	52.1067
29	51.0668
30	50.0544
31	49.0684
32	48.1082
33	47.1729
34	46.2616
35	45.3737
36	44.5084
37	43.6651
38	42.843
39	42.0414
40	41.2599
41	40.4977
42	39.7543
43	39.0292
44	38.3217
45	37.6313
46	36.9576
47	36.3001
48	35.6582
49	35.0316
50	34.4198
51	33.8223
52	33.2388
53	32.6688
54	32.112
55	31.568
56	31.0364
57	30.517
58	30.0092
59	29.5129
60	29.0278
61	28.5534
62	28.0895
63	27.6359
64	27.1922
65	26.7582
66	26.3337
67	25.9183
68	25.5118
69	25.114
70	24.7247
71	24.3437
72	23.9707
73	23.6054
74	23.2479
75	22.8977
76	22.5548
77	22.2189
78	21.8899
79	21.5676
80	21.2518
81	20.9424
82	20.6392
83	20.3421
84	20.0508
85	19.7654
86	19.4855
87	19.2111
88	18.9421
89	18.6783
90	18.4196
91	18.1659
92	17.917
93	17.6729
94	17.4334
95	17.1984
96	16.9679
97	16.7416
98	16.5196
99	16.3016
100	16.0877
101	15.8778
102	15.6716
103	15.4692
104	15.2705
105	15.0754
106	14.8837
107	14.6955
108	14.5107
109	14.3291
110	14.1507
111	13.9754
112	13.8032
113	13.6341
114	13.4678
115	13.3044
116	13.1438
117	12.986
118	12.8308
119	12.6783
120	12.5284
121	12.3809
122	12.236
123	12.0935
124	11.9533
125	11.8154
126	11.6798
127	11.5465
128	11.4153
129	11.2862
130	11.1593
131	11.0343
132	10.9114
133	10.7905
134	10.6714
135	10.5543
136	10.439
137	10.3255
138	10.2138
139	10.1038
140	9.9956
141	9.889
142	9.7841
143	9.6807
144	9.579
145	9.4788
146	9.3801
147	9.2829
148	9.1872
149	9.0929
150	9
151	8.9085
152	8.8183
153	8.7295
154	8.642
155	8.5557
156	8.4708
157	8.387
158	8.3045
159	8.2231
160	8.1429
161	8.0639
162	7.986
163	7.9092
164	7.8334
165	7.7588
166	7.6852
167	7.6126
168	7.541
169	7.4704
170	7.4008

Table 2.9 : Resistance Vs Temperature Data for the Composition $Ni_{0.9}Mn_{2.1}O_4$ (TA3)

Temp. °C	Resistance KΩ
27	44.9845
28	44.112
29	43.2621
30	42.434
31	41.627
32	40.8405
33	40.0739
34	39.3265
35	38.5978
36	37.8871
37	37.194
38	36.5179
39	35.8583
40	35.2147
41	34.5867
42	33.9737
43	33.3754
44	32.7913
45	32.221
46	31.6641
47	31.1202
48	30.589
49	30.07
50	29.5629
51	29.0675
52	28.5834
53	28.1102
54	27.6476
55	27.1954
56	26.7533
57	26.321
58	25.8982
59	25.4847
60	25.0803
61	24.6846
62	24.2974
63	23.9186
64	23.5479
65	23.1851
66	22.8299
67	22.4822
68	22.1418
69	21.8086
70	21.4822
71	21.1626
72	20.8495
73	20.5428
74	20.2424
75	19.9481
76	19.6597
77	19.377
78	19.1
79	18.8285
80	18.5624
81	18.3015
82	18.0457
83	17.7949
84	17.5489
85	17.3077
86	17.0712
87	16.8391
88	16.6115
89	16.3881
90	16.169
91	15.954
92	15.743
93	15.5359
94	15.3327
95	15.1332
96	14.9373
97	14.745
98	14.5562
99	14.3709
100	14.1888
101	14.01
102	13.8344
103	13.662
104	13.4925
105	13.3261
106	13.1626
107	13.0019
108	12.844
109	12.6888
110	12.5363
111	12.3865
112	12.2391
113	12.0943
114	11.9519
115	11.812
116	11.6743
117	11.539
118	11.4059
119	11.275
120	11.1463
121	11.0197
122	10.8951
123	10.7726
124	10.6521
125	10.5335
126	10.4168
127	10.302
128	10.189
129	10.0778
130	9.9683
131	9.8606
132	9.7546
133	9.6502
134	9.5474
135	9.4463
136	9.3467
137	9.2486
138	9.152
139	9.0569
140	8.9632
141	8.8709
142	8.7801
143	8.6906
144	8.6024
145	8.5155
146	8.4299
147	8.3456
148	8.2625
149	8.1807
150	8.1
151	8.0205
152	7.9421
153	7.8649
154	7.7888
155	7.7138
156	7.6398
157	7.5669
158	7.495
159	7.4241
160	7.3542
161	7.2853
162	7.2174
163	7.1504
164	7.0843
165	7.0191
166	6.9548
167	6.8914
168	6.8289
169	6.7672
170	6.7063

Table 2.10 : Resistance Vs Temperature Data for the Composition $Ni_{0.75}Mn_{2.25}O_4$ (TA6)

Temp. °C	Resistance KΩ
27	32.0228
28	31.4556
29	30.9022
30	30.362
31	29.8347
32	29.3199
33	28.8173
34	28.3265
35	27.8472
36	27.379
37	26.9216
38	26.4747
39	26.0381
40	25.6113
41	25.1942
42	24.7865
43	24.3879
44	23.9981
45	23.617
46	23.2443
47	22.8797
48	22.523
49	22.1741
50	21.8327
51	21.4986
52	21.1716
53	20.8516
54	20.5383
55	20.2316
56	19.9313
57	19.6372
58	19.3492
59	19.0671
60	18.7908
61	18.5201
62	18.2549
63	17.995
64	17.7403
65	17.4908
66	17.2461
67	17.0063
68	16.7712
69	16.5407
70	16.3147
71	16.0931
72	15.8757
73	15.6625
74	15.4534
75	15.2482
76	15.0469
77	14.8494
78	14.6556
79	14.4654
80	14.2788
81	14.0955
82	13.9157
83	13.7391
84	13.5657
85	13.3955
86	13.2283
87	13.0641
88	12.9029
89	12.7445
90	12.5889
91	12.4361
92	12.2859
93	12.1384
94	11.9934
95	11.8509
96	11.7109
97	11.5733
98	11.438
99	11.305
100	11.1743
101	11.0457
102	10.9193
103	10.7951
104	10.6728
105	10.5526
106	10.4344
107	10.3181
108	10.2037
109	10.0912
110	9.9805
111	9.8716
112	9.7644
113	9.6589
114	9.5551
115	9.4529
116	9.3524
117	9.2534
118	9.156
119	9.0601
120	8.9656
121	8.8727
122	8.7811
123	8.691
124	8.6022
125	8.5148
126	8.4287
127	8.3438
128	8.2603
129	8.178
130	8.0969
131	8.0171
132	7.9384
133	7.8608
134	7.7844
135	7.7091
136	7.6349
137	7.5617
138	7.4897
139	7.4186
140	7.3486
141	7.2795
142	7.2114
143	7.1443
144	7.0782
145	7.0129
146	6.9486
147	6.8851
148	6.8226
149	6.7609
150	6.7
151	6.64
152	6.5808
153	6.5223
154	6.4647
155	6.4079
156	6.3518
157	6.2964
158	6.2418
159	6.188
160	6.1348
161	6.0823
162	6.0305
163	5.9794
164	5.929
165	5.8792
166	5.83
167	5.7815
168	5.7336
169	5.6863
170	5.6397

Table 2.11: Resistance Vs Temperature Data for the Composition $Ni_{0.55}Mn_{2.45}O_4$ (TA10)

Temp. °C	Resistance KΩ
27	15.4489
28	15.2403
29	15.0359
30	14.8355
31	14.6391
32	14.4466
33	14.2578
34	14.0727
35	13.8912
36	13.7132
37	13.5386
38	13.3673
39	13.1992
40	13.0343
41	12.8726
42	12.7138
43	12.5579
44	12.405
45	12.2548
46	12.1074
47	11.9627
48	11.8206
49	11.681
50	11.544
51	11.4093
52	11.2771
53	11.1472
54	11.0196
55	10.8941
56	10.7709
57	10.6498
58	10.5308
59	10.4138
60	10.2988
61	10.1857
62	10.0746
63	9.9653
64	9.8579
65	9.7522
66	9.6482
67	9.546
68	9.4455
69	9.3466
70	9.2493
71	9.1535
72	9.0593
73	8.9666
74	8.8754
75	8.7856
76	8.6973
77	8.6103
78	8.5247
79	8.4404
80	8.3574
81	8.2757
82	8.1952
83	8.116
84	8.038
85	7.9611
86	7.8855
87	7.8109
88	7.7375
89	7.6651
90	7.5938
91	7.5236
92	7.4544
93	7.3862
94	7.319
95	7.2528
96	7.1875
97	7.1231
98	7.0597
99	6.9972
100	6.9355
101	6.8748
102	6.8148
103	6.7558
104	6.6975
105	6.64
106	6.5834
107	6.5275
108	6.4724
109	6.418
110	6.3644
111	6.3115
112	6.2593
113	6.2078
114	6.1569
115	6.1068
116	6.0573
117	6.0085
118	5.9603
119	5.9128
120	5.8658
121	5.8195
122	5.7738
123	5.7286
124	5.6841
125	5.6401
126	5.5966
127	5.5537
128	5.5114
129	5.4696
130	5.4283
131	5.3875
132	5.3472
133	5.3074
134	5.2681
135	5.2293
136	5.191
137	5.1531
138	5.1157
139	5.0787
140	5.0422
141	5.0061
142	4.9705
143	4.9353
144	4.9005
145	4.8661
146	4.8321
147	4.7985
148	4.7653
149	4.7324
150	4.7
151	4.6679
152	4.6362
153	4.6049
154	4.5739
155	4.5433
156	4.513
157	4.4831
158	4.4535
159	4.4242
160	4.3952
161	4.3666
162	4.3383
163	4.3103
164	4.2826
165	4.2552
166	4.2281
167	4.2014
168	4.1749
169	4.1486
170	4.1227

Table 2.12 : Resistance Vs Temperature data for the Composition $Ni_{0.4}Mn_{2.6}O_4$ (TA13)

Temp. °C	Resistance KΩ
27	5.8641
28	5.7312
29	5.6022
30	5.4769
31	5.3552
32	5.237
33	5.1222
34	5.0105
35	4.9021
36	4.7966
37	4.6941
38	4.5944
39	4.4974
40	4.4031
41	4.3113
42	4.2221
43	4.1352
44	4.0506
45	3.9683
46	3.8881
47	3.8101
48	3.7341
49	3.6601
50	3.588
51	3.5177
52	3.4492
53	3.3825
54	3.3174
55	3.254
56	3.1922
57	3.1319
58	3.0731
59	3.0158
60	2.9599
61	2.9053
62	2.852
63	2.8001
64	2.7494
65	2.6998
66	2.6515
67	2.6043
68	2.5582
69	2.5132
70	2.4693
71	2.4263
72	2.3844
73	2.3434
74	2.3033
75	2.2642
76	2.2259
77	2.1885
78	2.152
79	2.1162
80	2.0812
81	2.047
82	2.0136
83	1.9809
84	1.9489
85	1.9176
86	1.8869
87	1.857
88	1.8276
89	1.7989
90	1.7708
91	1.7433
92	1.7163
93	1.6899
94	1.6641
95	1.6388
96	1.614
97	1.5897
98	1.5659
99	1.5426
100	1.5197
101	1.4974
102	1.4754
103	1.4539
104	1.4328
105	1.4122
106	1.3919
107	1.372
108	1.3526
109	1.3335
110	1.3147
111	1.2964
112	1.2783
113	1.2606
114	1.2433
115	1.2263
116	1.2096
117	1.1932
118	1.1771
119	1.1613
120	1.1458
121	1.1306
122	1.1156
123	1.101
124	1.0866
125	1.0724
126	1.0585
127	1.0449
128	1.0315
129	1.0183
130	1.0054
131	0.9927
132	0.9802
133	0.968
134	0.9559
135	0.9441
136	0.9324
137	0.921
138	0.9097
139	0.8987
140	0.8878
141	0.8771
142	0.8666
143	0.8563
144	0.8461
145	0.8361
146	0.8263
147	0.8167
148	0.8072
149	0.7978
150	0.7886
151	0.7795
152	0.7706
153	0.7619
154	0.7533
155	0.7448
156	0.7364
157	0.7282
158	0.7201
159	0.7122
160	0.7043
161	0.6966
162	0.689
163	0.6815
164	0.6742
165	0.6669
166	0.6598
167	0.6527
168	0.6458
169	0.639
170	0.6323

Table 2.13 : Change in Room Temperature Resistance of the Thermistors with Nickel Content (%)

Sample Id	Nickel Content (%)	Room Temperature Resistance in KΩ
TA1	1	55.4030
TA2	0.95	51.228
TA3	0.9	46.80
TA4	0.85	42.3811
TA5	0.8	37.8001
TA6	0.75	33.2543
TA7	0.7	28.9089
TA8	0.65	24.0765
TA9	0.6	20.386
TA10	0.55	15.879
TA11	0.5	11.2512
TA12	0.45	9.882
TA13	0.4	6.142

2.9.7 Calculation of β and resistance ratio :

The thermistors can be accurately specified interms of β value over a limited temperature span.

For a thermistor resistance R1 at temperature T1 is expressed as

$$R1 = A \exp (ß/ T1) \text{ ---------- } (2.3)$$

The resistance R2 at temperature T2 can be given as

$$R2 = A \exp ((ß/ T2) \text{ ---------- } (2.4)$$

Taking the ratio: $R1 / R2 = \exp (ß(1/ T1 - 1/ T2))$

$$\beta = \frac{1}{(1/T1 - 1/T2)} \times \ln (R1/R2) \text{ ---------- } (2.5)$$

A program has been developed for calculation of β by dividing their measurement range into five equal segments and taking average for the

thermistors developed (TA1-TA13) by oxalic precursor route. The listing and the results are summarised as follows:

```
************************************************
REM PROGRAM
REM PROGRAM FOR CALCULATION OF BETA
REM OVER A INTERVAL OF 50 DEGREE CENTIGRADES.
INPUT "ENTER SAMPLE NUMBER"; S
INPUT "RESISTANCE AT 25oc"; R25
INPUT "RESISTANCE AT 50oC"; R50
INPUT "RESISTANCE AT 75oC"; R75
INPUT "RESISTANCE AT 100oC"; R100
INPUT "RESISTANCE AT 150oC"; R150
B1 = 2.303 * ((348.15 * 298.15) / (348.15 - 298.15)) * LOG(R25 / R75)
B2 = 2.303 * ((373.15 * 323.15) / (373.15 - 298.15)) * LOG(R50 / R100)
B3 = 2.303 * ((423.15 * 373.15) / (423.15 - 373.15)) * LOG(R100 / R150)
B4 = (1 / ((1 / 298.15) - (1 / 348.15))) * LOG(R25 / R75)
B5 = (1 / ((1 / 323.15) - (1 / 373.15))) * LOG(R50 / R100)
B6 = (1 / ((1 / 373.15) - (1 / 423.15))) * LOG(R100 / R150)
T1 = B1 - B2
T2 = B2 - B3
T = ((T1 + T2) / 2) / 100
B = (B4 + B5 + B6) / 3
PRINT "SAMPLE", S, "BETA", B, "TOLERANCE +/-"; T; "%"
END
************************************************
```

Table 2.14: Beta values and tolerances for thermistors

Composition	Beta Value	Beta Tolerance	Resistance Ratio
$NiMn_2O_4$	1834.253	4.150391E-05	4.688796
$Ni_{0.95}Mn_{2.05}O_4$	1788.887	0.0003125	4.513001
$Ni_{0.9}Mn_{2.1}O_4$	1770.32	1.489258E-04	4.442968
$Ni_{0.85}Mn_{2.15}O_4$	1745.971	3.051758E-05	4.352747
$Ni_{0.8}Mn_{2.2}O_4$	1687.77	4.260254E-04	4.144464
$Ni_{0.75}Mn_{2.25}O_4$	1615.319	1.489258E-04	3.899033
$Ni_{0.7}Mn_{2.3}O_4$	1565.041	2.062988E-04	3.737414
$Ni_{0.65}Mn_{2.35}O_4$	1450.028	5.004883E-05	3.392298
$Ni_{0.6}Mn_{2.4}O_4$	1368.035	0.6764856	3.197052
$Ni_{0.55}Mn_{2.45}O_4$	1228.739	9.399414E-04	2.815376
$Ni_{0.5}Mn_{2.5}O_4$	989.6518	3.173828E-05	2.30179
$Ni_{0.45}Mn_{2.55}O_4$	940.8755	6.738281E-04	2.209107

2.9.8 Verification of Steinhart-hart equation:

A common method to characterise a thermistor is to use the Steinhart-Hart equation:

$$1/T = A + [B * \ln(R)] + [C * \ln(R)^3] \text{ ---------- } (2.6)$$

Where:

T = Degrees Kelvin

R = Resistance

A,B,C = Curve-fitting constants.

The parameters are typically measured at three data points; min(A), middle(B), and max(C) and then the three simultaneous equations for A, B, and C are solved. A program listing in QBASIC for verification the equation is as follows :

********** Listing starts here **********

```
REM Program to verify Steinhart-hart equation
REM T is expressed in Kelvin.
REM Least squares fit program to find the thermistor coefficients
REM C1 and C2 in the following equation:
REM 1/T = C1 + C2 * (ln R)
REM Variables:
REM T[i], R[i] temperature and resistance data values.
REM Y[i] = 1/T[i] the dependent variable (depends on R[i])
REM in the Steinhart - Hart equation (above).
REM X[i] = ln(R[I]) the value of the ith function of the independent
REM variable ln(R) (natural log of resistance)
DEFDBL A-Z
DEFINT I, J, K, L
DIM R[400], T[400], Y[400], X[400]
C[3]=0
PRINT "What is the data file name"; : INPUT D$
OPEN "i", 1, D$
REM **** read and echo T(i), R(i) from the data file ****
REM (terminate read on R=-1)
I=0
PRINT "Data:"
G$="Point Temperature (Celsius) Resistance (ohms)"
```

```
        H$=" ### #####.## ########.##"
        PRINT G$
        PRINT
JMP1:I=I+1
        INPUT #1, T(I), R(I)
         IF R(I)<0 THEN GOTO JMP
        X(I)=LOG(R(I)) : Y(I)=1/(T(I)+273.15)
        PRINT USING H$; I, T(I), R(I)
        GOTO 1130
JMP: N=I-1
        CLOSE
        REM **** accumulate sums ****
        SX=0 : SY=0 : SXY=0 : SXX=0
        FOR I = 1 TO N
        SX=SX+X(I)
        SY=SY+Y(I)
        SXY=SXY+X(I)*Y(I)
        SXX=SXX+X(I)*X(I)
        NEXT I
        REM **** print out results ****
        C[2]=(N*SXY-SX*SY)/(N*SXX-SX*SX)
        C[1] = (SY-C[2]*SX)/N
        PRINT
        G$="Key in: C1 C2"
        P$=" #.## #.##"
        PRINT G$
        PRINT USING P$; C[1]*1000!, C[2]*10000!
        C1=INT(C[1]*1000000!)/1000000!
        C2=INT(C[2]*1E+07)/1E+07
        PRINT
        PRINT " T T T"
        PRINT " R ACTUAL CALC ERROR"
        PRINT " ======== ========= ========== ========="
        P$= " ######## ####.## ####.## ####.##"
        FOR L=1 TO N
        X=LOG(R(L))
        TCALC=1/(C1+C2*X)-273.15
        PRINT USING P$;R(L),T(L),TCALC,T(L)-TCALC
        NEXT L
```

********** Listings Ends here **********

The thermistor table of sample TA10 was passed to the above program and the results are compared as follows:

Table 2.15: Verification of Steinhart-Hart Equation

Input Data File Passed to Program		Output Data File Generated by Program	
25	15.879	25	15.88
30	14.8355	30	14.84
35	13.8912	35	13.89
40	13.0343	40	13.03
45	12.2548	45	12.25
50	11.544	50	11.54
55	10.8941	55	10.89
60	10.2988	60	10.30
65	9.7522	65	9.75
70	9.2493	70	9.25
75	8.7856	75	8.79
80	8.3574	80	8.36
85	7.9611	85	7.96
90	7.5938	90	7.59
95	7.2528	95	7.25
100	6.9355	100	6.94
105	6.64	105	6.64
110	6.3644	110	6.36
115	6.1068	115	6.11
120	5.8658	120	5.87
125	5.6401	125	5.64
130	5.4283	130	5.43
135	5.2293	135	5.23
140	5.0422	140	5.04
145	4.8661	145	4.87
150	4.7	150	4.70
0	-1		

Program in C++ for Calculation of β and its tolerance:

```
# include <stdio.h>
# include <string.h>

/* Program for calculation of Beta over an interval of 50 degree
centigrades*/

int main (void)

{
   float R25, R50, R75, R100, R150, B1, B2, B3, B4, B5, B6, T1, T2, T, B;
   Cout << "Enter Sample Number" << endl;
   Cin >> S;
   Cout << "Resistance at 25 Degree" << endl;
   Cin >> R25;
   Cout << "Resistance at 50 Degree" << endl;
   Cin >> R50;
   Cout << "Resistance at 75 Degree" << endl;
   Cin >> R75;
   Cout << "Resistance at 100 Degree" << endl;
   Cin >> R100;
   Cout << "Resistance at 150 Degree" << endl;
   Cin >> R150;

   B1 = 2.303 * (( 348.75 * 298.15) / (348.15 - 298.15 )) * log10 (R25/R75);
   B2 = 2.303*(( 373.15 * 323.15) / (373.15 - 323.15 ) * log10 ( R50/R100);
   B3 = 2.303*((423.15 * 373.15) / (423.15 - 373.15)) * log10 (R100/R125);
   B4 = (1/((1/298.15)-(1/348.15)))*log10 (R25/R75);
   B5 = (1/((1/323.15)-(1/373.15)))*log10 (R50/R100);
   B6 = (1/((1/373.15)-(1/423.15)))*log10 (R100/R150);
   T1 = B1 - B2;
   T2 = B2 - B3;

   T = (( T1 + T2)/2)/100;
   B = (B4+B5+B6)/3;
   Cin << "sample" << " " << S << " " << "BETA" << " " << B << " " <<
   "Tolerance" << " " << T << endl;
}
```

Program in C++ for Verification of Steinhart-hart equation:

```
********** PROGRAM LISTING STARTS HERE **********
# include <fstream.h>
# include <stdio.h>
# include <string.h>
# include <iostream.h>

void main ()
{
    log R[400], T[400], Y[400], X[400];
    ifstream infile;
    infile . open ("data.dat");
        if (infile.fail ())
            { cout << "Error reading file" << endl;
              exit (1); }
        infile.getline (buffer,200); k=0;

        while (! Infile.eof ())
            { char stmp [2] [20];
              int qa =0;
              int len=0;

                  if (buffer ! = '\0')
                  {
                        for (int i=0; i <strlen (buffer); i++)
                          {  ch = buffer [I];
                             if (ch != '    ')
                                { stmp [qa] [len] = ch;
                                  len ++;  }
                             else
                                { stmp [qa] [len] = '\0';
                                  len = 0; qa++}
                          }
                  }
        T[K] = afoi (stmp [0]);
        R[K] = afoi (stmp [1]);

        infile.getline (buffer,200); K ++;
```

```
{
    infile.close ();
    int N=0;

        for (int i = 0; i < 400;  i ++)
          {
              if ( R[i] < 0)
                    N --;
                    break;
          }

              else
           {        X[i] = log10 (R[I]};
                    Y[i] = 1/ (T[i] + 273.15);
                    N++;
           }
}

SX = 0; SY = 0; SXY = 0; SXX = 0;

        for (i=0; i<N; i++)

        {       SX   = SX + X[i];
                SY   = SY + Y [i];
                SXY  = SXY + X[i] * Y[i];
                SXX  = SXX + x [i] * X[i];
        }

c[2] = [ N * SXY - SX * SY) / (N * SXX - SX * SY)];
c[1] = ( SY - c[2] * SX) /N);
c1   = ( c[1] * 1000000)/ 1000000);
c2   = ( c[2] * 1000000)/ 1000000);

        for [ int i =0; i < N; i++)
        {
                X= log10 (R[i]);
                TCALC = 1/ (c1 + c2 * x) - 273.15;

                cout << "Resistance" << "  " << "Temperature" << "  "
                     << "TCALC" << " " << T(L) - TCALC" <<
                     << " " << endl;
```

```
                    cout << " R[i] " << "  " << T[i] << "  " << TCALC << "  "
                        << T[i] - TCALC << "  " << endl;

                }
            }
}
```

********** PROGRAM LISTING ENDS HERE **********

Significance of β value:

As outlined in the previous section, a simple approximation for the relationship between Resistance and Temperature for an NTC thermistor assumes an exponential relationship between them. This approximation is based on simple curve fitting to experimental data and also on an intuitive feel for electrical behaviour of semiconductor devices.

The exponential approximation is a mathematical model that applies an equation that can be expressed in the form:

$RT = \exp(ß/T)$ ----------(2.6a)

Where:

RT is the Resistance in ohms at temperature T

T is the absolute Temperature in Kelvin

A is a linear factor

"exp" is the exponential function

ß is the exponential factor known as "beta" value or sensitivity index of the thermistor material.

The ß value is a very important parameter in the description and specification of thermistor materials and thermistor components. When the natural log of both sides of the equation is taken, the relationship becomes:

$\ln(RT) = C + (ß/T)$ ----------(2.6b)

Where C is a constant factor, ($C = \ln(A)$) from the equation above.

If ln(RT) is plotted versus 1/T, then the slope of the resulting curve will be equal to beta, ß. This equation provides a reasonable approximation to measured data, but as mentioned in the previous section, the thermistor materials are not ideal materials. For the exponential model to apply over a large temperature range (greater than 50 °C) the beta value has to vary, therefore the beta value is not constant over extensive ranges. In fact, the beta value is also temperature dependent and it decreases with temperature.

Although this simple exponential model for the relationship between Resistance and Temperature of a thermistor is limited over large temperature spans, concepts derived from it are of importance in the thermistor industry and in the specification of NTC thermistors. Some of these concepts are developed in the following sections with the intention of explaining some of the basic calculations and specifications used in the industry.

Practical application of the beta value:

It is common practice to specify thermistor materials in terms of beta value over a particular temperature span.

For a temperature T1 and thermistor resistance R1 at this temperature T1:

$R1 = A \exp (ß/ T1)$ ----------(2.6c)

For a temperature T2 and thermistor resistance R2 at this temperature T2:

$R2 = A \exp ((ß/ T2)$ ----------(2.6d)

Taking the ratio: $R1 / R2 = \exp(ß(1/ T1 - 1/ T2))$

The expression for ß then becomes:

$\beta = \{1/ (1/T1 - 1/T2)\} \times \{\ln (R1/R2)\}$ ----------(2.6e)

Where:

ß has units of temperature (Kelvin)

"ln" represents the natural logarithm (log base e)

inverse of the exponential function.

In this form, published beta values can be used to calculate resistance or temperature values when other items in the equation are known.

The beta value can then be regarded a quantitative value of thermistor materials that is assigned as a material constant and that indicates the relationship of material resistivity to temperature.

Because the beta value is an indication of the relationship between the resistivity of thermistor material and temperature, it can also be used to calculate alpha (a) value (temperature coefficient) for a thermistor made

from the same material. Recalling the definition of the alpha value as the percentage change in resistance per °C, given by equation (2.6f)

$\alpha = -(\beta / T^2) \times 100$ (% per °C) ----------(2.6f)

The beta value is a single expression that can be regarded as a material constant. It depends on basic material properties, and beta values derived from measurements provide an indication of general thermistor material quality.

Although deviations in beta value from nominal values affect the tolerance of thermistors and are indicative of material quality, such deviations are not widely published by thermistor manufacturers. Typically, manufacturers will list the nominal Beta Value only or will list the nominal Beta Value with a tolerance expressed in K.

β Values of the thermistors in this work:

The major achievement of the thermistors fabricated by us is their moderate β value with its minimal tolerance. The β values are in the range of 940 to 1834 with minimal tolerance ranging from ± 0.003% to ±0.009%.

Figure 2.6: Photograph showing various processing stages: from precursor to final product

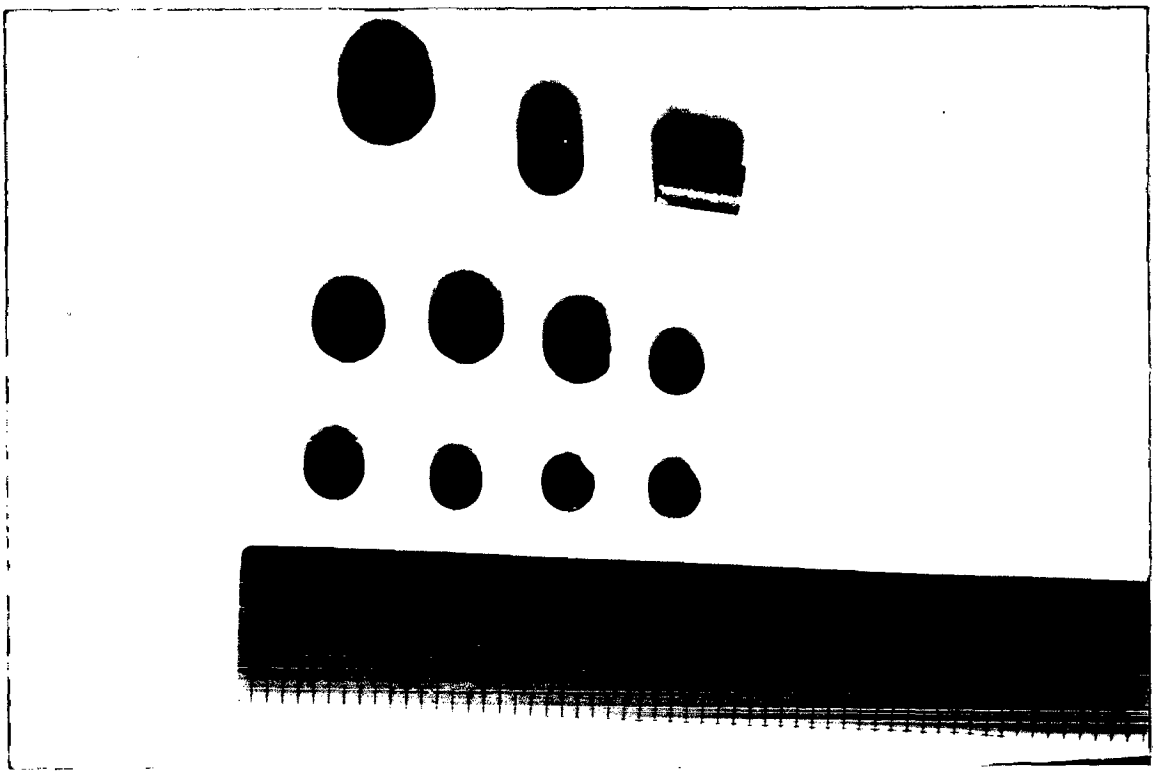

Figure 2.7: A Photograph of Thermistor Samples

2.10 Part III : Device Fabrication

The main challenges in the application of thermistor in critical electronic systems is their ageing, drift and interchangeability. All these shortcomings forces the users to calibrate or even tune the entire electronic system which is a costly and time consuming affair. This section presents an improved manufacturing set-up to fabricate thermistors. The thermistors fabricated with this set-up have exhibited significant reduction in ageing and less batch -to -batch tolerance.

2.10.1 Specifying Thermistor Tolerance :

There are two dominant factors that determine the resistance tolerance of thermistors. The first is the manufacturing tolerance in the NTC's nominal resistance. The second factor is the tolerance in the material constant β, which determines the variation of resistance with temperature. Manufacturers [135-138,1140-145] specify both above tolerances at the rated temperature. For example, DR/R_N = 3%, and Dβ/β = 0.5% at 25°C are representative for NTC thermistors used as temperature sensors in air conditioners[181]. When the tolerances for a thermistor are specified in this manner, the use of the equation

$$R_T = R_N e^{\beta\left(\frac{1}{T} - \frac{1}{T_N}\right)} \quad \text{----------(2.7)}$$

is implied. Two thermistors with very close resistance and β tolerances will track each other over a wide temperature range, and are called interchangeable.

2.10.2 Specifying Interchangeability or Curve Matching :

This is another measure of tolerance and is expressed as a temperature tolerance over a temperature range. For example, a value of ±0.1°C over a 0 - 70°C temperature range is typical for interchangeable disc NTC thermistors, and ±0.2°C over a 0-100°C range is typical for interchangeable chip NTC thermistors. Interchangeability gauges how close the resistance-temperature curves of two thermistors match. High interchangeability helps keep costs down since equipment does not need to be calibrated or adjusted for individual thermistors. Interchangeability is also a major advantage where NTC thermistors are used as cheap, disposable temperature probes, for example, in medical applications.

2.10.3 Thermistor fabrication with Lead Attachment :

In this section, we are presenting a novel technique of attaching leads to NTC thermistors. A batch of thermistors was fabricated with conventional lead attachment technique and the other with the new technique. The thermistors fabricated with the new technique were found to have better specifications than that of the conventional ones.

2.10.4 Conventional Method :

The presintered powder obtained by oxalic precursor route (described in Part- II) is used here. About 5 grams of the powder ($NiMn_2O_4$)

was put into a crucible (equally divided into three parts) and mixed with distilled water to make a heavy slurry. Three pairs of low resistivity nickel wires each of about 0.25mm diameter and 3 cm length were placed across an alumina combustion boat, each wire in the pair being separated by about 2mm. By means of a clean glass rod globules of the thermistor slurry were transferred on the crucible and placed across the lead wires to form thermistor beads. The boat of the thermistor beads was then placed in a furnace and fired at about 1060°C for six hours. The furnace was switched off and the samples were allowed to cool down to room temperature. Each thermistor bead was mounted on a piece of teflon sheet using two connecting screws in order not to disturb the thermistor lead contacts when making electrical connections. The entire process is shown in the figure 2.8 given below.

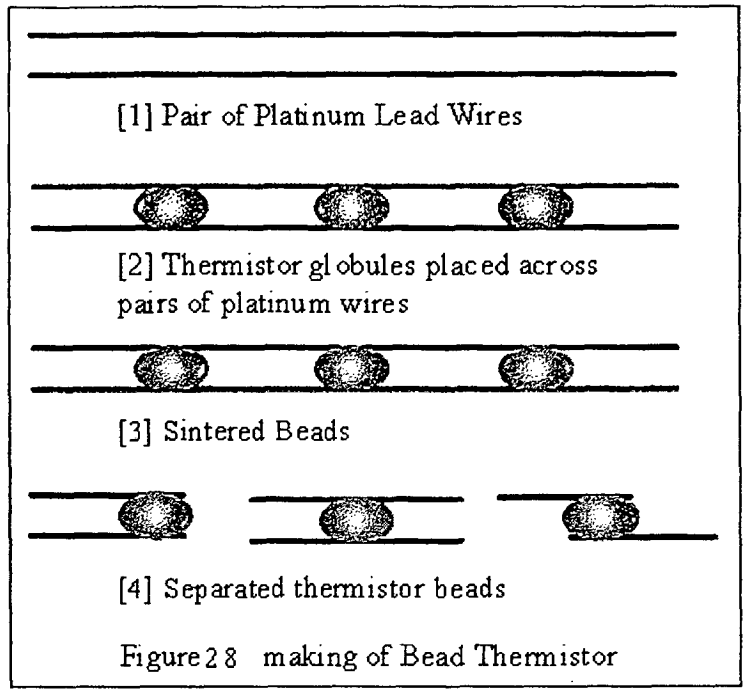

Figure 2 8 making of Bead Thermistor

It is required to check, whether the Nickel-thermistor contact is "Ohmic" (i.e. nonrectifying) and without voltage dependence. The linear current Vs voltage characteristics ensured that the semiconductor zone adjacent to the contacting metal has no carrier depletion zone and are Ohmic in nature.

The three samples were also tested for interchangeability, reproducibility and ageing by using an automated set-up described in Chapter 3. Results are shown below in the form of graphs: Although all the sample were made up of the same dimensions, composition and same amount of precursor, they showed tolerance in resistance-temperature characteristics as given in table 2.16.

Table 2.16: Interchangeability of thermistor samples by conventional method.

Temperature °C	Sample1 Resistance KΩ	Sample 2 Resistance KΩ	Sample 3 Resistance KΩ
25	54.7000	55.3321	52.3010
30	49.6759	50.5598	46.7898
35	45.0129	46.1160	42.0301
40	40.7585	42.0357	37.9096
45	36.9245	38.3274	34.3331
50	33.5000	34.9823	31.2200
55	30.4607	31.9810	28.5021
60	27.7750	29.2983	26.1221
65	25.4089	26.9063	24.0314
70	23.3281	24.7767	22.1893
75	21.5000	22.8822	20.5611
80	19.8946	21.1970	19.1177
85	18.4847	19.6977	17.8342
90	17.2461	18.3628	16.6896
95	16.1574	17.1732	15.6660
100	15.2000	16.1121	14.7480

The reasons attributed to the tolerance are poor control on the geometry, varying electrode shape and lead wire attachments from sample to sample . Ageing tests were also conducted on the thermistors fabricated by using the present method.

2.10.5 A Novel Method of thermistor Fabrication :

As described in the above at 2.15, the thermistors manufactured by the conventional method exhibit a poor performance interms of interchangeability and ageing. The primary cause of ageing in a porous sample is the loss of oxygen during exposure to elevated temperature [124]. In order to achieve higher densities, the die was

modified as shown in photograph at figure 2.9. The lower ram has two drilled holes to facilitate the insertion of leads. Experiments were conducted with the same amount of precursor and with the same composition and sintering conditions used in the conventional lead attachment method. The results are summarised in table 2.16.

Table 2.17 : Interchangeability of thermistor samples by new method

Temperature °C	Sample 1 Resistance KΩ	Sample 2 Resistance KΩ	Sample 3 Resistance KΩ
25	55.4650	55.7650	55.1150
30	51.1302	51.4266	50.4810
35	46.8318	47.1278	46.1177
40	42.7346	43.0318	42.0907
45	38.9351	39.2337	38.4274
50	35.4800	35.7800	35.1300
55	32.3828	32.6837	32.1845
60	29.6355	29.9366	29.5680
65	27.2175	27.5186	27.2527
70	25.1021	25.4027	25.2095
75	23.2600	23.5600	23.4100
80	21.6621	21.9616	21.8270
85	20.2810	20.5800	20.4357
90	19.0915	19.3904	19.2137
95	18.0711	18.3703	18.1410
100	17.2000	17.5000	17.2000

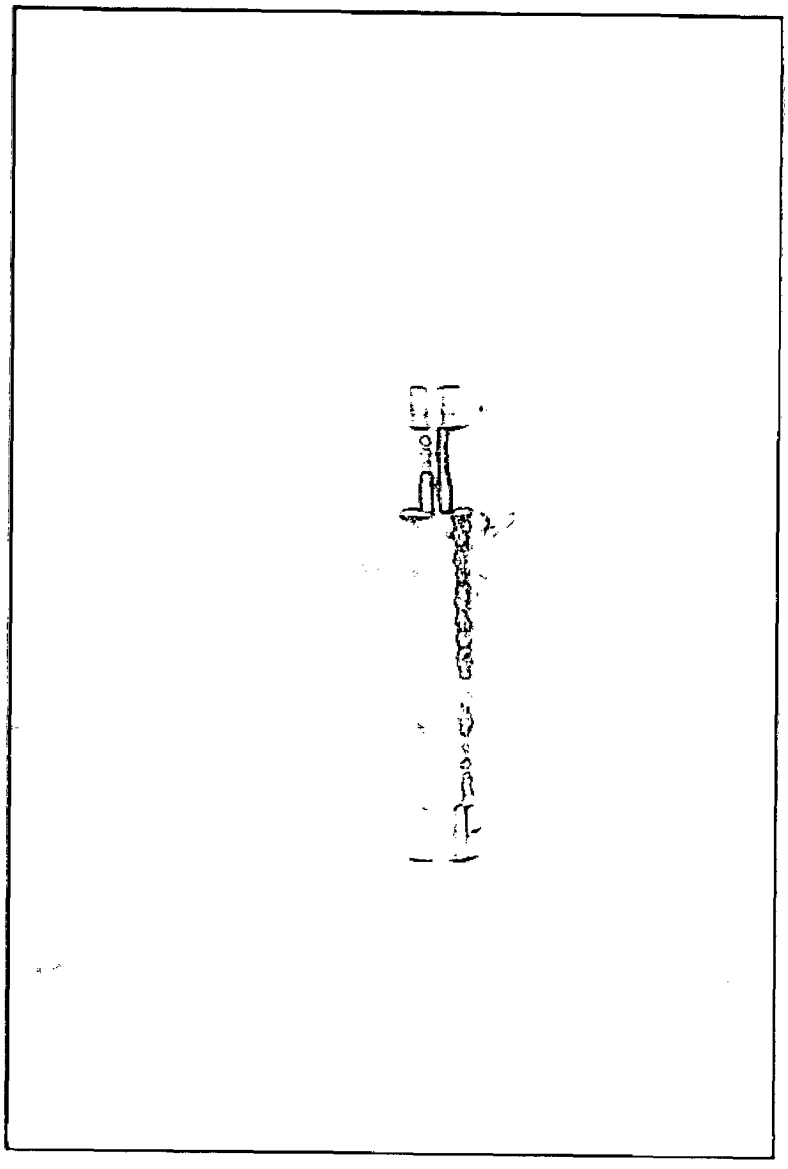

Figure 2.9 : Modified jig for thermistor manufacturing

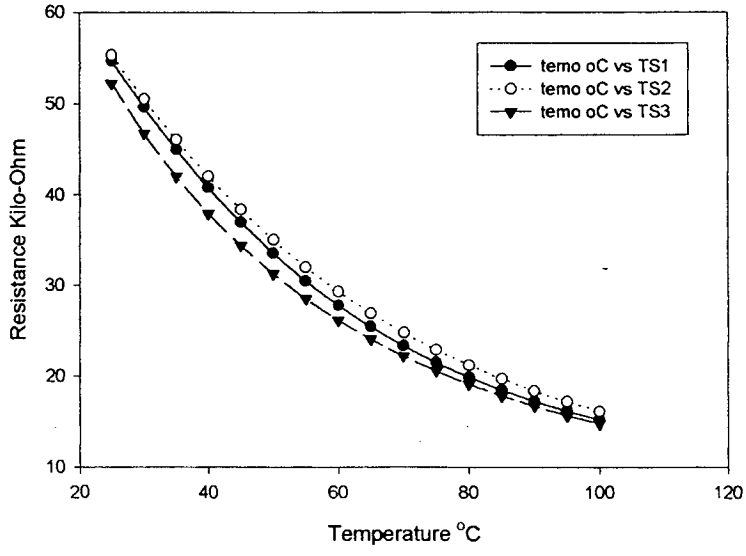

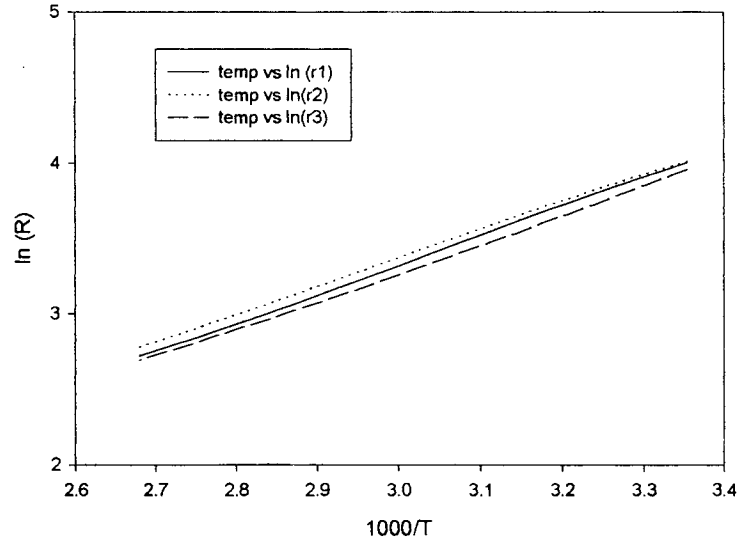

Figure 2.10 : Interchangeability of the thermistors fabricated by conventional lead attachment technique (Top graph Resistance Vs Temperature and bottom ln (R) Vs 1000/T)

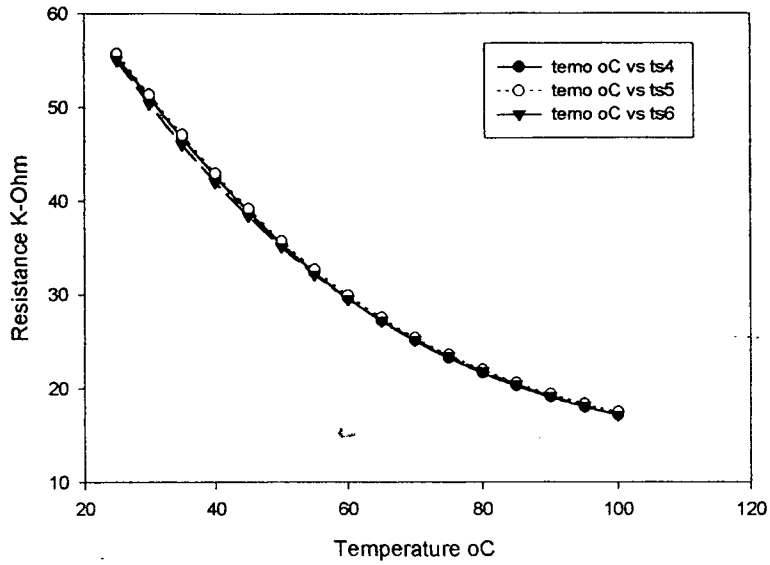

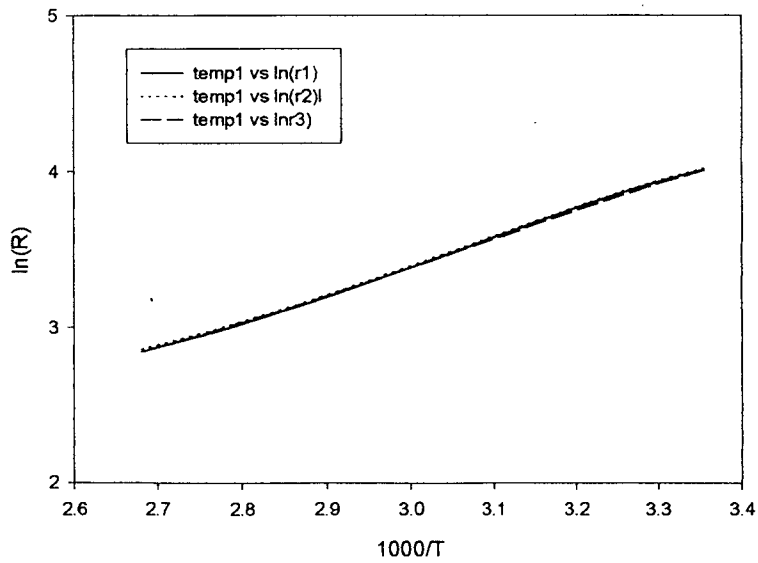

Figure 2.11 : Interchangeability of the thermistors fabricated by new lead attachment technique (Top graph Resistance Vs Temperature and bottom ln (R) Vs 1000/T)

CHAPTER 3

Instrumentation : Test and Characterisation

3.1 Introduction :

Chapter 2 presented the fabrication of nickel manganite based NTC thermistors. After making the device, it is essential to characterise it for finding the specifications. The Long Term Stability of thermistors is also an important issue in most of the temperature sensing applications. System designers are usually concerned with circuit development for thermistors with varied specifications which assure the end user an accurate, long-term measurement capability. It is extremely important therefore that the users should know the percentage drift of resistance versus temperature characteristics of the thermistors so that the readings can be corrected in digital environment. In addition to finding the technical specifications, customer needs to have an estimation of reliability. Reliability specifications are more important in thermistors because, in a batch, some of them are bound to follow the infant mortality due to manufacturing imperfections. It is better that the weak samples be detected at an early stage by using accelerated testing mechanism. Therefore, in order to facilitate the drawing up of specifications of the device and for quality assurance a proper characterisation of the thermistors is essential.

The three important specifications, zero-power resistance (Ro), time constant (T.C.), and dissipation constant (D.C.) influence the measured value of the resistance of a thermistor which will affect temperature values that are calculated from the resistance measurements. An understanding of these factors is critical in developing thermistor applications [23-27,33,

46-48,54] and in measurement of thermistors [59-60,78,95]. In order to calculate these specifications, it is essential to record the resistance Vs temperature, current Vs voltage and resistance Vs time characteristics of the thermistor.

A manual set-up to record the various characteristics is shown in the figure 3.1. However, some of the drawbacks associated with the manual set-up are lengthy characterisation process, possibility of damage of the sensor during characterisation, difficulty in analysing the data, plotting the graphs etc.

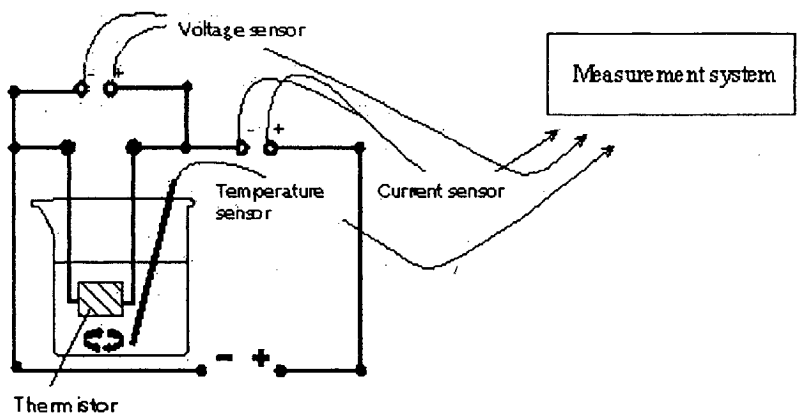

Figure 3.1: Manual setup for thermistor characterisation

By making the system fully automatic, all the drawbacks mentioned above can be eliminated. In addition to this PC characterises the device in compressed test time by employing techniques like accelerated testing. The sensor damage can be intelligently prevented by shutting down the system when found to consume more current. The data analysis also

becomes very easy with the help of packages like sigma plot, spss etc. The present chapter describes a fully automated PC based characterisation set-up for NTC thermistors.

3.2 Failure Mechanism in Thermistors :

The thermistors have found to follow the classical bathtub curve[129]. At the initial period if there is a manufacturing aberration or structural irregularity, the device fails. This period is called as infant mortality period. After the infant mortality period the behaviour of the thermistors becomes stable, any failure in this period is random in nature. In industrial applications of thermistors, failure occurs due to ageing (accelerated ageing due to excessive humidity, temperature etc.) and random failure due to transients and vibration. At very high temperature, the epoxy coating of the thermistor may be destroyed which forms a crack on its body. Lead corrosion occurs due to absorption of moisture which deteriorates its mechanical strength and changes the R Vs T characteristics.

The reliability of thermistors can be ensured through testing. The present chapter describes various test set-ups which includes different environmental stresses like temperature shock, moisture effects etc. Instrumentation systems are also developed to find out the time constant and dissipation constant of the thermistors.

3.3 PC based set-up for Thermistor Characterisation :

The block diagram of the PC based characterisation set-up is as shown in figure 3.2. It comprises of a high temperature furnace, OP-27 based instrumentation amplifier and ADC to monitor the temperature, and HP34401A DMM for resistance measurement. A RTD based analog ON-OFF controller is used for temperature controller of the furnace.

3.3.1 Furnace Design and Construction :

A fundamental feature of the computerised characterisation set-up is a high temperature tubular furnace controlled through the computer to impart predetermined number of temperature cycles. The temperature range of interest is 1100°C for material synthesis and 400°C for characterisation. Kanthal (920-30% Cr, 50% Al rest Fe) which has a maximum safe operating temperature of 1350°C is used as a heating element. Resistivity of Kanthal is 140 μ Ohm-cm and does not change much with temperature. The diameter of the wire used is 21 gauge and has resistance specification of 0.808 Ω/ft. To produce a temperature of about 1000°C in a tubular furnace, it is sufficient if the same wire can produce about 200°C in a straight stretched wire. From the data sheets, the current required to maintain such a temperature in 21 gauge wire is 2.7 amp $\approx$ 3 A.

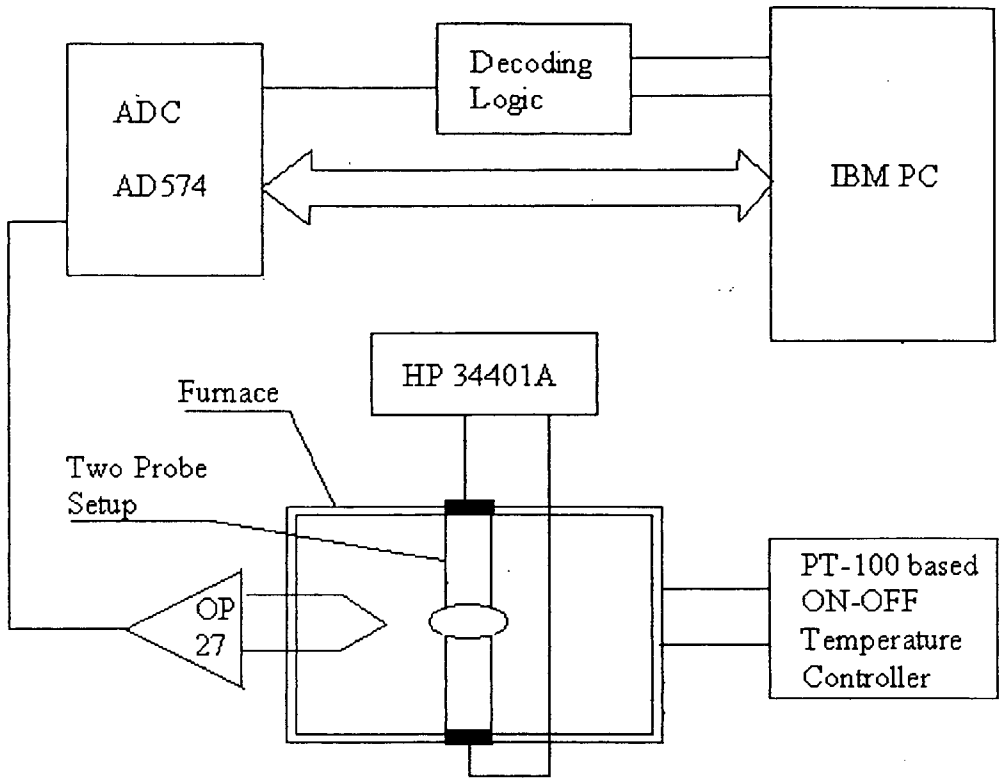

Figure 3.2: PC based Test and Characterisation setup

Therefore the resistance of the Kanthal element to be wound for 230 Volts A.C. mains operation of the furnace is

$$230 / 3 \text{ Amp} \approx 80\ \Omega.$$

Therefore the length of the wire required for furnace construction is $80/0.808 \approx 100$ ft.

The power which would be dissipated in the furnace is

$$\text{power} = 3^2 \times 80 = 720 \text{ Watts.}$$

To facilitate the sudden changes of temperature, low temperature coefficient materials are used for the furnace construction. Translucent fused silica is a good material for furnace tube. To get uniform temperature

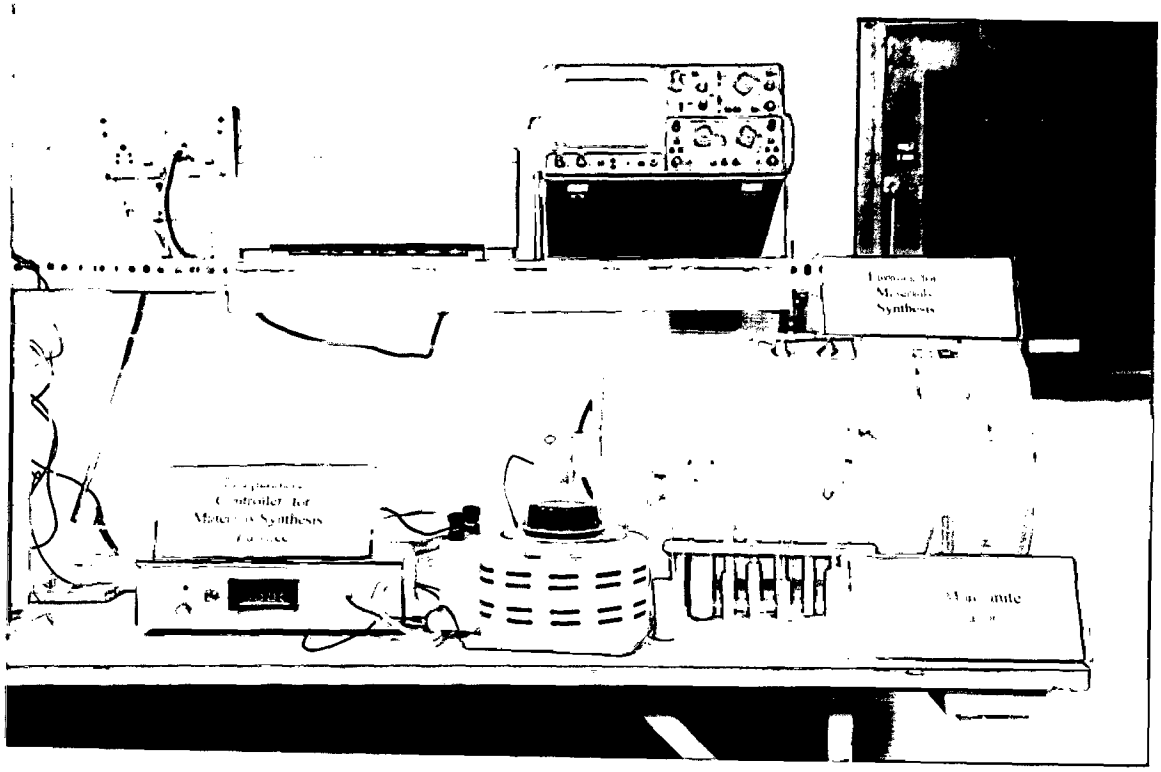

Figure 3.3 : Photograph of the furnace used for materials synthesis

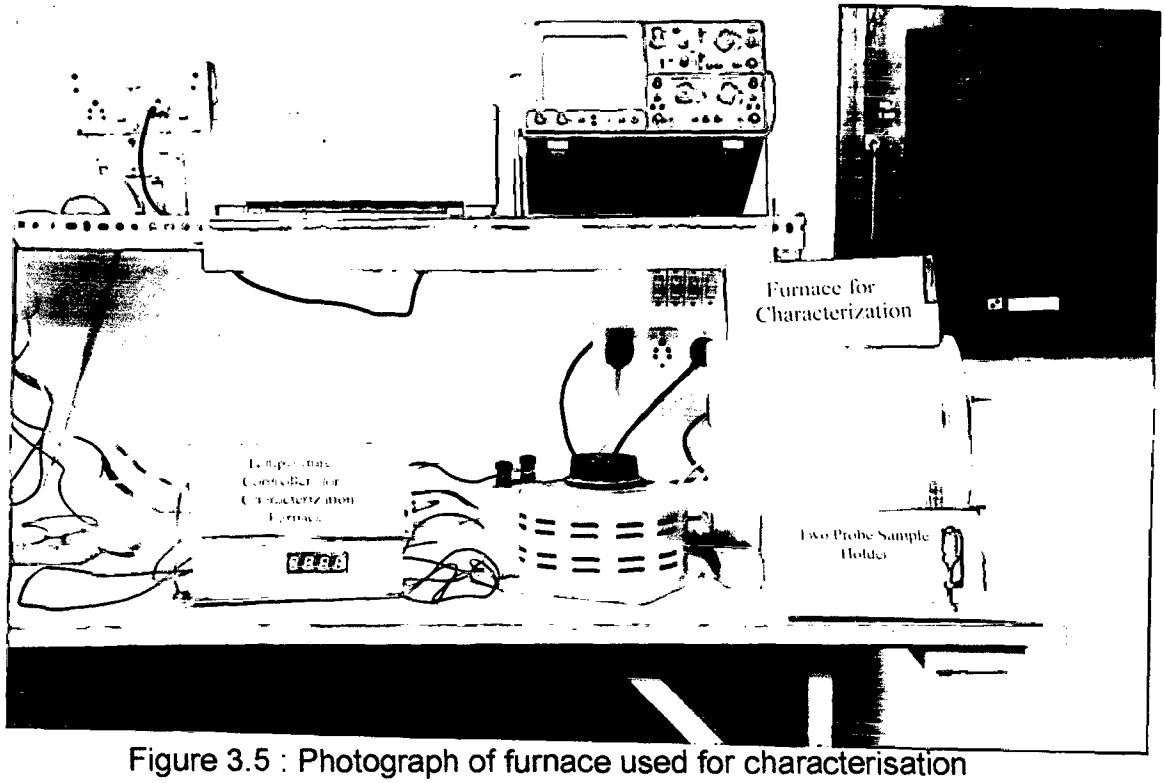

Figure 3.5 : Photograph of furnace used for characterisation

throughout the furnace, length was chosen to be 22". Length of the furnace tube is 21" and 1 ½ " inner diameter with a wall thickness 4 mm. The calculated length of the Kanthal element is wounded on the inner outer surface. For better grip a rough outer surface is preferred. To shield the heat being radiated to the outside, pads of silica wool are placed. A photograph of the furnace constructed is shown in figure 3.3.

3.3.2 Thermocouple based temperature controller :

The circuit diagram for a thermocouple based on-off controller for the above mentioned furnace is shown in the figure 3.4. First stage of the controller is a low drift, low noise, voltage amplifier which senses the thermocouple voltage. The gain of this stage is 40 dB and is constructed out of Op-Amp CA3140E (RCA). The second stage is a comparator constructed with Op-Amp LM-741. Instead of keeping this op-amp open loop, the gain is limited to 60 dB which avoids the jittering of the output. The comparator compares the voltage due to the thermocouple with a preset which corresponds to some required temperature. The two Zener diodes (6.2V) ensure voltage stability even if there are voltage fluctuations. The output of the comparator is given to a current SL100 transistor. A relay capable of handling 5 amp of current is connected in series with the collector of SL-100. The op-amps are configured in such a way that, when the thermocouple voltage due to the furnace temperature exceeds the set voltage, the relay will trip off and cut the supply to the furnace. The temperature controller gives control within $\pm$ 0.8°C. A 3 ½ LED digital panel

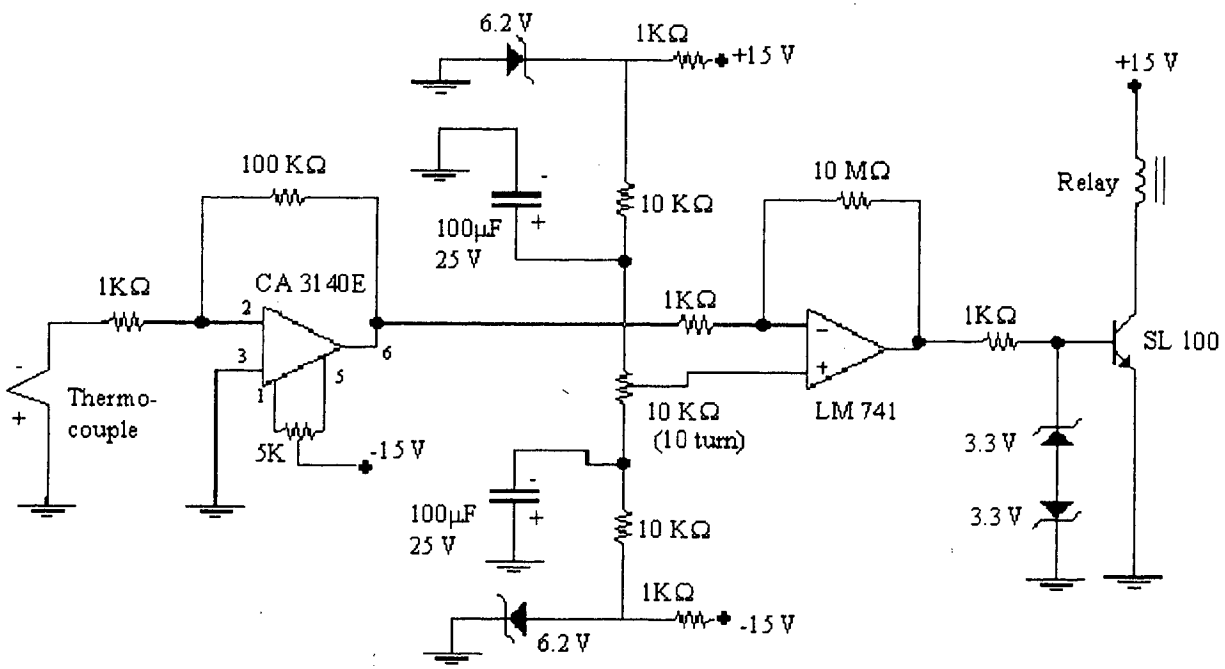

Figure 3.4: Circuit Diagram of Thermocouple based temperature controller.

meter 128/188 (along with ICL7107) is connected for displaying the temperature setpoint.

3.3.3 Furnace for Characterisation :

The furnace described shown in the photograph at figure 3.3 is only suited for material preparation and not for characterisation. Because during characterisation, precision measurements are of prime importance and any power frequency noise pick up can interfere with preamplifier signals. Therefore a d.c. powered furnace is essential for such measurements. Photograph of the furnace used for characterisation is shown in a photograph at figure 3.5.

3.3.4 D.C. High wattage Power Supply for Furnace :

A variable regulated power supply of rating 3 to 24 V, 3 A. has been constructed to power the furnace used for characterisation. The circuit diagram of the high wattage d.c. power supply is as shown in the figure 3.6. The regulated power supply can be adjusted from 3 to 25 volts and is current limited to 2 amps as shown, but may be increased to 3 amps by selecting a smaller current sense resistor (0.3 ohm). The 2N3055 and 2N3053 power transistors are mounted on the suitable heat sinks and the current sense resistor selected is rated at 3 watts or more. Voltage regulation is controlled by 1/2 of a 1458 op-amp. For op-amp. 1458 it is recommended that the supply voltage to pin 8 be limited to 30 VDC, which can be accomplished by adding a 6.2 volt Zener or 5.1 K resistor in series with pin 8. (The maximum DC supply voltage for the 1458 is 36 V.) The

power transformer is capable of supplying the desired current while maintaining an input voltage at least 4 volts higher than the desired output, but not exceeding the maximum supply voltage of the op-amp under minimal load conditions. The power transformer shown is a center tapped 25.2 volt AC with 4 amp current which will provide regulated outputs of 24 volts at 3 amps, 15 volts at 6 amps, or 6 volts at 6 amps. The 6 amp output is obtained using the center tap of the transformer with the switch in the 18 V position.

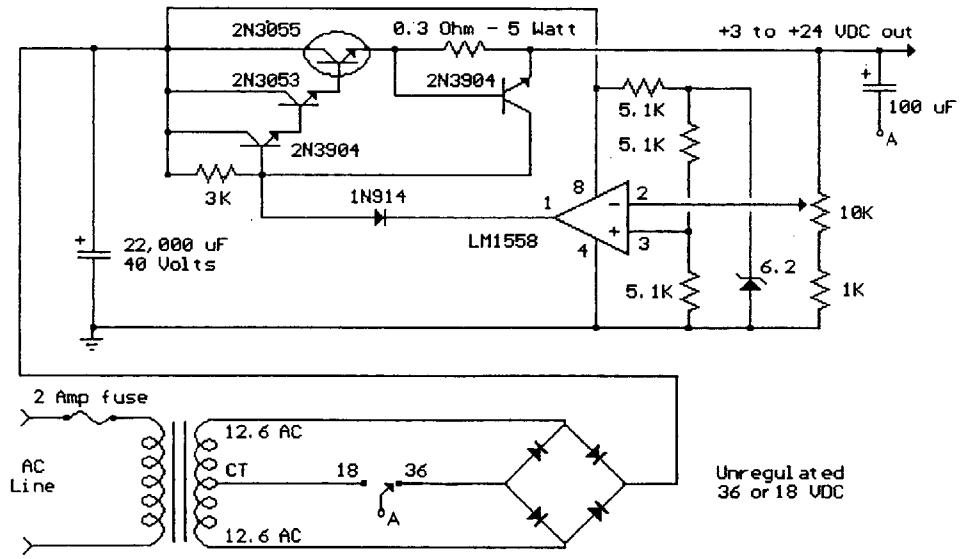

Figure 3.6 Circuit Diagram of high wattage d.c. power supply.

The 10K panel mounted potentiometer can be varied to get the suitable voltage/current as per the furnace heating requirement.

3.3.5 Temperature Controller for the d.c. powered Furnace :

A precision ON-OFF type temperature controller based on PT-100 is designed for controlling the temperature of the furnace. The controller has a variable set-point adjustment, so as to very the value of the temperature to be controlled. The circuit diagram is shown in figure 3.7. The design is as follows:

- Design of Bridge :

The bridge circuit for the sensor consists of constant current source to develop a voltage proportional to the change in resistance of PT100. Another current source of the same current value, biases a fixed resistance of 110Ω wire wound resistor to produce voltage. At 27°C (normal room temperature value) when RTD resistance is 110Ω, the bridge is balanced and the differential voltage V_{AB} is zero. As temperature increases the voltage V_{AB} also proportionately increases. PT100 has a resistance of 100Ω at 0°C and temperature coefficient of resistance α = 0.00392 Ω/°C.

- Constant Current Source Design :

Zener diode of breakdown voltage 6.2 Volts and a 470Ω resistor are chosen to keep the transistor base voltage constant at value 12-6.2V = 5.8 Volts.

Voltage at the emitter terminal of transistor = 5.8 + 0.6 = 6.4 Volts. Voltage drop across emitter resistor R_E = 5.6 Volts. The power dissipation constant for PT100 is 25 mW/°C. In order to avoid the self heating the current through the RTD is restricted below 2.5 mA.

Emitter resistance required for this Re = 5.6 / 2.5 mA $\approx$ 2.2 KΩ.

Using approximate equation for the change in resistance of RTD,

$$Rt = Ro (1 + \alpha \Delta T)$$

where Ro = 100 Ω for PT100 and α = 0.00392 $\Omega/^{\circ}C$

The lowest furnace temperature to be controlled is 27°C. Hence PT100 possess resistance,

$$R_{30^{\circ}C} = 100 [1 + 0.00392(27^{\circ}C)] = 110\Omega$$

The maximum temperature limit is 300°C.

$$R_{300^{\circ}C} = 100 [1 + 0.00392 (300^{\circ}C)] = 217\Omega$$

Therefore, the voltage V_A = Ic x 217 = 2.5 x 10^{-3} x 217= 0.542 V.

$$V_B = 2.5 \times 10^{-3} \times 110 = 0.275 \text{ V}$$

$$\Delta V = 0.26 \text{ V}$$

- Design of Bridge Amplifier :

The required output voltage Vo = 5Volts. Thus the gain for differential amplifier is

$\Delta V / \Delta Vin = 5/ 0.26 \approx 20$

The bridge amplifier is based instrumentation op-amp IC 725 which gives low noise with high input impedance.

Required gain of the Amplifier = Rf / R1 = 20 i.e. Rf = 20 x R1 = 238.1 K

The Ri is selected to be 10K, ¼ W. The Rf is 22K, 1/4W fixed resistor in series with 22 K multiturn potentiometer as shown in the circuit diagram.

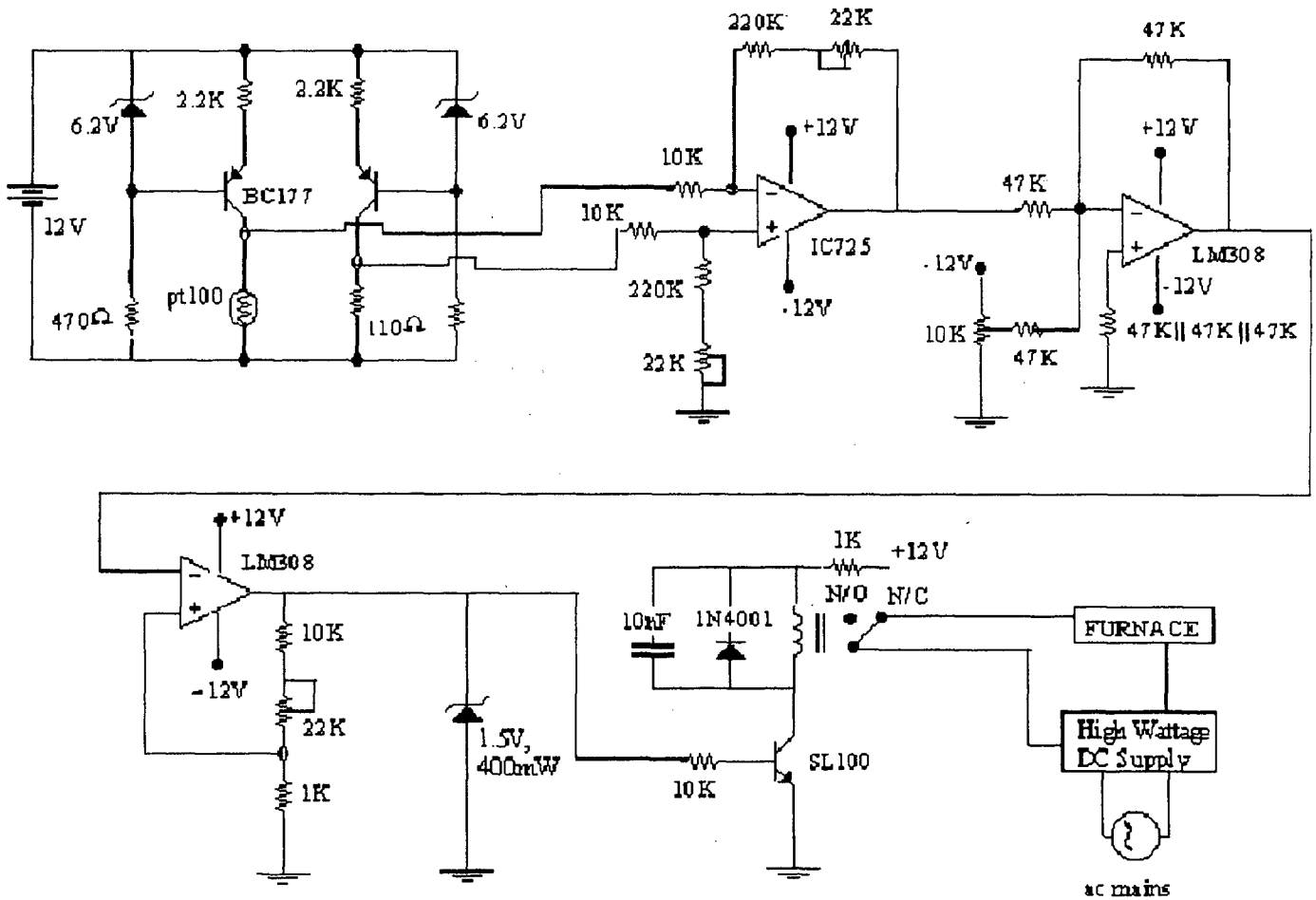

Figure 3.7: Circuit diagram of PT-100 based temperature controller

- Design of Error Amplifier :

To fix the setpoint, a multiturn potentiometer of 10K is selected. The input and feedback resistors are selected to be 47K. The offset compensating resistor R_{OM} should be a parallel combination of the three 47K resistors.

- Design of Schmitt Trigger :

The design of Schmitt Trigger depends on the total output swing required at the output which is ± 5 V = 10 Volts. Hystersis of 5% is introduced in the output,

i.e. (5/100) x 10 = ± 0.5 Volts.

i.e. ± 0.25 = ± βV

Where β = Ra / (Ra + Rb) and V = Vz = 5.1 Volts

Consider V = 5 Volts;

Now 0.25 = 5 x [Ra / (Ra + Rb)]

i.e. Rb = 19 Ra

Ra is chosen as 1K, ¼ W, then Rb = 19K. The resistor Rb is selected as a series combination of 10K, ¼ W fixed resistor and 22K multiturn potentiometer.

- Design of Relay Driver :

The transistor SL100 is used as a switch to turn on or off the dc power supply of the furnace. A resistor of 10 K is used to limit the base current and 1K resistor to limit the collector current of the transistor. The ac mains voltage is supplied to the heater through the normally closed

(N/C) terminal of the relay. When the relay is excited, it switches to normally open (N/O) terminal thus breaking ac supply to the heater.

A 3 ½ LED digital panel meter 128/188 (along with ICL7107) is connected for displaying the temperature setpoint

3.3.6 ADC Interface to PC :

The circuit diagram of the ADC interfaced to IBM PC is shown in the figure 3.8. A OP-27 based variable gain amplifier is used to amplify the thermocouple output. The OP-27 features low noise (80 nV Vpp , 0.1 Hz to 10 Hz), minimal drift (0.2 $\mu V/^{o}C$), high speed (slew rate: 2.8 $V/\mu S$, 8MHz Bandwidth), excellent CMRR (126 dB at Vcm OF $\pm 11V$), and high precision open loop gain (1.8 Million). A low input bias current is achieved by using bias current cancellation circuit. The output stage of OP-27 has a good load driving capability with a guaranteed swing of $\pm$ 10V into 600 Ω load. The PSRR and CMRR exceed 120 dB in addition to a long term drift of 0.2 μV/month, gives OP-27 a performance level previously attained only by discrete designs.

The thermocouple used in the present set-up is chromel-alumel. The thermocouple gives a voltage of 20.65 mV at 500 ^{o}C and 41.269 mV at 1000 ^{o}C before amplification. This input voltage is scaled in the full range of ADC. To achieve the scaling, the gain of the amplifier is kept at 236.63. This requires the input resistor to be 1 KΩ and feedback resistor to be a wire wound potentiometer of 250 KΩ set at 235 K.

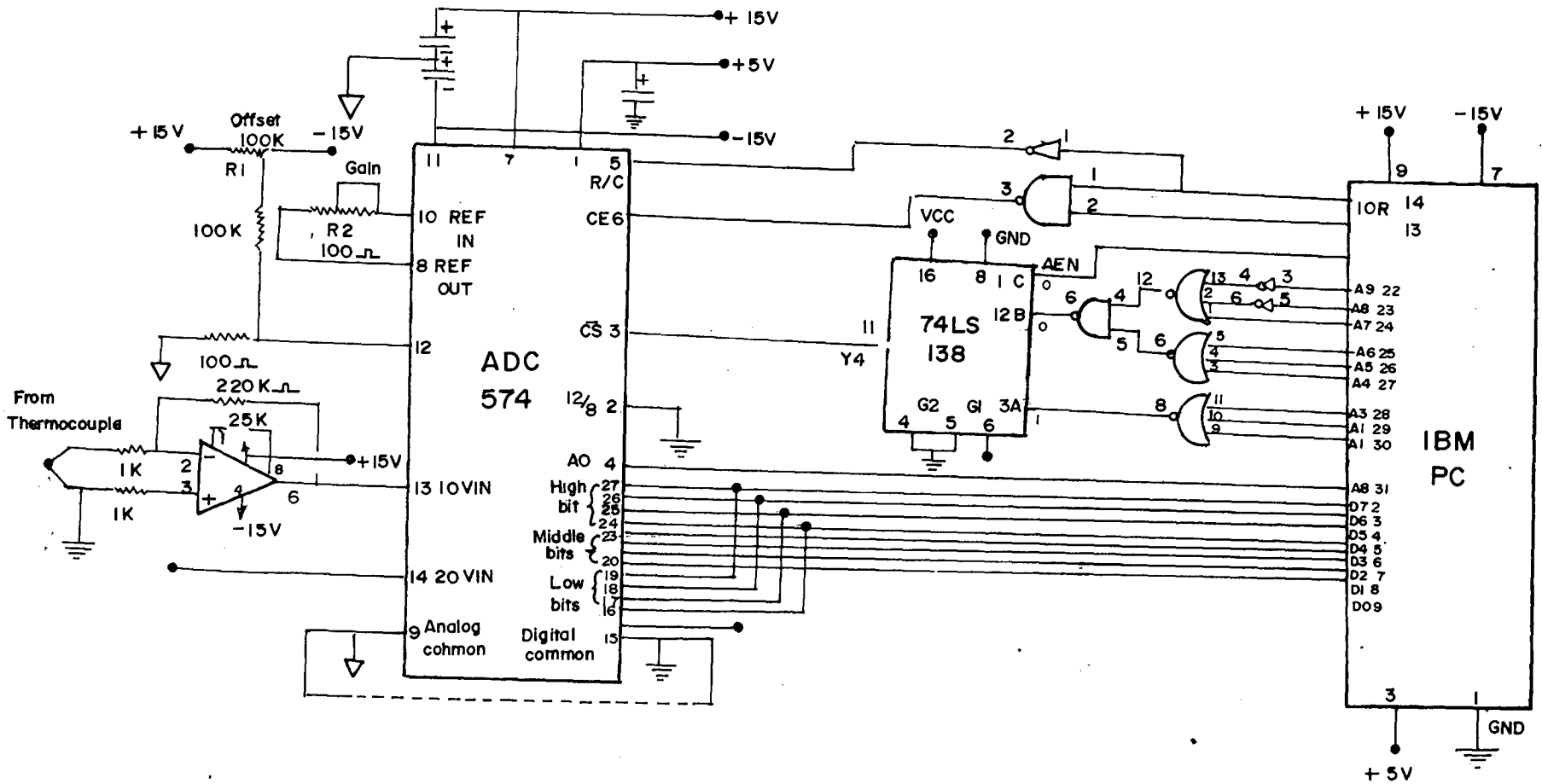

Figure 3.8 : Interfacing Diagram of AD574

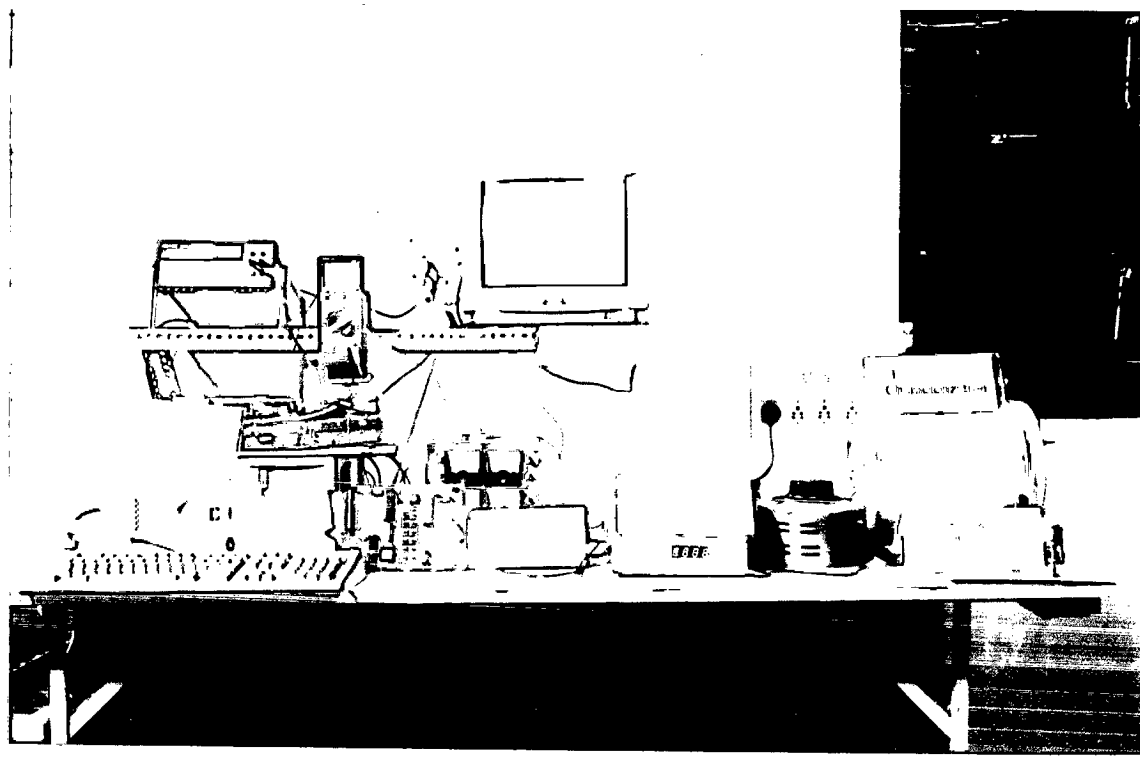

Figure 3.9:Photograph of PC based set-up for thermistor characterisation

The Analogue to Digital converter used for digitising the thermocouple output is AD574, a complete 12 bit successive approximation ADC with tri state output buffer circuitry for direct interfacing with microprocessors. The conversion time of the ADC is 35 μSec. The temperature compensated buried Zener reference provides the primary voltage reference to the ADC which guarantees excellent stability with both time and temperature. There are two 5 KΩ input scaling resistors to allow either a 10V or 20 V span. The 10 KΩ bipolar offset resistor is grounded for unipolar operation and connected to the 10V reference for bipolar operation. In the present interface the ADC is configured for a !0V span and unipolar mode of operation.

The circuit diagram 3.8 shows interfacing of AD574A to the Pentium processor of an IBM PC. Since the device resides in I/O space, its address is decoded only from the lower ten address lines gated with AEN (active low) to mask out internal DMA cycle which use the same I/O address space. This active low signal is applied to CS, IOR and IOW which are further gated together and given to chip enable (CE) to initiate the conversion. Since the data bus width is limited to 8 bits, the AD574A data resides in two adjacent addresses selected by A0. The decoding scheme by using 74LS138 a 3 to 8 decoder has also been shown in the circuit diagram. This assigns address 300H to lower nibble and 301H to high nibble.

The software routines developed for the ADC are included in the listings. AD574A provides an output signal (STS) which indicates that it is busy in conversion. This signal can be polled or used for invoking an interrupt routine. However, looking at the speed of the ADC, in this set-up it is assumed that it converts the sample till the output instruction executes. To avoid the contention, a small delay is introduced after write instruction. The program HELP_ADC.C presents interactive user interface to the user and gives the information about the interfacing details of the ADC. Other program ADC.C reads the temperature of the furnace and plots the same interms of bar charts with a time stamp.

3.3.7 Measurements using DMM :

HP34401A digital multimeter is a high performance instrument capable of measuring resistance, DC and AC voltage and current, as well as frequency. The HP34401A has a built-in microprocessor, memory and other electronics components that give it numerous features such as built-in math functions, recording and storing up to 512 readings, giving the maximum, minimum and average of the readings. In addition, it can be remotely programmed using the SCPI (Standard Commands for Programmable Instruments) language and read by computer via a General Purpose Interface Board (GPIB) port. The DMM gives the performance needed for fast, accurate bench and systems testing, and provides a combination of resolution, accuracy and speed. The typical specifications are 6 1/2-digit display, 0.0015% basic 24-hr dcV accuracy and 1,000

readings/sec direct to GPIB assures that the results are accurate, fast, and repeatable. The detailed specifications are given in the application manual[129].

3.4 Instrumentation Set-up for Determination of Time Constant:

When a thermistor is being used to monitor the temperature of it's environment then the accuracy of measurement of the resistance of the thermistor is critical. In case of systems where the temperature is changing with time, the dynamic thermal response of the thermistor must be considered. The thermal time constant specification, is used to qualify the dynamic response of the thermistor. The Thermal Time Constant for a thermistor is the time required for a thermistor to change its body temperature by 63.2% of a specific temperature span when the measurements are made under zero-power conditions in thermally stable environments.

Some of the dominant factors that affect the T.C. of a thermistor are: the mass and the thermal mass of the thermistor itself; Custom assemblies and thermal coupling agents that couple the thermistor to the medium being monitored; mounting configurations such as a probe assembly or surface mounting, thermal conductivity of the materials used to assemble the thermistor in probe housings; the environment that the thermistor will be exposed to and the heat transfer characteristics of that environment.

The following section describes the design and development of instrumentation set-up to determine the thermal time constant.

- Principle:

The determination of time constant of the thermistor involves the measurement of the variation of its resistance as a function of time, in response to a step change in the temperature input. However, it is very difficult to produce a sharp thermal pulse. The temperature step may be produced either by electrical power dissipated in the sensor (Joule Heating) or by incident radiation on the sensor.

- Description of the set-up:

A schematic of the set-up is as shown in figure 3.10 . The 100W incandescent lamp is fixed at one end of the wooden box and the sensor is mounted at the other end. A shutter fitted to relay moving arm exposing/closing the incidence of radiation on the sensor. Experiments were conducted on some of the bulkier samples specially fabricated in order to have large time constant (Refer Chapter II). The variation of the sensor resistance is measured by monitoring the amplifier output voltage through ADC. This variation is as shown in the graphs 3.11 a and b. Figure 3.11 a shows the response to the step increase in the radiation and figure 3.11b to a step decrease for two different thermistor samples. Using the non-linear curve-fitting techniques the time constants for the curves were found out.

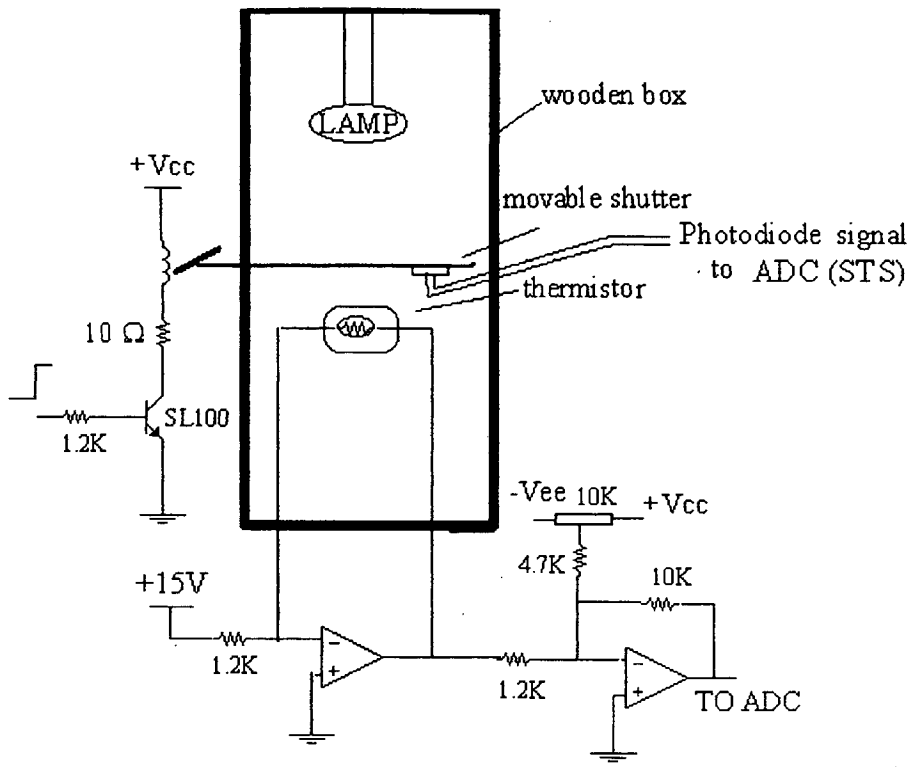

Figure 3.10: Schematic of Instrumentation set-up for determination of time constant

It may be noted that there could be an error in measurement of time constant, due to rise time offset of the relay used. To compensate this error, a photodetector in photovoltaic mode was used beneath the movable shutter and the output of the detector was used to initiate the ADC conversion process. The time constants of various thermistors fabricated in the present work were found to be in the range 0.5 to 3 Seconds.

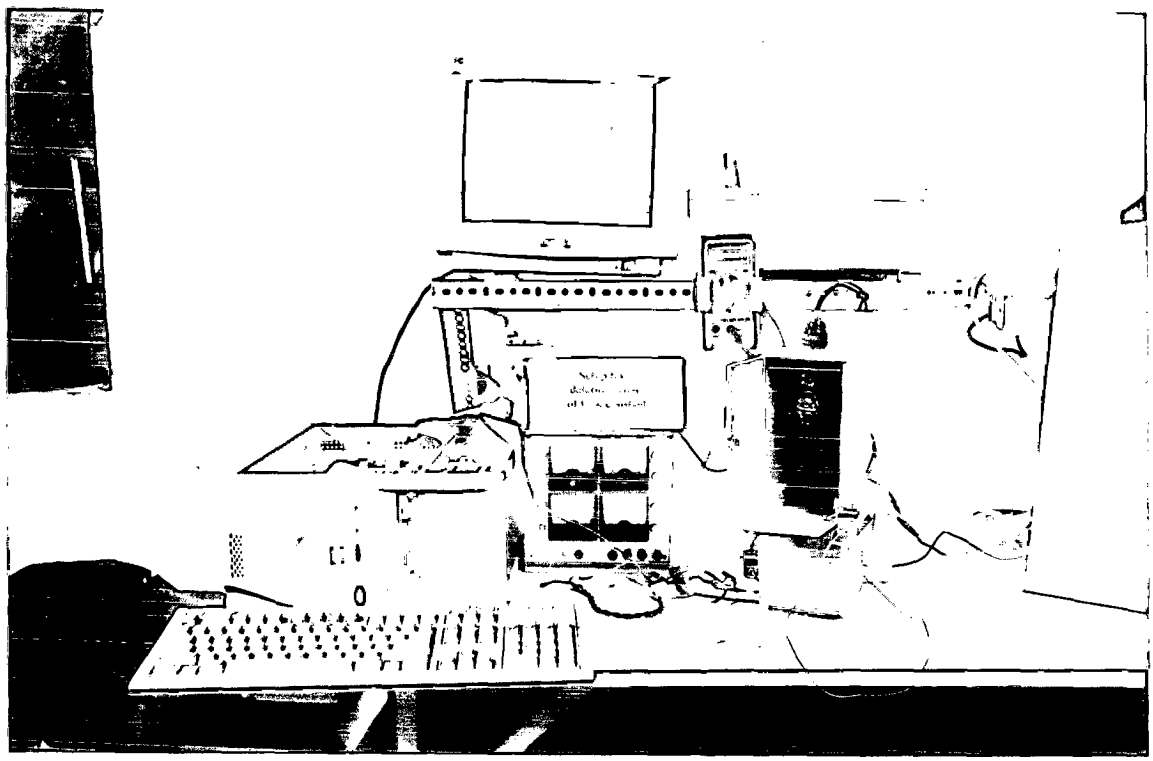

Figure 3.12 : Photograph of PC based set-up for determination of time constant.

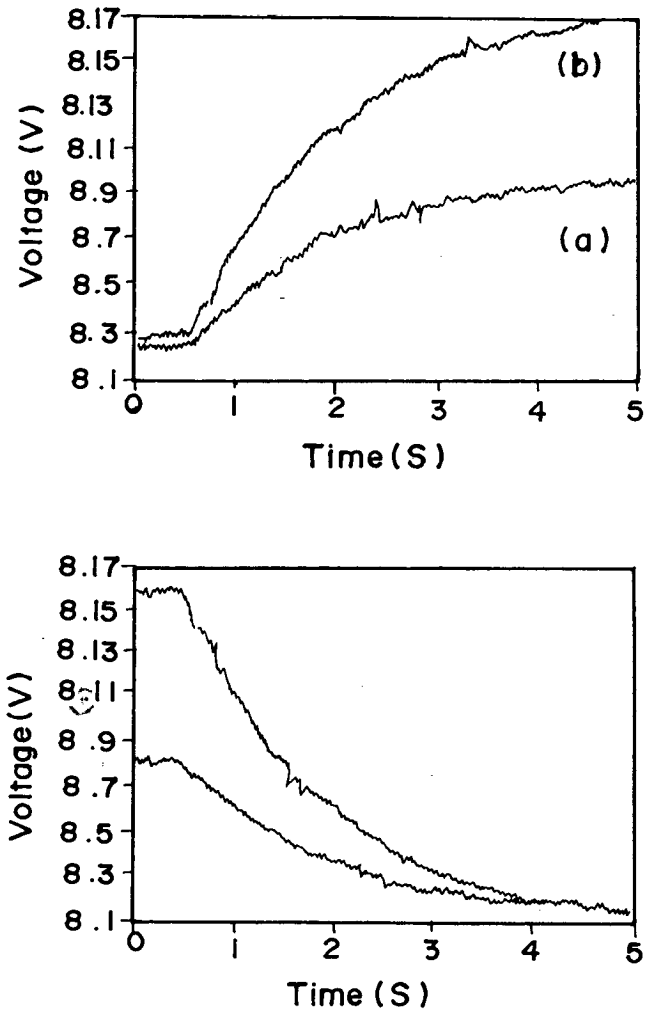

Figure 3.11: Graphs showing

(a) Thermistor characteristics for step increase in incident radiation,

(b) Thermistor characteristics for step decrease in incident radiation.

3.5 Set-up for Determination of Dissipation Constant (D.C.):

The resistance of the thermistor measured depends on its power dissipation and also on the thermal dynamics of the system. A technical specification which quantifies both the parameters is its dissipation constant. The dissipation constant is defined as the power required to raise the thermistor body temperature by 1°C from room temperature in a particular measurement medium. It is expressed in units of mW/°C. The dissipation constant is a very important parameter in circuit design and application considerations. In practise the dissipation constant will be affected by : the mass or thermal mass of a thermistor; the mounting of the thermistor in a probe assembly; the thermal dynamics of the environment where the thermistor is used for monitoring and the range switching of measuring instrument that change the current levels while tracking the resistance changes of the thermistors. The dissipation constant is also an important factor in applications that are based on the self-heating effect of thermistors. In particular, the resistance change of a thermistor due to change in dissipation constant can be used to monitor levels or flow rates of liquids / gasses. For example as flow rate increases, dissipation constant of a thermistor in the flow path will increase and the resistance will change in a manner that can be correlated to flow rate.

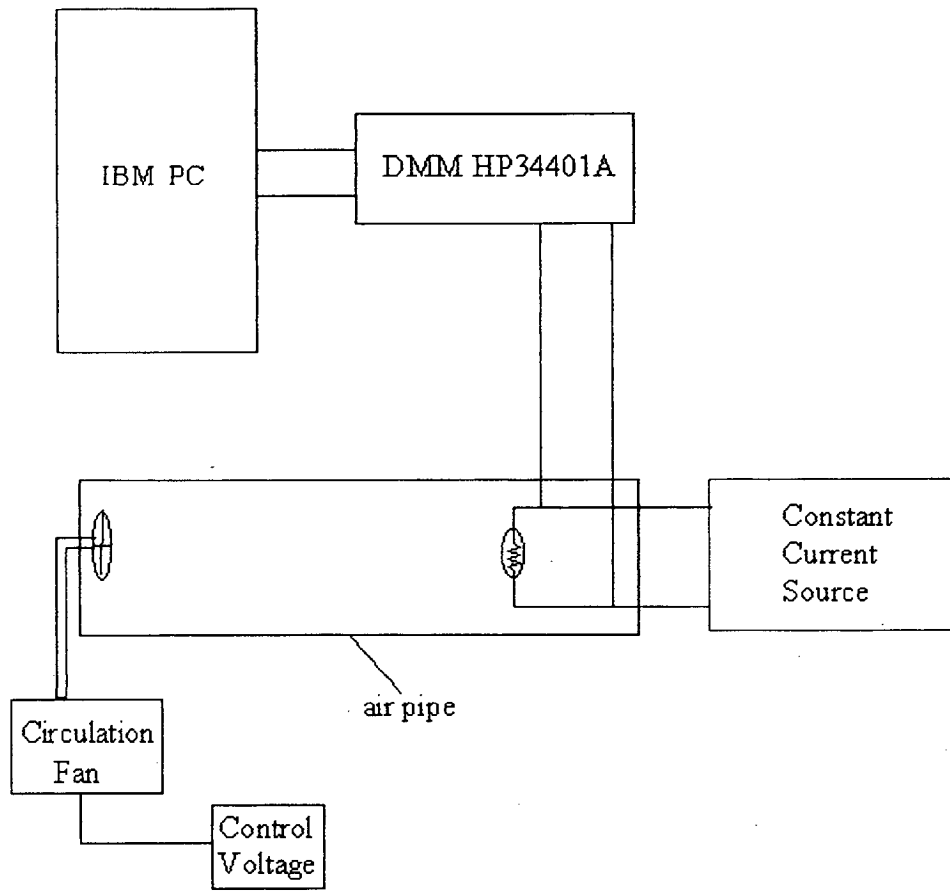

Figure 3.13 : Schematic of set-up for determination of dissipation constant

The plotting of V-I characteristics of NTC thermistors is a time consuming process especially when the thermal time constant of the sensor is large. It is also necessary to maintain the ambient parameters (like temperature, humidity etc.) constant during recording of V-I characteristics. It is therefore desirable to make the duration of the experiment as short as possible.

A PC based instrumentation set-up for measurement of dissipation constant is shown in figure 3.13. The measurements were carried out in still as well as moving air at room temperature. A thermostat used for this purpose is shown in figure 3.14. It consists of a Zener diode based LM335 a precision temperature sensor to monitor the temperature, the transistor SL100 to switch the heater ON and OFF to keep the temperature at the setpoint established by R2 a 10 K 10 turn potentiometer.

The experiments were also carried out in moving air, with the thermistor placed in an air pipe of diameter 20 cm. The air velocity was varied by using a circulator fan as shown in figure 3.13.

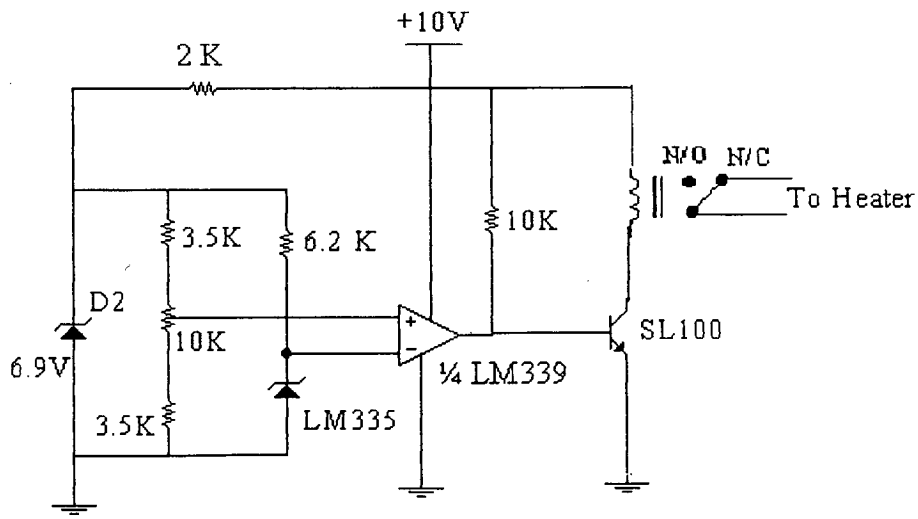

Figure 3.14 : Circuit Diagram of Thermostat

The experiment is started with the thermistor placed in the constant ambient temperature in order to get equilibrium state. The current in the

sensor is gradually increased and the time-dependent voltage characteristics is recorded in order to get the equilibrium voltage value. The DMM HP34401A was configured in remote mode to acquire the readings after a certain time interval depending on the time constant of the thermistor. The program used for this is listed at the end of the chapter (i.e. dc_measure.c)

The initial current steps applied are relatively small so that the power dissipated at first three to five measuring points is negligible. This implies that the first three to five points of a V-I characteristics lie on the straight line, having the slope $\Delta V / \Delta I = R(Ta)$. Since there is no considerable change of thermistor resistance occurs at the beginning of the V-I characteristics, the measurements are carried out quickly, by skipping few data points which is generally true for sensors having both a small or large time constant. When power dissipation produces a significant increase in temperature of the sensor, the stationary V-I characteristics becomes non-linear.

The damage may occur due to overheating of the thermistors in the self heating region. The set-up is programmed to give alarm to prevent the damage to the sensor. The technique used here is, the software compares the adjacent voltage readings. The self heating condition is detected when the voltage readings start decreasing. The system gives an alert message on the screen to reduce the current step. The software also calculates the turn-over voltage and calculates the safe current based on the

relation : I < 2 * Im, where I is the current through the thermistor, Im is the current corresponding to the turn-over voltage.

The circuit diagram 3.15, shows design of a constant current source used in the above set-up.

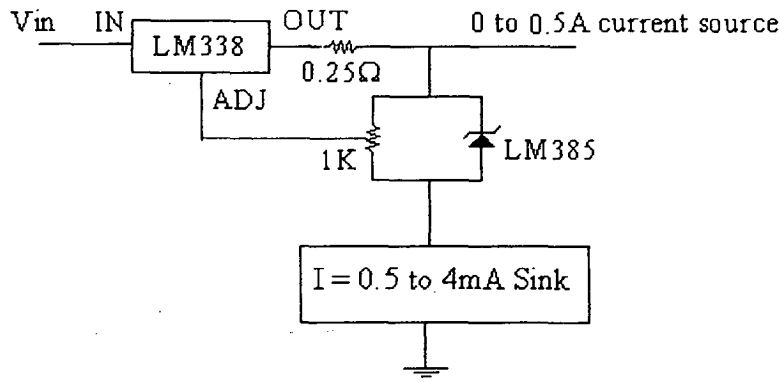

Figure 3.15 : circuit Diagram of Constant Current Source

The circuit has two ranges, lower current sink from 0.5 to 4 mA and a variable current source from 0 to 0.5A. Both of them can be used to configure thermistor in the self heating region. The 1K pot selects a portion of the floating 1.23 V reference voltage, and tricks the LM338 into correspondingly adjust the voltage across the 0.25 ohm current-sense resistor. For using the current sink, the thermistor has to be connected in the sink mode.

A V-I characteristics recorded on a thermistor sample TA1 is as shown in the graph 3.16. Ohm's law is obeyed for very small values of currents as the self heating is minimal. The initial anomaly in the characteristics is attributed to the presence of moisture on the thermistor

Figure3.16Static Current-Voltage Characteristics of the $NiMn_2O_4$ thermistor exhibiting the turnover voltage

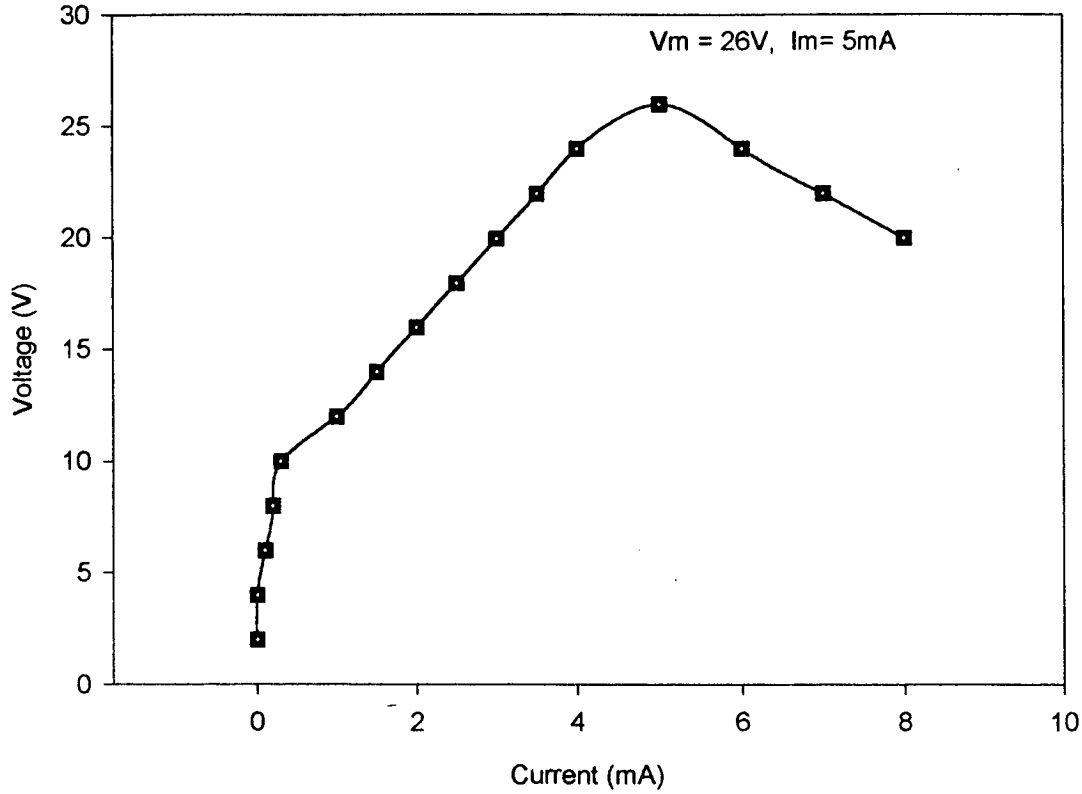

Variation of Power Dissipation with Temperature for the thermsitor

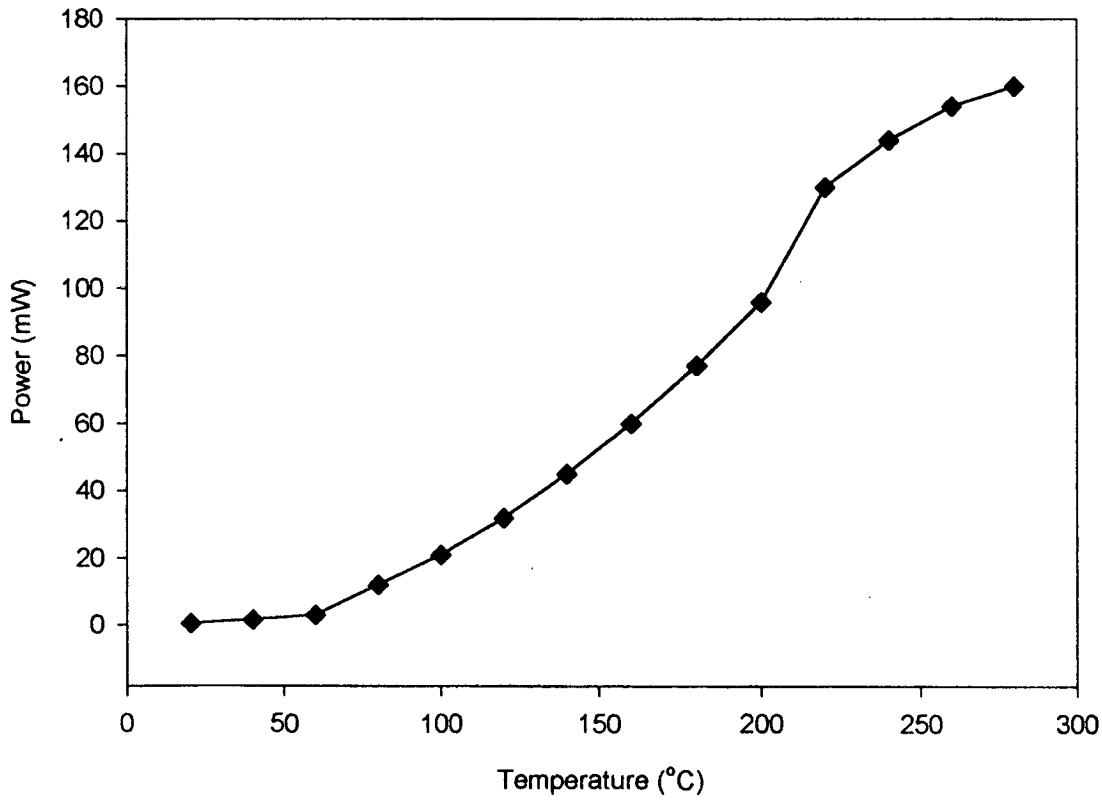

surface. For higher values of voltage and current, the thermistor self-heating starts. After a maximum voltage Vm known as turn over voltage, with slightest increase in current results in rapid decrease in resistance corresponding to negative resistance. From the I-V characteristics,

Vm = 26 V and Im = 5mA. Thus Rm = Vm/Im = 5.2K

From the R Vs T characteristics, the value of 5.2K corresponds to temperature Tm = 150°C. Thus the useful range of the thermistor is upto 150°C. The value of Tm can also be obtained by using the equation

$$Tm = \beta/2 \left[1-(1- 4To/\beta)^{1/2} \right]$$

which gives Tm=160°C. Thus within the exponential errors, the value of turn-over temperature obtained by both the methods agrees well.

3.6 Accelerated Testing of NTC Thermistors:

Because of the increased use of thermistors, specially by the biomedical community, in the late 1970's the National Bureau of Standards (NBS), now the National Institute of Standards and Technology (NIST), imposed extensive tests to find out their failure rates. One way to find the failure rates is gathering field information regarding the components and then predicting for the other components based on standard equations. However, it was found that the reliability predictions by the above method itself is not much reliable for devices like thermistors. An alternate way is to actually operate the component at their normal operating temperature for months and years together[130] to check their satisfactory working. Testing time of the order of 560 days has been reported in the literature.

A white paper on Reliability model [144] of thermistors has been published by BetaTherm a well known company in thermistor manufacturing. The procedure adopted by the company is as follows: The thermistors to be tested are stressed by operating them at a temperature higher than their normal operating temperature. It is important that the stress temperatures are not so high that other failure mechanisms are introduced. After this the R Vs T characteristics is recorded. The procedure is repeated till the thermistor shows drift or failure.

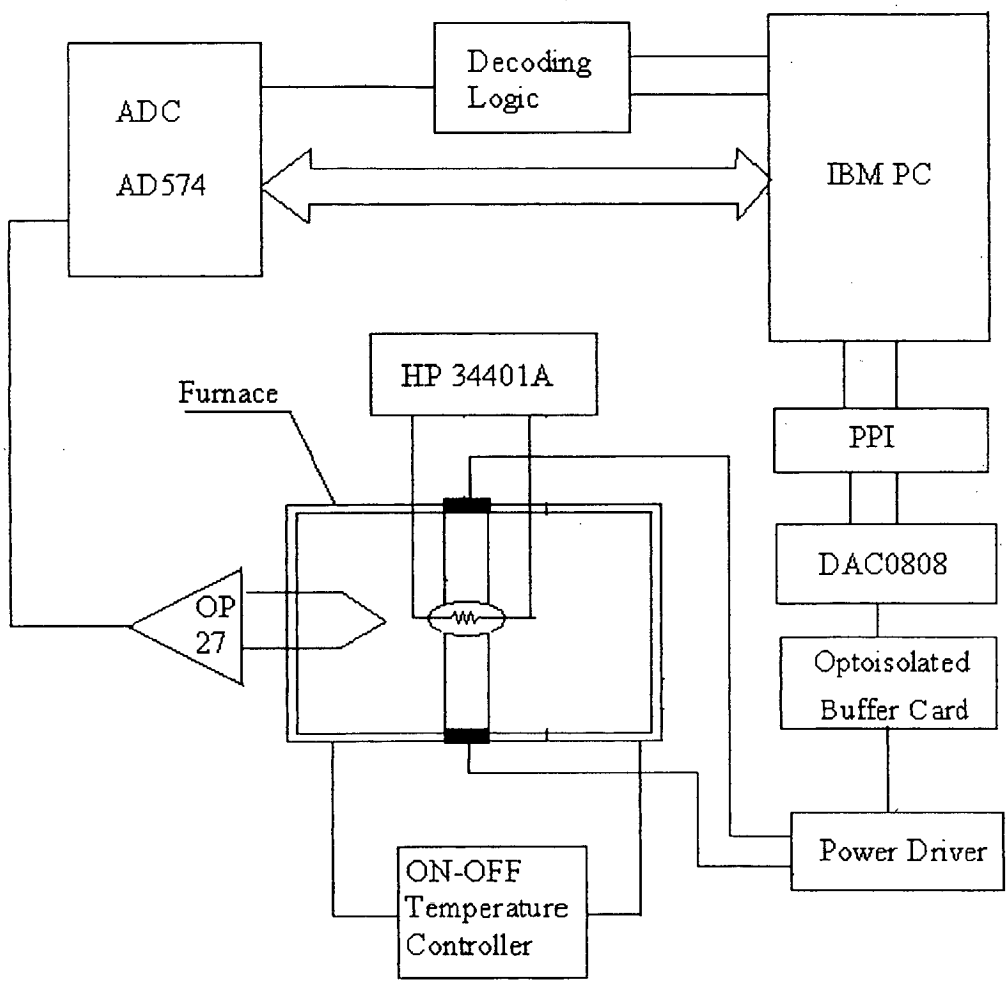

Figure 3.17 : Schematic of PC based set-up for accelerated testing .

The above said procedure has been automated by using the PC based set-up shown in figure 3.17 . Various test waveforms are generated through DAC by using the programs listed at the end of the chapter. The digital to analog converter used is an 8 bit monolithic DAC0808, featuring a full scale output current settling time of 150nS while dissipating only 33mW with only ±5V supplies. The present application does not require reference current trimming since the full scale output current is typically ±1 LSB of 255 (Iref/256). The details regarding the specifications of the DAC may be found from the application catalogue of National Semiconductor Corporation. The interfacing diagram of the DAC is as shown in the figure 3.18. The sawtooth waveform is applied to the furnace through the power driver module. The resistance Vs temperature characteristics is recorded per every cycle of the sawtooth waveform. The ageing characteristics is shown in the graph at figure 3.19.

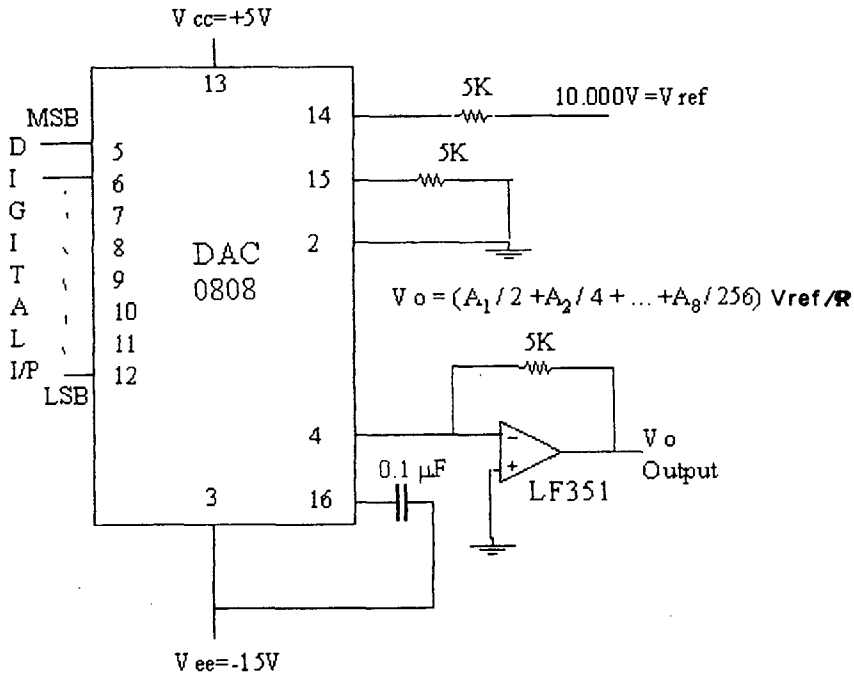

Figure 3.18: DAC 0808 interfacing diagram

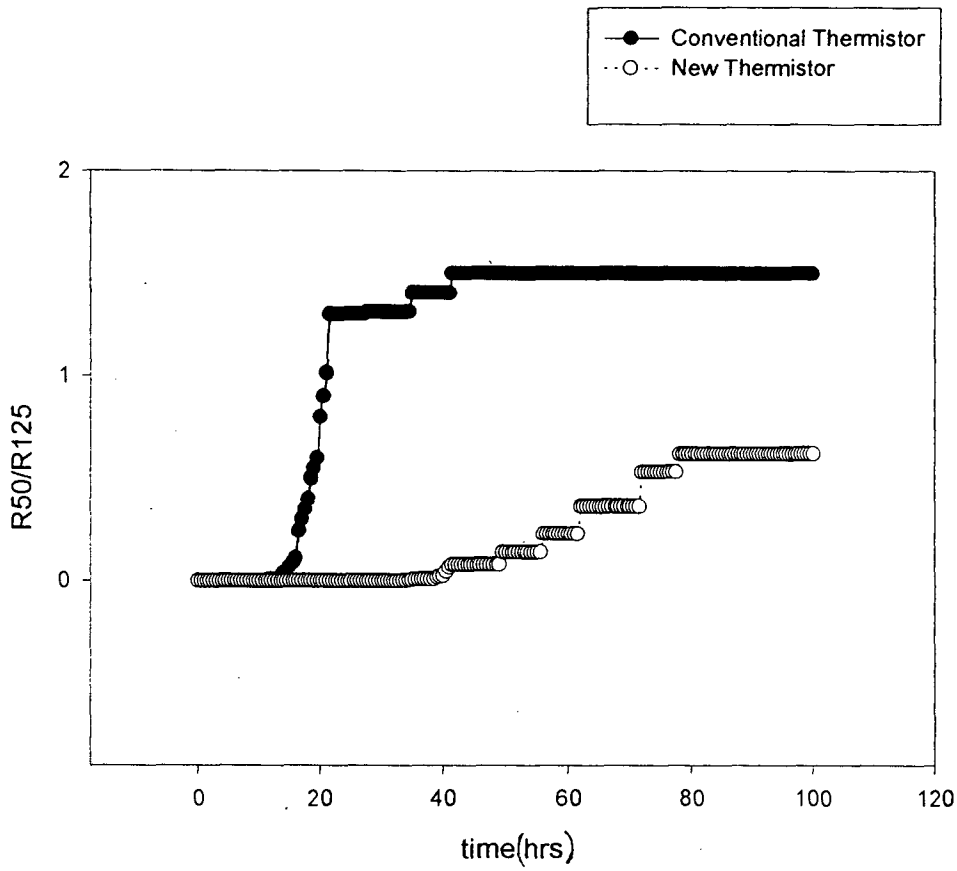

Figure 3.19 : Ageing behaviour of thermistors

3.7 Characterisation of Moisture Effects on Thermistors:

It has been reported[131] that humidity severely affects the characteristics of thermistors. The R Vs T characteristics have found to change with the absorption of moisture and the long term effects like lead corrosion, were also detected. In the course of our investigation, experiments were conducted on few samples preserved in a dissector and others left open. During R Vs T characterisation, the samples kept in the dissector were found to conform their previous characteristics. On the other hand the samples kept outside, showed significantly reduced room temperature resistance. When these samples were subjected to a temperature cycle upto 70^{o} and then characterised, exhibited their previous characteristics. The changes in the characteristics was attributed to the presence of moisture on the thermistor surface. Moisture (or relative humidity) characterisation is a vital aspect of thermistor reliability. A set-up is therefore designed for moisture characterisation of the thermistor samples.

3.7.1 Principle: The sensing mechanism is based on a capacitor probe. A parallel plate capacitor has been designed in which the test thermistor sample is placed. The moisture content of the thermistor influences the dielectric constant and in turn changes the capacitance of the capacitor.

3.7.2 Construction: The design of capacitor probes for sensing applications has been discussed in depth in literature [200-203]. The sensor

consists of a concentric cylinder type of structure. A plastic case is used as a sample holder and two parallel aluminium

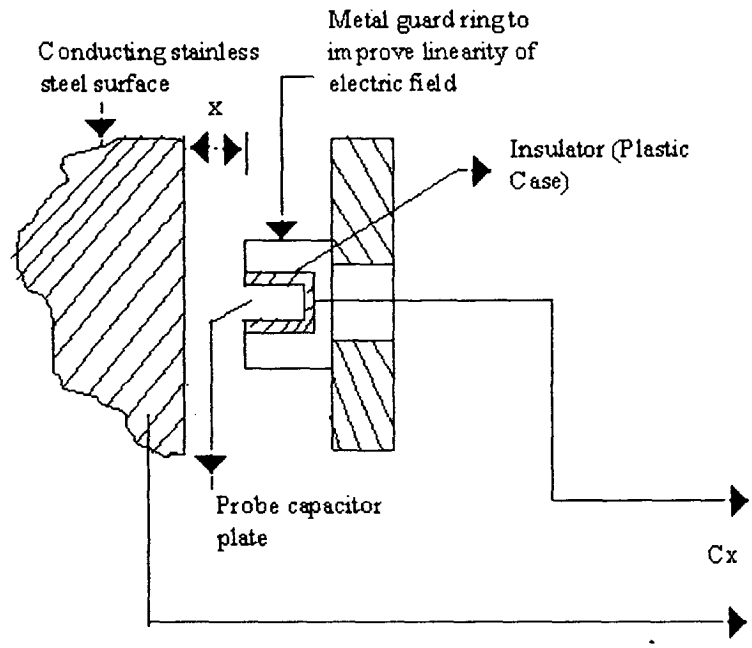

Figure 3.20: Schematic of moisture probe

plates are placed in parallel around it. The schematic is shown in the figure 3.19. A photograph of the probe is shown in figure 3.20.

3.7.3 Calibration of Probe: The moisture probe was calibrated by using the following calibration salts. These salts cause the air in a closed container to attain the given value of relative humidity. A small amount of water is added to these salts with an equilibrium point greater than the ambient relative humidity. The salts with drier equilibrium points gradually remove water vapour from the air and eventually become too soupy for effective calibration.

Table 3.1 : Calibration of moisture probe

Salt	Relative Humidity at 25°C %	Capacitance pF
Ammonium Sulfate	80	161
Ammonium Nitrate	63	144
Potassium carbonate	42	132
Potassium Acetate	22	124

3.7.4 Signal Conditioning : The transducer is connected to the signal conditioner by short lengths of miniature coaxial cable and is largely insensitive to the stray capacitance between the sensor electrodes and earth. This limits the length of connecting leads used were approximately 1.5 metres. The signal conditioning board has four modules. The module A1 is a highly linear RC oscillator. It is based on Op Amp LF356 which is a monolithic JFET input operational amplifiers incorporating well matched, high voltage JFETs on the same chip with standard bipolar transistors. The reasons for choosing this operational amplifier is due to the requirement of following specifications: high slew rate; wide bandwidth; extremely fast settling time; low voltage and current noise; a low 1/f noise. The module A2 is a high performance AC amplifier based on operational amplifier LF353. This follows by a buffer and equaliser module (A3) and a display driver (A4) module. Operational amplifier LF353 used in all these circuits is a wide bandwidth dual JFET input operational amplifier with low supply current,

large gain bandwidth product and fast slew rate. A glass tube attachment is done to the moisture probe to facilitate the moisture conditions. The characteristics is as shown in the graph at figure . A time period of about 1 minute is required to obtain an equilibrium of moisture in the enclosure after the thermistor sample placed in the probe.

Figure 3.23 shows variation in room temperature resistance of a thermistor sample TA3 under constant moisture conditions.

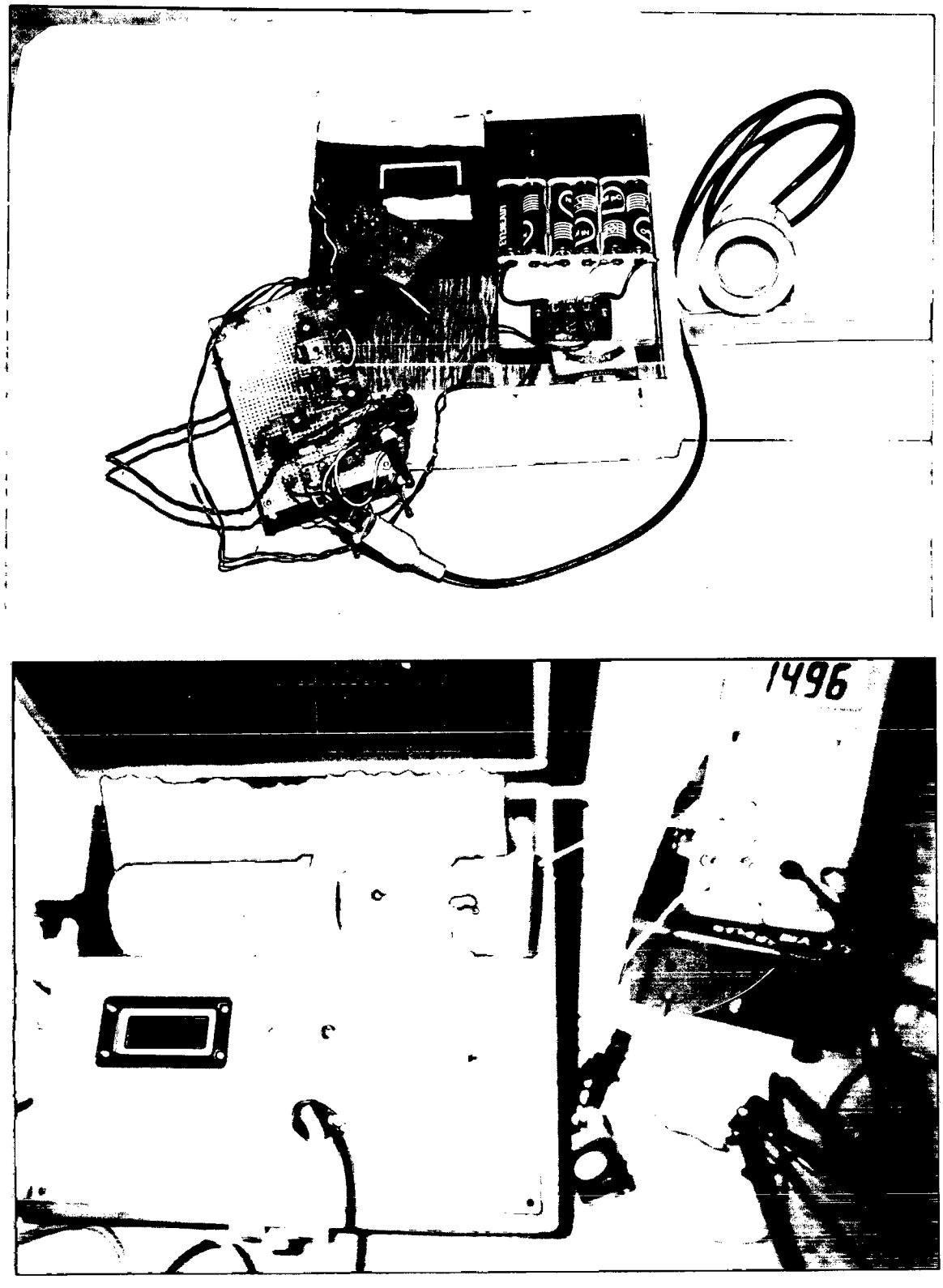

Figure 3.21 : Photographs of set-up for characterising effects of moisture on thermistors.

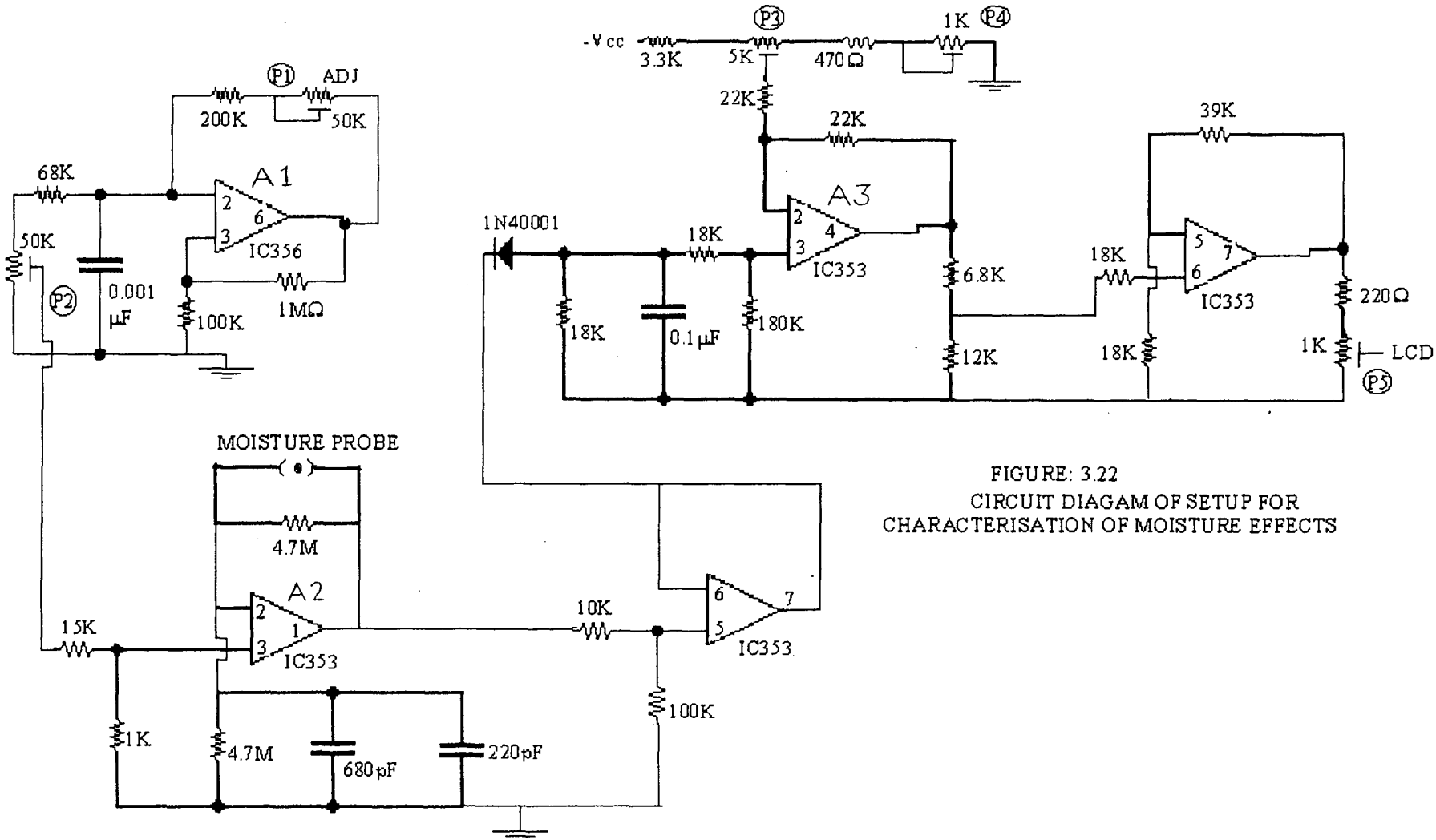

FIGURE: 3.22
CIRCUIT DIAGAM OF SETUP FOR
CHARACTERISATION OF MOISTURE EFFECTS

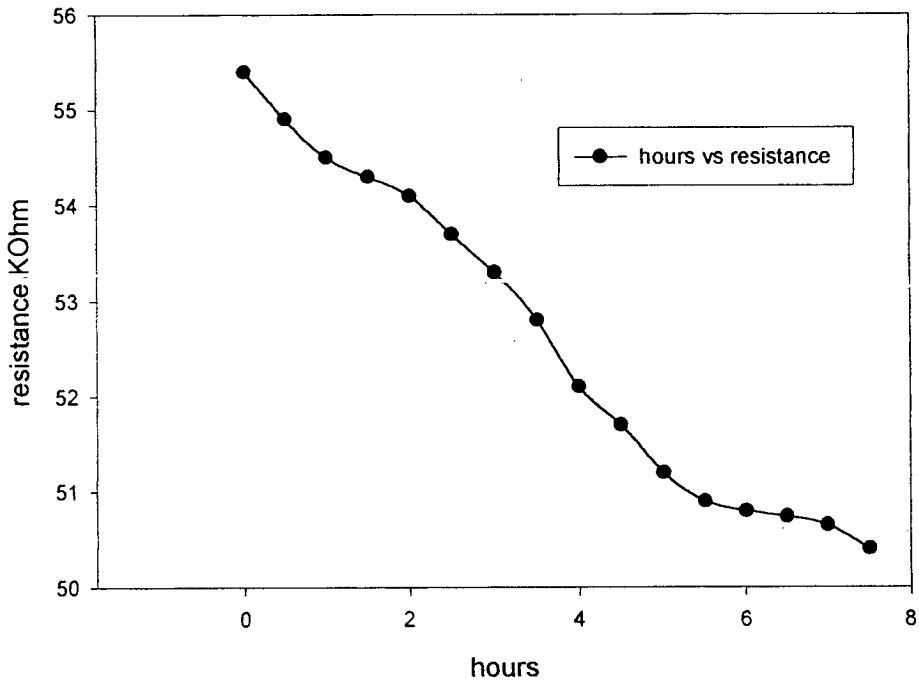

Figure 3.23 : Graph showing variation of room temperature resistance Vs Hours at Constant moisture Conditions

3.8 Software Listings :

HELP_ADC.C
PROGRAM FOR INTERACTIVE USER INTERFACE WHICH ALSO PRESENTS INFORMATION ABOUT ADC

```
#include<stdio.h>
#include<conio.h>
#include<bios.h>
#include<stdlib.h>
#include<dos.h>
#include<math.h>
#include<graphics.h>

main()
{
int gd,gm;
char ch;
detectgraph(&gd,&gm);
initgraph(&gd,&gm," ");
setgraphmode(VGAHI);
setfillstyle(SOLID_FILL,WHITE);
floodfill(0,0,CYAN);
settextstyle(TRIPLEX_FONT,HORIZ_DIR,4);
setcolor(LIGHTGRAY);
outtextxy(180,20,"SPECIFICATION");
setcolor(BLACK);
line(5,40,175,40);
line(5,40,5,460);
line(630,460,630,40);
line(630,40,410,40);
line(5,460,150,460);
line(585,460,630,460);
setviewport(10,60,620,470,1);
m0:  clearviewport();
setcolor(LIGHTCYAN);
settextstyle(DEFAULT_FONT,HORIZ_DIR,2);
outtextxy(10,40,"# ANALOG TO DIGITAL CONVERTER");
setcolor(DARKGRAY);
outtextxy(10,43,"_ _____ __ _____ _____");
setcolor(WHITE);
line(0,400,385,400);
line(560,400,630,400);
settextstyle(SANS_SERIF_FONT,HORIZ_DIR,1);
outtextxy(70,70,"     -  AD574  -") ;
```

```
        settextstyle(DEFAULT_FONT,HORIZ_DIR,1);
        outtextxy(70,110," * COMPLETE 12 BIT A/D CONVERTER WITH
                    REF CLOCK & 3STATE OUTPUT.");
        outtextxy(70,140," * FULL 8 and 16 BIT MICROPROCESSOR
                   BUS INTERFACE.");
        outtextxy(70,170," * Maximum Conversion Time 35
                    microcecond");
        outtextxy(70,200," * DIGITAL ERROOR CORRECTION.");
        outtextxy(70,230," * +/- 1 LSB Max. Zero Offset
                    Error");
        outtextxy(70,260," *ESD PROTECTION : 1500 Volts MIN.");
        outtextxy(70,290," * LOW POWER : 240 mW Typ.");
        outtextxy(70,320," * EFFICIENT PERFOMANCE AT : +- 12 V
                    or+- 15 V.");
        outtextxy(70,350," * MONOLITHIC BiMOS CONSTRUCTION &
                   PLCC PACKAGE.");
        setcolor(CYAN);
        outtextxy(420,395," M .. main menu");


mess1: ch=getch();

        if(ch=='m' || ch=='M')
        {
        cleardevice();
        exit(0);
        }
        goto mess1;

        }
```

HELP_DAC.C
PROGRAM FOR INTERACTIVE USER INTERFACE WHICH ALSO PRESENTS INFORMATION ABOUT DAC

```
        #include<stdio.h>
        #include<conio.h>
        #include<bios.h>
        #include<stdlib.h>
        #include<dos.h>
        #include<math.h>
        #include<graphics.h>

        main()
        {
```

```
        int gd,gm;
        char ch;
        detectgraph(&gd,&gm);
        initgraph(&gd,&gm," ");
        setgraphmode(VGAHI);
        setfillstyle(SOLID_FILL,WHITE);
        floodfill(0,0,CYAN);
        settextstyle(TRIPLEX_FONT,HORIZ_DIR,4);
        setcolor(LIGHTGRAY);
        outtextxy(180,20,"SPECIFICATION");
        setcolor(BLACK);
        line(5,40,175,40);
        line(5,40,5,460);
        line(630,460,630,40);
        line(630,40,410,40);
        line(5,460,150,460);
        line(585,460,630,460);
        setviewport(10,60,620,470,1);
m0:     clearviewport();
        setcolor(LIGHTCYAN);
        settextstyle(DEFAULT_FONT,HORIZ_DIR,2);
        outtextxy(10,40,"# DIGITAL TO ANALOG CONVERTER");
        setcolor(DARKGRAY);
        outtextxy(10,43,"_ _____ __ _____ _____");
        setcolor(WHITE);
        line(0,400,385,400);
        line(560,400,630,400);
        settextstyle(SANS_SERIF_FONT,HORIZ_DIR,1);
        outtextxy(70,70,"      -  DACPORT 0808  -") ;
        settextstyle(DEFAULT_FONT,HORIZ_DIR,1);
        outtextxy(70,110," * COMPLETE 8 BIT D/A CONVERTER.");
        outtextxy(70,140," * CURRENT OUTPUT -- ");
        outtextxy(70,170," * SINGLE SUPPLY OPERATION : +5V TO
                           +15V.");
        outtextxy(70,200," * EXTREMELY FAST ACCESS TIME : 1 micro
        sec.");
        outtextxy(70,230," * FULLY MICRO PROCESSOR INTERFACE
        POSSIBLE");
        outtextxy(70,260," * SINGLE LASER-WAFER-TRIMMED CHOP FOR
        HYBRIDS");
        outtextxy(70,290," * LOW POWER : 75 mW Typ.");
        outtextxy(70,320," * GUARANTEED MONOTONIC OVER TEMP
        ARATURE.");
        outtextxy(70,350," * SMALL 16 PIN DIP & 20 PIN PLCC
        PACKAGE.");
```

```
        setcolor(CYAN);
        outtextxy(425,395," M .. main menu");


mess1:  ch=getch();

        if(ch=='m' || ch=='M')
        {
        cleardevice();
        exit(0);
        }
        goto mess1;

        }
```

Acclerated_Testing.C
PROGRAM FOR OUTPUTTING VARIOUS WAVEFORMS THROUGH DAC FOR ACCELERATED TESTING.

```
        /* THIS PRGRAM OUTPUTS SQUARE-WAVE TRIANGULAR WAVE
        OR  /* SAWTOOTH WAVE AT THE OUTPUT OF DAC. THE
        VOLTAGE LEVELS  AND FREQUENCY IS CONTROLLABLE
        WITHIN LIMITS.      */

        #include<stdio.h>
        #include<dos.h>
        #include<math.h>

        main()

        short int a,b,i,wave_type;
        int c;
        printf("\nPlease enter lower limit, upper limit, and half period\n");
        printf("\n in mlliseconds.\n");
repl:   printf("\n\nlower limit (less than 40)\n");
        scanf("%d",&a);
        if(a>0&&a<41)
        {
        printf("\nPlease enter upper limit between 50 & 250.\n");
        goto repu;
        }
        else
        {
        printf("\n\nnumber should be between 0 & 40.\n");
        goto repl;
        }
```

```
repu:  scanf("%d",&b);
       if(b>49&&b<251)
       {
       printf("\nPlease enter number between 10 and 250 for half
    period.\n");
       goto rept;
       }
       else
       {
       printf("\nThe number should be between 50 and 250\n");
       goto repu;
       }
rept:  scanf("%d",&c);
       if(c>9&&c<251)
       {
       goto type;
       }
       else
       {
       printf("\nThe number should be between 10 and 250\n");
       goto rept;
          }
type: printf("\nSelect waveform of output.\n");
       printf("Enter 1 for square-wave.\n");
       printf("     2 for triangular wave.\n");
       printf("     3 for saw-tooth wave.\n");
       scanf("%d",&wave_type);
       switch(wave_type)
       {      case 1:
              goto square;
              case 2:
              goto triang;
              case 3:
              goto sawtooth;
              goto type;
       }
triang: printf("\nTriangular output from DAC.");
        outportb(0x31b,0x89);
out1:   for(i=a;i<b;i++)
        {
        outportb(0x318,i);
        delay(c);
        }
        for(i=b;i>a;i--)
        {
```

```
        outportb(0x318,i);
        delay(c);
        }
        goto out1;

square: printf("\n Squarewave at output of DAC.");
        outportb(0x31b,0x89);
out2:   outportb(0x318,a);
        delay(c);
        outportb(0x318,b);
        delay(c);
        goto out2;

sawtooth:   printf("\nSawtooth output from DAC.");
            outportb(0x31b,0x89);
out3:       for(i=a;i<b;i++)
            {
            outportb(0x318,i);
            delay(c);
            }
            goto out3;}
```

ADC_DAC.C
PROGRAM FOR CONTROLLING BOTH ADC & DAC

```
#include<graphics.h>
#include<dos.h>
#include<stdlib.h>
#include<stdio.h>
#include<conio.h>

 main()
 {
        int num;
        char ch;
start:  clrscr();
        gotoxy(4,4);
        printf("\n\tTHIS OPTION ALLOWS YOU TO CONTROL THE
       ADC");
        printf("\n\n   DO YOU WISH TO CONTROL-");
        printf("\n\n    1. INPUT TO ADC & OUTPUT TO DAC");
        printf("\n    2. INPUT TO ADC & OUTPUT TO DPM");
        printf("\n    3. EXIT WITHOUT ACESS          ");
        printf("\n\n Type a number to make a choice :: ");
```

```
                fflush(stdin);
                scanf("%d",&num);

                switch(num)
                {
                case 1:
                        goto dac;
                        break;
                case 2:
                        goto dpm;
                        break;
                case 3:
                        exit(0);
                        }
        clrscr();
                        gotoxy(2,2);
                printf("\n Please enter a valid key");
                printf("\n  Press any key to continue ");
                getch();
                goto start;

dac:            poke(0xd000,0x03ff,0x04);
                exit(0);
dpm:            poke(0xd000,0x03ff,0x05);
                exit(0);
ramp:           poke(0xd000,0x03ff,0x03);
                exit(0);
                }_
```

PROGRAM FOR CONTROLLING DAC

```
#include<graphics.h>
#include<dos.h>
#include<stdlib.h>
#include<stdio.h>
#include<conio.h>

 main()
 {
 int num;
start:  clrscr();
gotoxy(4,4);
printf("\n\tTHIS OPTION ALLOWS YOU TO CONTROL THE DAC");
 printf("\n\n  DO YOU WISH TO GENERATE  -");
```

```
        printf("\n\n    1. SQUARE WAVEFORM");
        printf("\n    2. TRIANGULAR WAVEFORM");
        printf("\n    3. RAMP WAVEFORM");
        printf("\n    4. EXIT");
        printf("\n\n          Type a number to make a choice :: ");

        fflush(stdin);
        scanf("%d",&num);
        switch(num)
        {
        case 1:
         goto square;
        break;
        case 2:
        goto tri;
        break;
        case 3:
        goto ramp;
        break;
        case 4:
        exit(0);}
        clrscr();
        gotoxy(2,2);
        printf("\n Please enter a valid key");
        printf("\n  Press any key to continue");
        getch();
        goto start;

square: poke(0xd000,0x03ff,0x01);
          exit(0);
tri:      poke(0xd000,0x03ff,0x02);
          exit(0);
ramp:     poke(0xd000,0x03ff,0x03);
          exit(0); }
```

DC_Const.c

```
/* Program for configuring DMM HP 34401A for Acquiring fast d.c.
   voltages and currents to calculate dissipation constant */

#include<graphics.h>
#include<dos.h>
#include<stdlib.h>
#include<stdio.h>
#include<conio.h>
```

```
#define ADDR 727L
HANDLE  hHpib;
/* Function Prototypes */
void open_hpib(void);
void close_hpib(void);
void rst_clear(void);
void meter_meas(void);
void check_error(char *func_name);

/************************************************/

void main(void)
{
open_hpib();          /*Open the hpib board*/
rst_clear();          /*Reset the instrument and clear error queue*/
meter_meas();         /*Set up the meter for measurement take
                            measurement*/
close_hpib();         /*close hpib board*/
}
/************************************************/
void open_hpib(void)
{
/* Open the hpib board so the program can use it*/
int      err;

err=HpibOpen(7L,&hHpib);
}

 /************************************************/
void close_hpib(void)
/* Close the hpib board so other programs can use it*/
{
int     err;

err=HpibClose(hHpib);
}


void rst_clear(void)
{
/* Reset the meter, clear the error queue, and wait for commands to
```

```
complete.  A "1" is sent to the output buffer from the *OPC?
Command when *RST and *CLS are completed. */

float value;

HpibOutputs(hHpib,ADDR, "*RST;*CLS;*OPC?", 15);
HpibEnter(hHpib,ADDR, &value);
}

void meter_meas(void)
{
/* Configure the meter for fastest reading rate.  The measurement
is made on the 10 volt range with the least resolution.*/
float value;
float rdg[500];
int   elements;
int   i;
elements=500;

HpibOutputs(hHpib,ADDR, "CONF:VOLT:DC 10,MAX", 19);        /*
                              set 10 volt range dc and max res*/
HpibOutputs(hHpib,ADDR, "DISP OFF;TRIG:DEL MIN",21);       /*
                    turn off disp and set trigger delay to min*/
HpibOutputs(hHpib,ADDR, "TRIG:COUN 500",13);               /* Set
                                        trigger count to 500 */
HpibOutputs(hHpib,ADDR, "*OPC?",5);                        /* Wait for
                              the above commands to finish */
HpibEnter(hHpib,ADDR, &value);     /* Enter the opc result */

HpibOutputs(hHpib,ADDR, "INIT;*OPC?",10);                  /* Start
                                                 taking readings*/
         /* Wait for all readings to go to memory*/
HpibEnter(hHpib,ADDR, &value);

HpibOutputs(hHpib,ADDR, "FETCH?",6);
HpibEntera(hHpib,ADDR, rdg,&elements);                     /* Enter
                    the readings from memory to pc */

for (i=0;i<500;i++)
printf("Reading: %f\n\n", rdg[i]);              /* Print the readings */

/* Call the function to check for errors */

check_error("meter_meas");
}
```

```
/*****************************************/

void check_error(char *func_name)
{
/* Read error queue to determine if errors have occurred */

char message[80];
int length = 80;

HpibOutputs(hHpib,ADDR, "SYST:ERR?", 9);
HpibEnters(hHpib,ADDR, message, &length);

while (atoi(message) !=0)       /* Loop until all errors are read*/
 {
printf("Error %s in function %s\n\n", message, func_name);
HpibOutputs(hHpib,ADDR, "SYST:ERR?", 9);
HpibEnters(hHpib,ADDR, message, &length);
}
}
```

CONTROL.C

PROGRAM FOR MONITORING TEMPERATURE OF FURNACE THROUGH THERMOCOUPLE AND PLOTTING THE BAR CHARTS. A SUBROUTINE IS INVOKED FOR TEMPERATURE CONTROL OF THE FURNACE USING PROPORTIONAL MODE

```
#include<stdio.h>
#include<dos.h>
#include<math.h>
#include<conio.h>
#include<time.h>
#include<stdlib.h>
#include<graphics.h>

void control1(void);

int s1,s2,s3,s4,l1,l2,l3,gm,gd,pb,kp;
int i,j,k,l,set2,set3,er1,er2,er3,con,con1,con2;
char *S1, *SET2,*SET3,*E1,*E2,*E3,*DAC;

main()
```

```
        {       hardinit();
        for(l=0;l<10000;l++)
                {
                getval();
                graph();
                } }
                getval()
        { repeat: clrscr();
        outportb(0x31d,0);
        outportb(0x31d,2);/* CHANNEL 1 OF ADC (S1) SELECTED.*/
        outportb(0x31d,1);/* START CONVERTION.*/
        outportb(0x31d,0);
        delay(100);
rep1:   i=inportb(0x31e);/* CHECK EOC. */
        j=i&1;
        if(j==0)
        {goto rep1;}
        else
        {
                s1=inportb(0x31c);/* S1 READ. */
        }

        /* REPEAT FOR CHANNEL 2 (S2). */
        outportb(0x31d,4);
        outportb(0x31d,6);
        outportb(0x31d,5);
        outportb(0x31d,4);
        delay(100);

        /* CALCULATION OF MANIPULATED OUTPUT AND OUPUT TO
        CONTROLLERS. */
        er1=30-s1;    /*SETPOINT CHANGED TO 30. ERROR
                        CALCULATED.*/
        pb=40;        /*PROPORTIONAL BAND IN PERCENT, (40%)*/
        con1=er3*100/pb;    /*PROPORTIONAL CONTROL OUTPUT TO
DAC CALCULATION.*/
        kp=2;/*PROPORTIONAL GAIN*/
        next:   outportb(0x31a,con);}
        graph()
        {
        gm=DETECT; gd=DETECT;
        initgraph(&gd,&gm," ");
        settextstyle(2,0,5);
        outtextxy(50,70,"SETPOINT AT S1 IS  ");
        outtextxy(350,70,"30");
```

```
outtextxy(400,70," DEGREE CELSIUS");
itoa(s1,S1,10);
outtextxy(350,85,S1);
outtextxy(400,85," DEGREE CELSIUS.");
outtextxy(50,85,"TEMPERATURE AT S1 IS ");
outtextxy(400,160," DEGREE CELSIUS.");
itoa(er1,E1,10);
outtextxy(50,100,"ERROR AT S1 IS ");
outtextxy(350,100,E1);
outtextxy(400,100," DEGREE CELSIUS.");
itoa(er2,E2,10);
outtextxy(50,220,"PROPORTIONAL OUTPUT FOR CONTROLLER
IS ");
outtextxy(415,220,DAC);
settextstyle(2,0,7);
setcolor(12);
outtextxy(50,5,"INDICATIONS OF SETPOINTS, ERRORS,AND
CONTROL");
settextstyle(8,0,3);
setcolor(10);
outtextxy(50,250,"REALTIME BAR GRAPH OF TEMPERATURES");
setcolor(15);
line(25,475,25,300);
line(1,450,450,450);
line(20,325,30,325);
line(20,425,30,425);
line(20,375,30,375);
line(18,400,32,400);
line(18,350,32,350);
line(18,300,32,300);
settextstyle(2,1,5);
setcolor(11);
outtextxy(5,325,"DEGREES CELSIUS");
settextstyle(2,0,4);
setcolor(14);
outtextxy(30,325,"125");
outtextxy(30,350,"100");
outtextxy(30,375,"75");
outtextxy(30,400,"50");
outtextxy(30,425,"25");
outtextxy(30,451,"0");
outtextxy(30,300,"150");
settextstyle(2,0,5);
setcolor(10);
outtextxy(120,460,"S1");
```

```
        setfillstyle(4,13);
        bar(120,450-s1,130,449);
        setfillstyle(6,13);
        bar(220,450-s2,230,449);
        setfillstyle(8,13);
        bar(320,450-s3,330,449);
        setfillstyle(10,13);
        bar(420,450-s4,430,449);
        setcolor(15);
        setlinestyle(2,0,1);
        line(100,450-30,140,450-30);
        line(200,450-set2,240,450-set2);
        line(300,450-set3,340,450-set3);
        settextstyle(2,0,5);
        setcolor(13);
        if(s4<60)

        /*DISPLAY OF MESSAGES AND SENDING OF CONTROL
        OUTPUTS.*/
next:
        outportb(0x318,con);
        delay(50000);
        }

                hardinit()
        {
                outportb(0x31b,0x89);
                outportb(0x31f,0x99);
        }
```

CHAPTER 4

Thermistor Based Smart Sensors

4.1 Introduction:

The past decade has witnessed a revolution in microelectronic circuits and devices. Today's microprocessors and micro-controllers are powerful and affordable and they have revitalised the instrumentation world. But the modest suitability of conventional sensors used in microprocessor based data acquisition systems is becoming bottleneck in diverse application fields. This problem is being overcome by the rapid development of digital-output sensors that are compatible with microprocessors[99,107]. These so called smart sensors [34,36,98, 102,106,109,110,168,169,176] have advantages like automatic calibration, automatic linearisation, insensitivity to interference, elimination of cross sensitivity and improved frequency response. It goes beyond saying that, the hardware is becoming more complex inside these sensors but the external hardware required is more simple. This new arrangement saves the cost of extra signal conditioning and digitisation. The present chapter reports thermistor based smart sensors. Part-I describes a modified Schmitt Trigger transducer. Part - II reports a non-linear analogue to digital converter, and the last part presents an architecture of an ASIC dedicated for thermistor applications.

4.2 Review of IC Sensors in Thermal Domain:

IC temperature sensors can be divided into two groups on-chip signal conditioning with a built in sensor and on-chip signal conditioning with an external sensor. Integrating both the modules on one chip results in

minimal noise pick-up, adaptive processing, the possibility of wireless interfaces, linearisation, calibration and cross sensitivity compensation.

However, this technique has few drawbacks such as drawbacks of single chip integration include non-standard processing steps, non-standard initial wafer sizes, and difficulty in predicting the behaviour of the material after fabrication. In spite of these drawbacks, single chip technique permits optimal interaction between the sensor and measurand, or else there is a possibility of damaging the sensing core and conditioning circuitry.

As early as 1966, Silicon and Germanium were predicted to be the leaders in IC temperature sensors. In fact the poor temperature characteristics of Germanium has enabled Silicon to take over the IC market. Variation in junction potential along with temperature, in the case of P-N junction diodes, was the basis of first-generation IC temperature sensors and is used till today. A programmable temperature monitoring chip with P-N junction as the temperature sensing core was even used for fishing application i.e. tagging Atlantic salmon [103]. The transistor, which is the basic unit of the IC, exhibits good temperature sensing when connected in the negative feedback loop of an op amp. This performance seems to be the reason for the dual transistor structures found in many IC temperature sensors. In these ICs, temperature sensing is done by monitoring changes in ΔV_{BE} (also known as PTAT) that results from operating identical bipolar transistors at different biasing conditions. With

the growing need for portable instruments, the focus has shifted now to low power designs for IC temperature sensors. CMOS transistors are being used quite often to reduce power consumption, also other techniques such as need based switching of the circuit, on/off frequency keying transmission to other modules, management of the submodules by keeping them in standby mode, and hardware/software partitioning, are being implemented in the effort to lower power dissipation. Techniques like multi-threshold CMOS (MTCMOS), super cur-off CMOS (SCCMOS) and variable threshold CMOS (VTCMOS) are few examples in this direction.

A CMOS monolithic temperature sensor based on compatible lateral bipolar transistors for the sensor and reference parts were developed with all CMOS circuits for ADC control, and calibration [107, 109]. However, the current gain of the lateral bipolar transistor and the leakage current to substrate depend on the IC processing technology, so the desired results are hardly feasible. That's why vertical bipolar substrate transistors are used in recent IC sensors [107]. The sensing is based on the PTAT mechanism with the output chopped suitably for the offset reduction and then passed through sigma-delta A/D module for digitisation. The chip is 1.5 mm^2 with a temperature measurement range -40°C to +120°C, a supply voltage as low as 2.2V, and power consumption as low as 7μW are reported.

IC based temperature setpoint switches are also popular in control applications. Switching the output of an IC takes pace when a sum of PTAT

and its complementary CTAT pass through zero at a selected temperature set by an external resistor [116]. This low cost IC has an open-collector output and works in the range of -40°C to +150°C with an accuracy of ± 1°C.

For a long time RTD has been the industry standard among temperature sensors. Its success is primarily due to its corrosion resistance, high melting point, and ease of purification. This sensor provides unequalled accuracy, sensitivity, stability, wide sensing range, and a better non-linearity characteristics. With the progress of hybrid IC technology, it is possible to design RTD based sensing cores on Si-based substrates. Honeywell, USA has begun designing temperature sensors for the automobile and HVAC industries [115]. To reduce the cost, they use a combination of nickel and iron in their TD series. Linearisation hardware is built into the chip and every care is taken to overcome the magneto-resistance of the permalloy. A reference BIMOS chip for processing Pt-100 signals over the range of -200°C to 850°C is also reported in reference [96]. The output signal is time multiplexed and has frequency modulated voltage that is suitable for microcontroller processing.

Microminiaturised amorphous Germanium thin film thermistors insulated by a thick PCVD silicon nitride layer) have been used as probes for measuring mass flow, heat conductivity, perfusion and local temperature gradient [112]. These probes are useful for on-line blood-flow measurements in physiological and other medical applications. Several

researchers have also worked out suitable methods of linearisation, self calibration and compensation [91,92,98,110]. The latest trends in this field indicate the demand for ICs based on RTDs and thermistors.

4.3 Part - I : NTC Thermistor based Modified Schmitt Trigger Sensor

4.3.1 CMOS Implementation of Thermistor Cell :

An implementation of CMOS based thermistor cell is as shown in figure 4.1. The feedback transistor Q2 has been biased to operate in weak inversion mode and therefore it exhibits a logarithmic dependence of its drain - source voltage on the thermistor current. This feedback action also maintains constant potential to the thermistor and thus ensures short response time. The transistor Q3 serves as a load device and column select switch. A sensor implementation like this has some unique feature like random sensor access and much higher dynamic range.

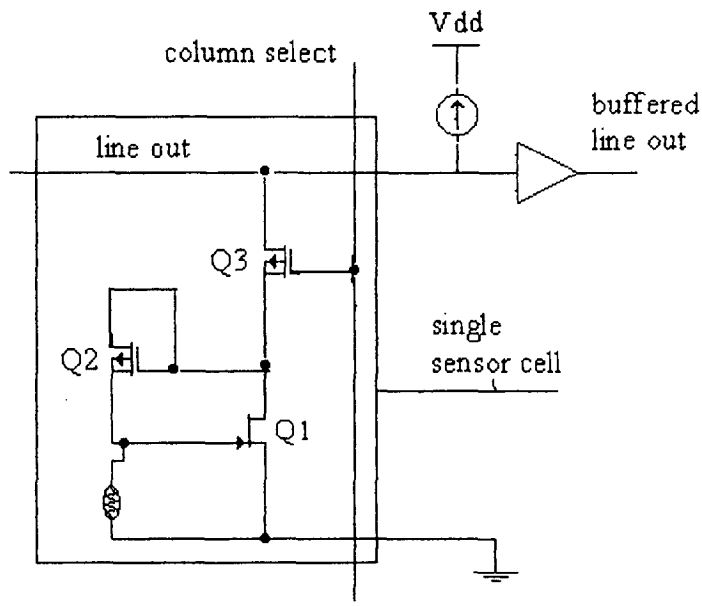

Figure 4.1 : Schematic of CMOS implementation of thermistor cell

4.3.2 Modified Schmitt Trigger Sensor :

4.3.2a The Conventional Flip-Flop Sensor :

One of the traditional example of a smart sensor design is the flip-flop sensor. Developments in this type of sensor type led to flip-flop sensors suitable for sensing many different physical parameters [99, 125-126]. The sensor consists of a flip-flop in which a circuit element, sensitive to the desired measurand, is embedded. As an example the flip-flop sensor developed for optical sensing is shown in the figure 4.2.

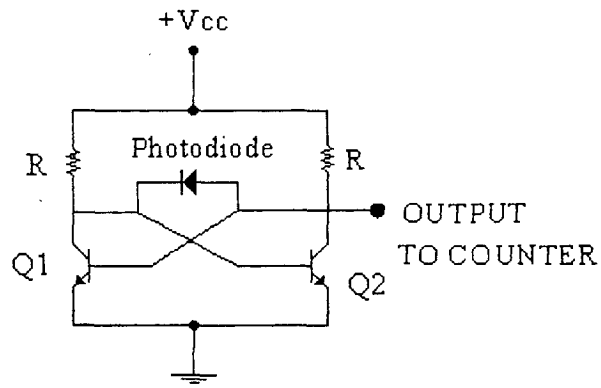

Figure 4.2 : An optical flip-flop sensor

The sensing action consists of alternately bringing the flip-flop into an unstable state and observing the stable state to which it switches by counting the number of ones and zeros. A non-zero value of the physical quantity results in a flip-flop imbalance and thus leads to a deviation in the ratio of ones and zeros from unity. A similar scheme works well with diode as a temperature sensor. The advantages of such flip-flop sensor include

the possible integration of the sensor with the ADC, in a simple structure. Flip-flop sensors can also be easily combined to form a matrix sensor using addressing techniques similar to those used in static RAMs. However the most striking drawback of the flip-flop temperature sensors is their sensitivity to glitches in addition to the limited sensing range. In order to eliminate this drawback the flip-flop transducer was modified with the NTC thermistor as a sensor. Built-in hystersis was introduced to minimise the sensitivity to noise and glitches. The circuit is designed so as to reduce the current consumption in thermistor in dormant state.

4.3.2b Modified Schmitt Trigger Temperature Transducer Design :

BJT Implementation :

The sensor design is based on the emitter coupled multivibrator. The thermistor is embedded in the circuit as shown in figure 4.3. The UTP and LTP calculations are as follows:

$$UTP = \frac{(R1 \parallel R5)}{R5 + (R1 \parallel R5)} \times Vcc \quad \text{----------} (4.1)$$

$$LTP = \frac{(R5 \parallel R6)}{(R1 + (R5 \parallel R6)} \times Vcc \quad \text{----------} (4.2)$$

At room temperatures, the thermistors have high resistance. Because of Rset, the base of T1 is at lower base voltage than the base of T2. The base of T2 is approximately at UTP. With the increase in

temperature, the resistance of thermistor (RT) decreases, causing the base potential of T1 to rise above UTP level. In turn, this causes T1 and T4 to turn ON, and T2, T3 to turn OFF. The advantages of this circuit are high input impedance and full output swing from 0 to Vcc. It also reduces the current burden on thermistor in

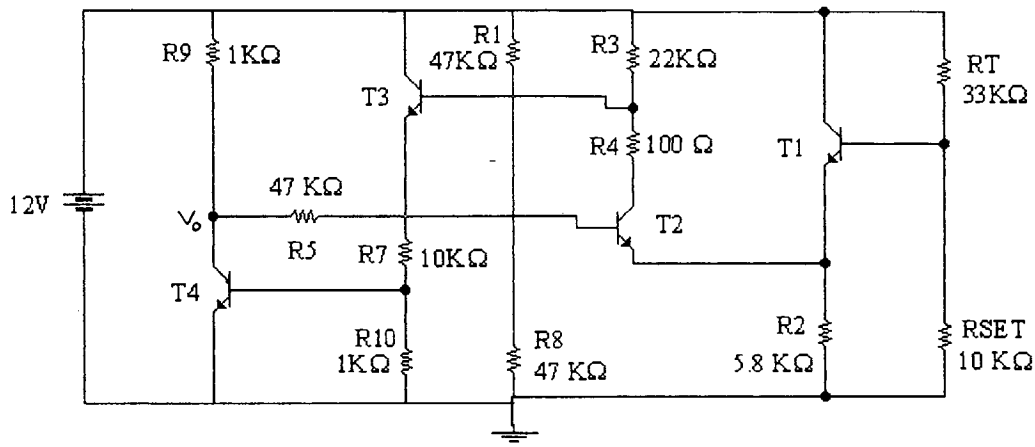

Figure 4.3: Schematic of Schmitt trigger transducer which features high input impedance and full output swing along with less current burden on thermistor.

dormant mode resulting in low power dissipation. The circuit is simulated using Electronics Workbench. The enlarged snapshot of the CRO screen is shown in figure 4.4, which confirms the results.

4.3.2c Simulation of the Schmitt Trigger Sensor using PSPICE:

The circuit in figure 4.3 was also simulated using SPICE-3 . The following transistor parameters were used in the simulation programs using

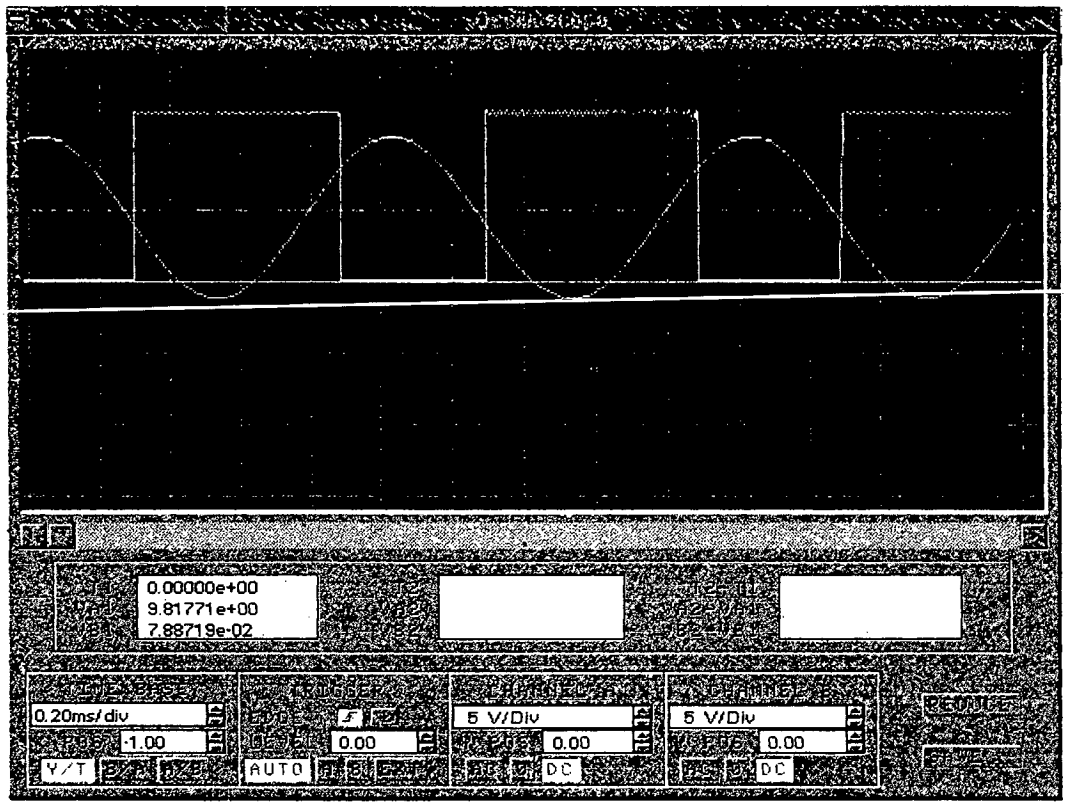

Figure 4.4: simulation of Schmitt Trigger Transducer using Electronics Workbench.

the standard Gummel Poon model. The real challenge in simulation lies in developing appropriate SPICE model for the NTC thermistor. However SPICE allows micro-modelling[127] of a device using the existing primitives. The netlist for the NTC thermistor developed by using the existing primitives in SPICE is given under 4.4.4.

.MODEL QBC547A/PLP NPN

(+ IS = 1.533E-14
+ NF = 1.002
+ ISE = 7.932E-16
+ NE = 1.436
+ BF = 178.7
+ IKF = 0.1216
+ VAF = 69.7
+ NR = 1.004
+ ISC = 8.305E-14
+ NC = 1.207
+ BR = 8.628
+ IKR = 0.1121
+ VAR = 44.7
+ RB = 1
+ IRB = 1E-06
+ RBM = 1
+ RE = 0.6395
+ RC = 0.6508
+ XTB = 0 + EG = 1.11
+ XTI = 3 + CJE = 1.61E-11
+ VJE = 0.4209
+ MJE = 0.3071
+ TF = 4.995E-10
+ XTF = 139
+ VTF = 3.523
+ ITF = 0.7021
+ PTF = 0
+ CJC = 4.388E-12
+ VJC = 0.2
+ MJC = 0.2793
+ XCJC = 0.6193
+ TR = 1E-32
+ CJS = 0
+ VJS = 0.75
+ MJS = 0.333
+ FC = 0.7762)
*$

4.3.2d SPICE Modelling of the NTC thermistor :

The thermistor macromodel [127] used has three terminals. Two terminals are for electrical domain, third is for thermal domain having a potential (voltage source) equivalent to thermal time constant, thermal boundary temperature and heat capacity. The following expression describes the resistance-temperature relation of thermistor.

$$R = Ro\, e^{\beta(1/T - 1/To)} \quad \text{---------- (4.3)}$$

The exponential relationship is modelled by using a voltage controlled voltage source (VCVS). The VCVS is developed by adapting the diode model within SPICE. Shockley's equation describes the polynomial expansion for diode and the same is used in SPICE as follows:

$$I_d = I_s \ [\exp (V_d V_t / n) -1] \text{ ----------(4.4)}$$

The netlist for the thermistor in series with the setpoint resistor Rset is as given below:

```
.SUBCKT THERMISTOR 10 3
9
G1 6 3 7 0 1
V1 5 0 {BSTA}
X1 5 9 4 DIVIDE
X2 4 2 EXP
X3 1 2 7 DIVIDE
*TCELL
VTC1 21 0 {TINF}
CTC1 9 0 {TAU/HC}
RTC1 9 21 {HC}
GX5 0 9 POLY(2) 10 0 7 0
0 0 0 0 1.0000
V2 10 6
E1 1 0 3 6 {-
(2.7128^(BETAA/300)/RO)}
.ENDS
```

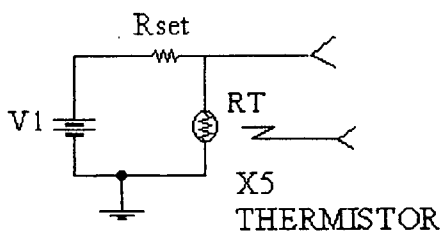

Figure 4.5: Macro-model of NTC Thermistor

```
.SUBCKT DIVIDE 1 2 4
*V4 = V1/V2
R1 1 0 1MEG
R2 2 0 1MEG
R4 4 0 1MEG
G1 0 3 1 0 1
G2 3 0 POLY(2) 2 0 3 0 0 0 0
0 1
R3 3 0 100MEG
E1 4 0 3 0 1
.ENDS
.SUBCKT EXP 1 2
R 1 0 1K
E 3 0 1 0 .0258642
V 3 4
RD 4 0 1MEG
D 4 0 DIODE
.MODEL DIODE D(IS=1)
I 0 4 -1
H 2 0 V 1
.ENDS

THERMIST & RSET
*SPICE_NET
.TRAN .05 10
*INCLUDE THERMAL.LIB
.OPTIONS ACCT ITL1=500
.PRINT TRAN V(2) IV(1) V(3)
R1 1 2 1.5k
X5 2 0 3 THERMISTOR {
RO=30k BETA=4k
*TAU = 1.5 HC=500 TINF=300}
V1 1 0
.END
```

4.3.2e CMOS Implementation of the Circuit :

The CMOS implementation of the Schmitt trigger is shown in figure 4.5. When the output is low, M6 is ON, M3 is OFF and P-channel section determines the switching points. If the output is high, M3 is ON, M6 is OFF and N-channel section determines the the switching points.

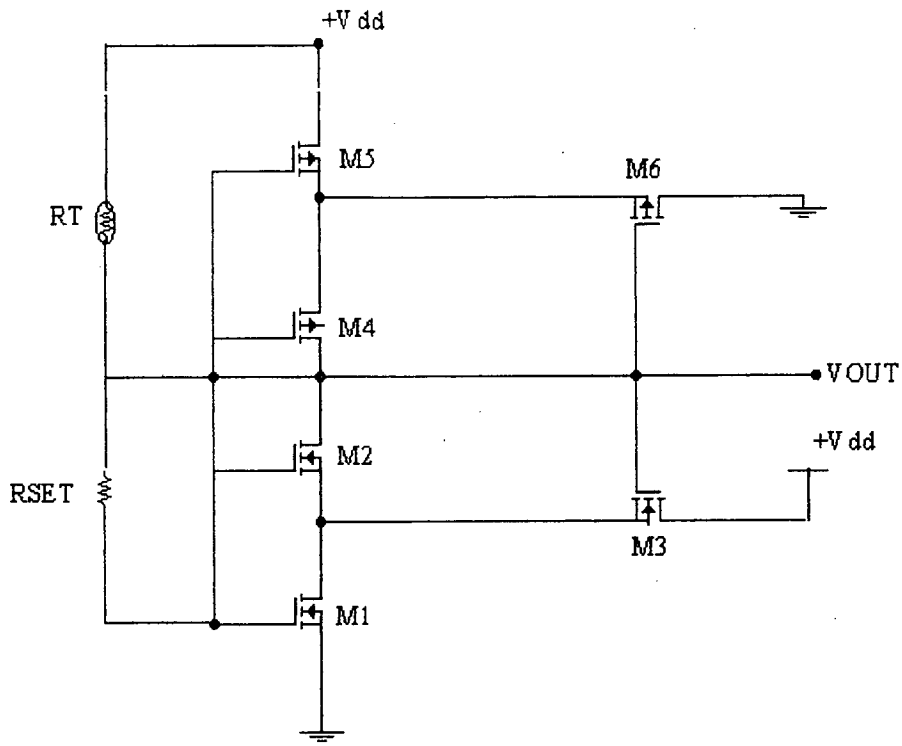

Figure 4.6 : CMOS implementation of Schmitt Trigger Transducer.

The netlist for determining the switching points of the circuit is as follows:

Netlist for Schmitt Trigger

```
vdd 1 0 3V
v2 4 0 pwl (0u 0v 8us 0v 12u 3v 16u 0v)
m1000  2  4  1  1 pmos w=3u  l=3u ad=36p pd=24u as=36p ps=24u
m1001  5  4  2  2 pmos w=10u  l=3u ad=36p pd=24u as=36p ps=24u
m1002  0  5  2  2 pmos w=12u  l=11u l=3u ad=36p pd=24u as=36p
ps=24u
m1003  3  4  0  0 nmos w=10u  l=2u l=3u ad=36p pd=24u as=36p
ps=24u
m1004  1  5  3  3 nmos w=7u  l=6u l=3u ad=36p pd=24u as=36p
ps=24u
m1005  5  4  3  3 nmos w=3u  l=3u l=3u ad=36p pd=24u as=36p
ps=24u
.include ami-c5n.md
.tran 0.01ns 20u
.control
reset
run
plot V(4) V(5)
.endc
.end
```

4.3.2f Sensor In IC Form:

The Schmitt trigger sensor circuit is easy to fabricate as an ASIC [38] because it is based on all NPN transistors. This IC implementation eliminates incorrect triggering (the result of mismatched VBEs on T1 and T2) by careful design of device layout in the photo-masking stage. To reduce further the effects of the tolerance and temperature coefficients on trigger level definition, a separate thin film network of metal resistors R1, R5 and R6 is needed (Refer Figure 4.3). The components added externally to this proposed ASIC are a thermistor and Rset, which can be chosen to suit the application.

In some biomedical applications where the measurand temperature range is small, the thermistor can even be placed on the substrate itself using hybrid techniques. A hybrid IC designed in this way combines the advantages of silicon processing with exotic sensing principles. The basic circuit shown in the figure 4.3 or 4.6 can even be arranged in rows and columns. The output of thus formed matrix sensor can be accessed via addressing techniques similar to those used in SRAM. The matrix sensor can be duplicated using VLSI technology.

4.3.2g Programmable Noise Immunity :

The noise immunity of the above reported Schmitt Trigger Transducer is a function of the hystersis introduced. The traditional flip-flop sensor is sensitive to even a weak glitch produced due to temperature drift or supply variation. The Schmitt trigger transducer can be made insensitive to the noise by first obtaining the accurate noise estimation [26] of the system where the sensor is to be used. Then the resistors R1, R2 and R5 can be chosen to widen the hystersis gap slightly more than the noise voltage. The digital output of the sensor can be processed by a microprocessor based system for ensemble averaging to minimise the low frequency noise.

However, there is a trade-off between sensitivity/resolution and noise immunity. For better sensitivity, the amount of hystersis should be minimal (as with a flip-flop sensor). In a Schmitt Trigger Transducer, the

noise immunity is greater, at the expense of lack of sensitivity in dead-band.

4.3.2h Projected Applications :

The thermistor based Schmitt Trigger Transducer can be used as a low cost high performance temperature switch in applications such as over/under temperature alarm, electric irons, over-temperature warnings in PC board applications, and more.

If the thermistor is biased in a self heated region, the circuit can be used as vacuum alarm, CO_2 detection or even as an ice indicator in transport applications. The hystersis of the circuit is user definable and can be set by choosing appropriate values of R1, R5, and R6. With a relay (e.g. a triac) as a load to control the AC cycle, the circuit can work as a proportional controller. During the dead-band, the final control element remains unaware of the measurand status. Thermistor arrays are required in many medical applications, including measuring regional cerebral blood flow. The micro-logic version of this circuit can be sued for this purpose with an array of thin-film thermistors suitably arranged on the substrate. This circuit can also be sued to study temperature changes in relation to change in the composition of anaesthetic gas. It can also be used to record chemical reaction enthalpy in a microcalorimetric device.

4.4 Part II : Analogue to Digital Converter With Non-linear Transfer Function for Thermistor Applications

4.4.1 Non-linear ADC for Thermistor Interfacing to Digital Systems :

The section 4.3 describes a sensor with digital output. However, when digital systems are to be implemented for temperature measurement, control, and protection, the Analogue to Digital Converter (ADC) can not be avoided. The ADC converts voltage equivalent of temperature, into a digital form, which can be read by the processor and manipulated as needed to support the application. However thermistor characteristics has some peculiar features that makes interfacing the device with the digital systems a challenge. The transfer function of thermistors is highly non-linear and hence a compensation for the non-linearity with a look-up table, is required in a digital system. However this leads to a loss of resolution. Several researchers [39-41,62,67,90-93]have worked on analog signal conditioning modules like log converter, shunting two thermistors, etc. to compensate the non-linearity. This technique results into erroneous measurement as the errors will add up from the thermistor-resistor combination, the amplifier offset voltage, the tolerance of gain-setting resistors, errors due to ADC, and the voltage reference error (which may be more than the intended application can tolerate). Another striking feature of thermistor-ADC interfacing is the need for variable resolution due to its variable dynamic range which can be described in terms of variation of temperature

coefficient of resistance, material constant and resistance ratio with temperature. The problem could be solved by dividing the measuring range into several subranges and using variable gain amplifier controlled by microprocessor. However this results in a substantial increase in the measurement time, an unnecessary expansion of hardware and possible increase of measurement errors[30]. The problem may be solved by using a non-linear ADC (NADC) with its transfer characteristics being the inverse of the thermistor characteristics. This section presents a novel modified pulse width modulation (PWM) ADC architecture suitable for thermistor interfacing. The transfer function of a pulse width modulation ADC s shaped as per the thermistor characteristics. This is achieved by varying the amplitude of the reference voltage to reach the temperature equivalence of the voltage to be digitised.

4.4.2 Pulse Width Modulation ADC :

The block diagram of a conventional technique of the pulse width modulated ADC is shown in figure 4.7.

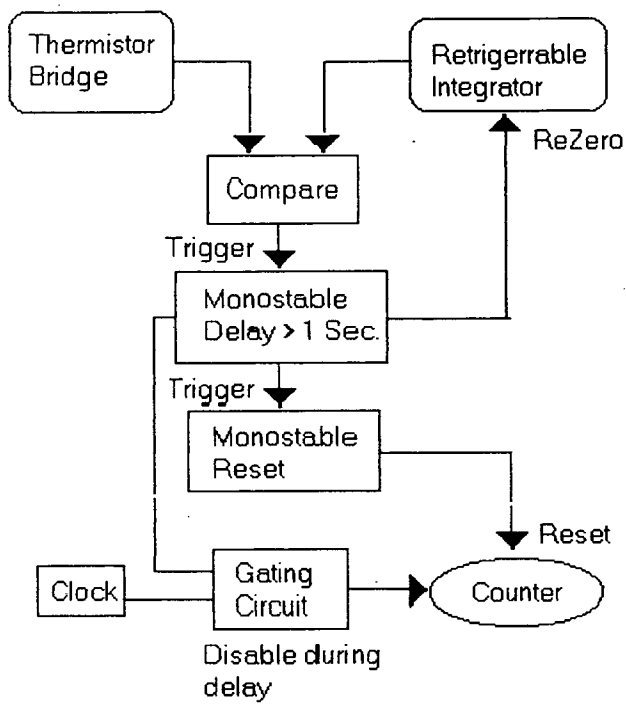

Figure 4.7 : Block Diagram of Conventional PWM ADC

The ADC operates by measuring the time in terms of pulse width of the output of the integrator to reach the output voltage of the thermistor bridge which is proportional to the temperature to be measured. A constant voltage (reference voltage) acts as input to the integrator and the value is chosen after carefully studying the measurand voltage range. The measurement cycle consists of (i) rezeoring the counter and integrator (ii) beginning of the integration and counting (iii) Stopping the integration when the integrator output equals that of bridge output (iv) Delaying few microseconds to allow the counter to read final value and simultaneously disabling it (v) Repeating the process.

In this method, the integrator output reaches the input voltage with a fixed slope equal to the time constant RC. This leads to a non-linear digital output code for a given temperature. To overcome this drawback, it is proposed to modify the architecture of conventional PWM ADC with an additional thermistor which is placed in the vicinity of the process. This forms the R of the integrator time constant and thus the slope of the output sawtooth waveform varies in a non-linear fashion and adapts itself with the characteristics of thermistor in the bridge.

4.4.4 The Modified Architecture:

Figure 4.8 shows the schematic of the modified architecture of PWM ADC to suit the thermistor requirements.

The thermistor bridge with the instrumentation amplifier gives the voltage equivalent of temperature at the inverting terminal of the comaprator. The saw-tooth waveform is generated by a integrator based on Op-amp and a transistor switch. The capacitor charges through Rt2 with a time constant Rt2C. The discharging is controlled by a 'rezero' pulse generated by the monostable multivibrator 1. At time t=0, the output of the thermistor bridge is higher than that of sawtooth amplitude. The capacitor C

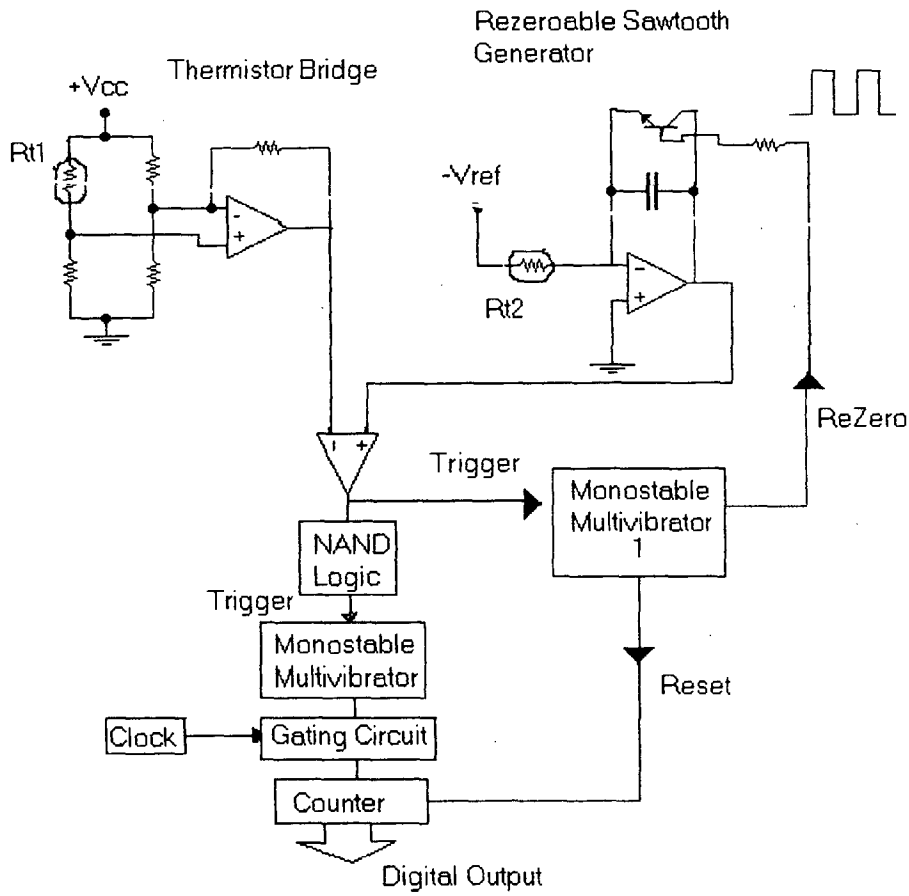

Figure 4.8 : Modified PWM ADC with Non-linear Transfer Function

starts charging with a slope equal to Rt2C towards the supply voltage thus generating a positive going ramp. The output of the comparator is low and the NAND logic ensures triggering of monostable. The monostable output is high which enables the gating circuit and the counter starts up counting. When the positive going ramp reaches the bridge voltage, the comparator output becomes high, triggering the monostable multivibrator 1, which gives a 'rezero' pulse to integrator, which makes the transistor ON, and thus initiates discharging of capacitor. After a delay of few microseconds a pulse is also given to the counter to reset it. The delay is intentionally kept to latch the final counter reading. The cycle of operations is repeated continuously thereby giving a digital equivalence of the temperature at the output of counter.

4.4.5 Simulation :

The circuit blocks shown in figure 4.8 were simulated successfully using Spice3. The instrumentation amplifier was simulated using two ideal op amps and a single active op amp. The thermistor response was simulated using the EXP model described in Section 5.4. From the overall simulation, the variation of slope of sawtooth waveform with temperature was evident. Timing diagrams of a typical simulation are shown in figure 4.9. The circuit was designed, fabricated and tested with op-amps like LM 741, instrumentation amplifier LM 725, monostable multivibrator IC 74121, AND gate 7400, universal counters ICM7226B and a 74c14 Schmitt trigger inverter based clock circuit. The thermistor TA1 (refer Chapter II, Part II)

were used with the bridge thermistor placed at the center of a tubular furnace and the second thermistor placed in the close vicinity. The monostable pulse width is designed to be 1 Second keeping in mind the temperature range right from room temperature to 150°C.

4.4.6 Conclusion :

Presently used linear ADC technology poses various limitations while processing output of sensors like thermistors having highly non-linear characteristics. In this section we have presented a novel modified PWM ADC architecture having a non-linear transfer function suitable for digitising thermistor output. In a way of digitisation the non-linearity of the thermistor is cancelled due to the adaptability of the sawtooth waveform. The circuit was successfully simulated using Spice3. The discrete version was constructed using general purpose ICs and was found to be working satisfactorily. The architecture suggested is suitable for integration in the form of a semi-custom IC.

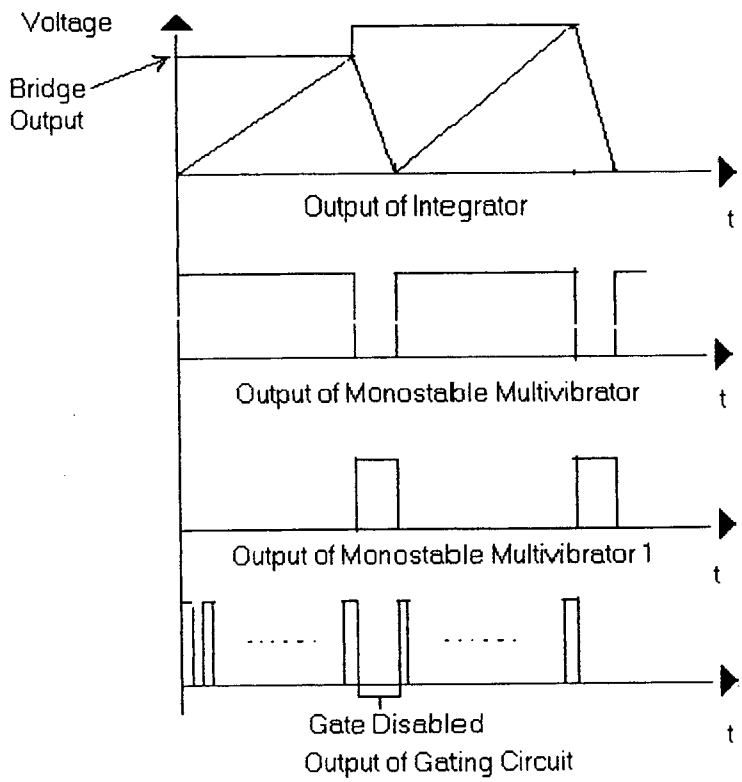

Figure 4.9 : Timing Diagrams of Modified PWM ADC

4.5 Part III : A Low Voltage ASIC for Biomedical Temperature Measurement

This section presents architecture of a low power digital ASIC based on NTC thermistor for biomedical temperature measurement applications. The thermistor is coupled externally to a low power astable multivibrator, which modulates its pulse width. The modulated pulse width is detected in terms of the number of clock pulses counted by a counter. The counter output is processed by on chip processor to display the temperature. The ASIC supports many advanced features like self configuration, prediction and self calibration and correction.

4.5.1 NTC thermistor for Body Temperature Measurement :

For centuries, elevated body temperature has been recognized as an indication of illness. As part of the traditional "vital signs," temperature trends remain a simple and direct way of tracking a patient's progress and is the means of clinical assessment and decision making. NTC thermistors have a long history in biomedical applications [76]. Miniaturized thermistor arrays with minimal heat dissipation and high temperature resolution have been used for detection of temperature gradients and temperature changes originating from metabolic activities[45]. Other temperature sensors like RTD and silicon based PN junctions have also been used in biomedical field [96]. Though thin films of RTD exhibit high reproducibility and accuracy in a four wire configuration, there applications are limited due to their size.

Monolithic CMOS, poly-Si, μ-Si or P-N junction based temperature sensors have the advantage of on chip integration, but are limited in temperature range and most importantly in measurement resolution. The intrinsic high resolution of thermistors besides their highest sensitivity is the main cause for their wide acceptance in clinical appliances. The other factors favouring their choice for clinical applications is their usage in small temperature range (268-323K) minimizing the linearisation problems. The increasing need for continuous recording, remote measurement and telemetering, makes thermistor the most appropriate sensor, as the lead resistance has very little effect on the overall characteristics. The cost effectiveness of the thermistor probes allows us to use them as disposable probes after application to patients with dangerous or highly infectious diseases, thus eliminating tedious sterilization procedures. There are however some detrimental factors like the limitations on homogeneity within a small mass of semiconductor substances of which the thermistor is synthesized. The uniformity from piece to piece is also difficult to achieve, considering the grain size within the sinter body. The problem of interchangeability (tolerance from unit to unit of the resistance temperature characteristics) also exists besides the ageing in characteristics. The response time of thermistors is an inverse function of their mass or size posing a typical speed Vs accuracy dilemma. Though the most of these problems have been taken care as discussed in chapter 2, they can not be fully eliminated. These residual effects could be intelligently tackled in a smart sensor

architecture operating in digital environment. This type of smart sensor revolutionizes the design of sensor systems, and makes it easier, cheaper, and faster [28]. The resulting systems becomes more reliable, more scaleable, and provide higher performance than traditional systems. This section presents a low power clinical ASIC based on thermistor.

4.5.2 Sensor Interface For The ASIC :

There are good number of ways to read and display the thermistor output. The most of the techniques are based on Wheastone's bridge and analog to digital conversion (ADC) with a microcontroller or microprocessor. With ADC interfacing the typical problems are sensor and ADC range incompatibility, errors introduced by conditioning circuits, limited resources to correct the non-linear transfer functions for sensors like thermistors etc. Although Wheatstone's bridge is a versatile technique to convert thermistor resistance into voltage, it suffers from extremely low level output susceptible to noise and the non-linearity of the bridge elements which considerably influences the output. With the advent of low cost microcontrollers, (having a rich set of mechanisms to measure frequency, pulse width, or period), the pulse width modulation scheme has really become very popular. Here the sensor modulates the on time of the pulse which can be sensed with the serial ports having capability to detect the pulse edges. This kind of resources available with today's microcontrollers simplifies the interface for resistive sensors. Besides the highest achievable measurement precision, the PWM scheme also

eliminates the need of power hungry analog to digital converters. The ASIC reported here comprises of an astable multivibrator in which the NTC thermistor is embedded as an external component. The output of the astable multivibrator is modulated as per the instantaneous temperature value. The modulated pulse width is measured in terms of clock pulses by using an electronic up counter circuit by activation of a gating circuit opened during the ON time of the output. The output of the counter is further processed by the on chip microprocessor that displays the output temperature on a suitable display. The block diagram of the ASIC is as shown in figure 4.10.

4.5.3 Sensing Core :

The sensing core for the ASIC is based on a very low power astable multivibrator [180] as shown in the following circuit diagram. The circuit is powered by 1.5V silver oxide cell, having a current rating of 160 mA per hour. The circuit has been designed with special emphasis on the low power aspect. It consumes average current of 300 nA and a power of around 450 nW at 1.5V supply. The output pulse width is modified by the thermistor Rth which can be externally connected to the chip and applied to patients body through a cuff.

4.5.4 The Processor And Associated Innovative Features Of ASIC :

The proposed ASIC is based around an eight bit RSIC processor core with 32Kb of dedicated scratchpad RAM, 8Kb in-system programmable Flash RAM and a further 512 bytes of non-volatile EEROM

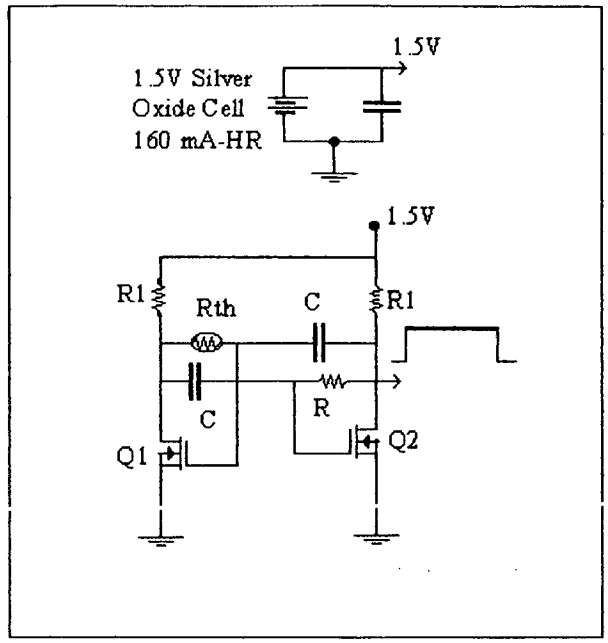

Figure 4.11 : Sensing Core of the ASIC

used to store configuration and calibration information. The non-volatile Flash RAM module saves all the data collected during a specified time which then can be printed out for clinical assessment. The processor proposed to be embedded on the ASIC is a simple 8 bit RISC type. The processor is supported by a set of registers viz. control register, finite impulse response (FIR) coefficient register and four registers to store the calibration coefficients. The control register is further supported by an interface to control signals. The chip supports a good number of control and handshake signals like start (starting measurement), test (self test), reset (resetting chip and counter), end of conversion (EOC), PRG (for

programming the EEPROM). The sensor signal register stores the output of the counter till it gets processed by the processor.

4.5.5 Digital To Analog Converter :

For the purpose of simulation, digital to analog converter is modeled using the ADC and DAC converter library provided by Open Verilog International (OVI) as follows [125,126].

```
module ideal_dac(in,out);
 input [0:dac_size-1] in;
 output out;
 voltage in,out;
 parameter real dac_size = 2 from (1:inf);
 parameter vth = 2.5;
 parameter real trise = 0 from [0:inf);
 parameter real tfall = 0 from [0:inf);

 real code;
 integer pow2 [0:dac_size];

 analog
 begin
  @(initial_step)
   for (i=0;i<=dac_size;i=i+1) pow2[i] = pow(2,i);

  code = 0;
  for (i=0;i<dac_size;i=i+1)
   code = code + (V(in[i]) > vth) ? pow2[i] : 0;
  V(out) <+ transition(code/pow2[dac_size],0,trise,tfall);
 end
endmodule
```

4.5.6 Salient Features Of The ASIC :

The ASIC supports many advanced features which helps in eliminating the limitations of the thermistor. The response time problem stated at the beginning, is eliminated by using prediction feature. The calibration, linearisation and regeneration of temperature is based on the Steinhart-Hart equation.

The chip can be made to support the auto-reconfiguration feature. This can be implemented by calculating the coefficients A,B,C at three data points minimum(A), middle(B), and maximum (C). Then the on board processor determines the A, B, and C coefficients. These coefficients are stored in calibration coefficient registers and used by the processor whenever required. An intelligent implementation detects the ageing of the thermistor. The chip automatically compares the resistance temperature values generated in several cycles and on detection of drift recalculates the Steinhart-Hart coefficients. The prediction feature is based on a latest U.S. patents[128,163] finite impulse response filter is configured so as to sample the temperature signal a plurality of times to calculate an estimate of the temperature measured and provide an estimated final temperature signal. The processor applies a weighting factor to each of the average value, the first derivative, and the second derivative of the signal, and further adds an offset factor selected in accordance with the ambient temperature, to calculate a prediction of the temperature of the object. The prediction feature allows completion of the temperature measurement much

before thermal stabilization is attained, thereby reducing the measurement time[128]. This reduces risk that the patient would not hold the probe in the correct position for the entire measurement period and requires less time of the attending medical personnel. Another advantage is that because body temperature is dynamic and may significantly change in short time span, a rapid determination offers more timely diagnostic information. In addition, the accuracy with which the temperature is predicted improves markedly as the processing and analysis of the data are more accurately performed.

4.5.7 Results :

Architecture of low power ASIC based on thermistor for clinical temperature measurement application has been proposed in this paper. The entire signal conditioning and processing blocks have been proposed to be integrated on chip. The analog blocks are successfully simulated using SPICE-3. The digital modules are simulated by using Verilog Hardware Description Language. The entire architecture contains few major hardware components like few shift registers, up counter, arithmetic and logic units etc. So it can be realized in a single VLSI chip. As the fabrication was not possible the features like reconfiguration, calibration using Steinhart-hart equation and prediction were tested by developing programs in 'C'. Based on the outputs of these programs the hardware requirement of the chip was finalized.

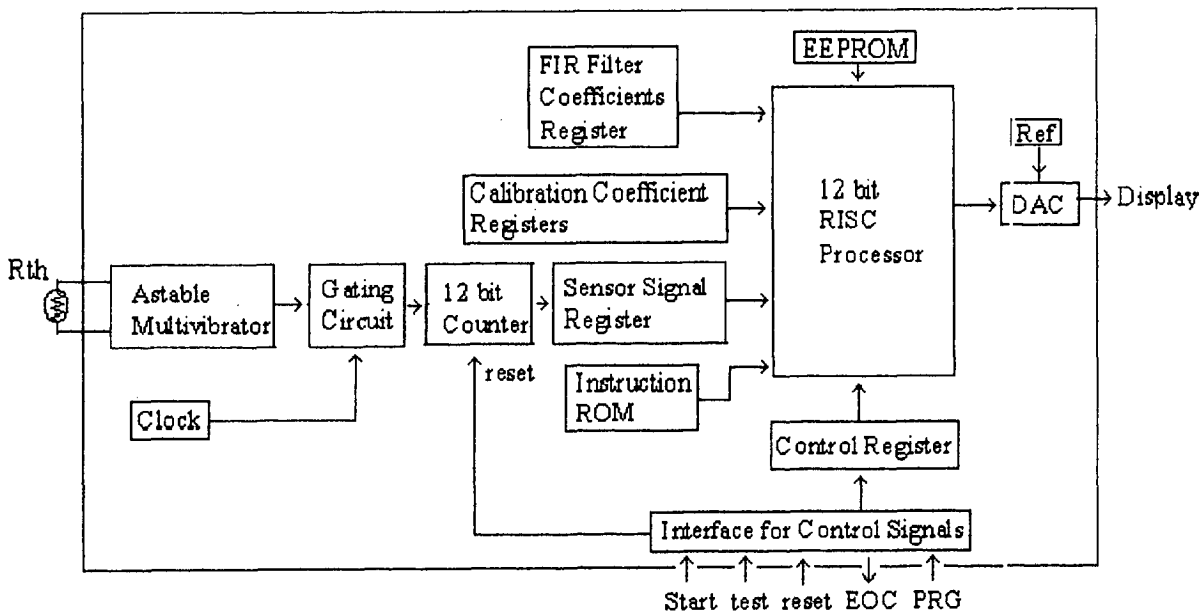

Figure 4.12: Block Schematic of the proposed ASIC

CHAPTER 5

Summary and Conclusion

5.1 Summary:

Life without any senses seems impossible. On the other hand; sensors of all kinds try to mimic the certain senses of living organisms, have developed in order to interact with the environment. Sensors are the most vital elements for building intelligent systems. Advanced sensor technology has been identified world over as one of the important technologies for the future. With the advent of information technology and easy availability of large processing power, advanced sensors will be utilised in several walks of human life. An analysis of the world market on production of sensors shows the following trend in sensing areas: temperature 33%; displacement and proximity 23%; flow and level 13%; pressure and force 8%; magnetic field 5%; optical 5%, chemical 3%, humidity 2%, and others 8%. [205-206] Thus, the authors claim that temperature sensors of ambient conditions are in heavy demand. The authors have also emphasised wider use of thermistor sensors because of their advantages like small size, high accuracy and resolution, highest sensitivity, low cost, least power dissipation etc. However, presently available thermistor products are still far from fully meeting the market needs. The present market requires thermistors to achieve further reductions in cost, high precision, better interchangeability, and realise a wider measurable temperature range by going lower in the materials constant among various other requirements. Most of the above mentioned

aspects for the improvement of thermistors are investigated in the present thesis.

The main aim of the thesis is development of high performance NTC thermistors. This requires an interdisciplinary approach of ceramics technology, solid state chemistry, electronics, hardware and software techniques. The global growth economics presented in chapter 1 justifies the importance of investigation on this topic. The same is further strengthened by presenting the good number of applications. Various thermistor configurations are also compared with a conclusion that the device specifications are more dependent on the fabrication technology rather than the style or geometry. The chapter justifies the main objectives of research work and systematic plan to improve various characteristics and specifications.

The follow-up of the importance of materials synthesis technique is persuaded in the chapter 2. At the outset, the choice of the material (i.e. nickel manganite) is justified and supported with research based on investigations of other researchers. Various synthesis techniques with their pros and cons are presented. Fabrication of nickel manganite based disc type NTC thermistors are reported in the first part of this chapter. One of the technique used in part I (i.e. oxalic precursor route) is extended to tailor the room temperature resistance of the thermistors varying the stoichiometry. The details are given in part II. The part III of this chapter,

presents the device fabrication aspects and an improved method of lead attachment.

Instrumentation systems for test and characterisation for the thermistors fabricated are presented in depth in chapter 3. The details of automated characterisation set-up to record the characteristics like resistance Vs temperature, current Vs voltage is presented. The time constant and dissipation constant are also calculated by using various other set-ups described here. The details of effects of moisture on samples is also reported and is followed by the listings of the software used for various characterisation.

The development of silicon micromachined sensors enables physical transducers to be integrated with control and signal processing electronics in a single, compact package. This type of "smart" sensors have revolutionised the design of sensor systems, making them more reliable, better packaging, which provide higher performance than traditional systems. These benefits are gained by embedding computing resources on the sensor itself. Chapter 4 presents three architectures of smart sensor design, namely, modified Schmitt trigger transducer, non-linear ADC and a low power ASIC.

5.2 Results and Conclusions:

From the present studies following results and conclusions drawn:

1. Despite the many drawbacks associated with NTC thermistors, their development is expected to continue on a larger pace, and the market

appears to be promising. Several emerging research trends contribute to such a perspective: (i) better understanding of sensing mechanisms due to increased efforts in basic studies in recent years; (ii) new and improved materials synthesis and device fabrication techniques; (iii) application of hardware and software techniques to minimise the drawbacks; (iv) developing sensor with embedded signal processing modules for more specific or focused applications.

2. The carboxylate precursors of nickel manganite were prepared by using fumarate, succinate, oxalate, tartarate and malonate. The XRD studies reveals a good agreement of observed d-values with the standard ones reported in JCPDS file [189]. This confirms the formation of $NiMn_2O_4$.The lattice parameter values calculated are in the range of 8.37 to 8.39. This is in good agreement with the reported values of 8.37 to 8.41 for $NiMn_2O_4$. The calculation of bond lengths (R_A and R_B and site radii (r_A and r_B) shows no remarkable change in their values for the fabricated samples. The percentage of Nickel and Manganese was found out by using AAS and agrees with the stoichiometric ratio in $NiMn_2O_4$. The TG/DTA studies shows that the total decomposition of different carboxylate precursor takes place between 325°C to 400°C. Dehydration of the carboxylate precursors takes place below 250°C.
3. Nickel manganite based disc type pellets prepared by using carboxylate precursor route, exhibited their NTC thermistor behaviour in domestic temperature range. All these thermistor samples have moderate value

of materials constant (β). The tolerance of β is in the range of ± 0.003% to ±0.009%. The resistance ratio is in the range of 5.09 to 6.31. These specifications are comparable and even better than those reported in the literature for disc thermistors. Moderate β values with minimum tolerance indicates a good measurement precision. Improved resolution is indicated by the high values of resistance ratio. This satisfies the our main objectives: optimisation for domestic applications; improving figure of merit; better resolution.

4. The precursors of nickel manganite with stoichiometry $Ni_{1-X}Mn_{2+x}O_4$ with $0 \leq x \leq 0.6$ were prepared by using oxalic precursor route. XRD studies of the decomposed oxalic precursor at different temperature reveals the total decomposition and formation of single phase nickel manganite at 600°C. The TG/DTA analysis shows the dehydration of the precursors below 200°C and a total decomposition at 325°C. The lattice parameter values are in the range of 8.37 to 8.39, which is in good agreement with the standard reported ones. The percentage of Nickel and Manganese in the oxalic precursors was found out by using AAS and agrees with the stoichiometric ratio in $NiMn_2O_4$. The disk type pellets fabricated exhibited a non-linear R Vs T characterisation in the range 27°C to 170°C. Wide variation in the room temperature resistance in the range of 55.4K to 6.1K was observed with change in stoichiometry. The β values of all these thermistors are in the range of 940 K to 1834 K. The resistance ratio is in the range of 2.20 to 4.68. Thus the power

consumption may be tailored by choosing the proper composition in this series having appropriate dormant resistance, which also constitutes one of the objectives.

5. The leads are attached to the thermistors with conventional method and a new method. With the same stoichiometry and dimensions, the thermistors fabricated with the conventional method exhibited poor interchangeability of the order of ± 1.5°C. The reasons attributed to poor interchangeability and ageing are poor control on the geometry, varying electrode shape and lead wire attachments from sample to sample. The new method with the modified jig, exhibited better interchangeability of the order of ±0.2°C and less ageing characteristics. All the thermistor samples prepared by carboxylate and oxalic precursor routes were found to follow the Steinhart-hart equation.
6. Zero power resistance variation with temperature, time constant and dissipation constant influence the measured temperature. An automated set-up for resistance VS temperature characterisation of thermistors is designed. The set-up comprises of a furnace, thermocouple amplifier, AD574 based analogue to digital converter and HP34401A DMM. The furnace for materials synthesis (temperature upto 1200°C) and characterisation (temperature upto 300°C) are designed. A thermocouple based temperature controller controls the temperature of materials synthesis furnace within ± 0.8°C. A d.c. high wattage power supply with ratings of 24 V at 3 A, 15 V at 6 A and 6V at 6A powers the

characterisation furnace. A RTD based temperature controller controls the temperature of this furnace.

7. The automated set-up designed to evaluate dissipation constant and time constant gave a dissipation constant in the range of 1.5mW/°C to 4 mW/°C and time constant in the range of 0.5 to 1 Second. With dissipation constant known, the value of current excitation can be decided. e.g. With measurement range 25°C to 50°C, with a desired resolution ΔT of 0.1°C and thermistor room temperature of 1K and dissipation constant 4 mW/°C, the maximum power must be restricted below Pmax = $\Delta T*D$ i.e. 0.4 mW to avoid self heating.
8. The conventional flip-flop sensor design was applied to thermistor and a modified Schmitt trigger sensor is proposed. The circuit was successfully simulated.
9. The architecture of PWM ADC was modified for thermistor applications and the same was simulated.
10. The architecture of low power thermistor based ASIC for clinical applications is proposed and simulated.
11. The above results indicate that all the objectives undertaken for the development of a high performance NTC thermistor are fulfilled.

Chemistry of Materials

The details of the chemical aspects of the samples developed in chapter 2 are covered under this appendix.

1. Chemical Analysis:

The percentage of Nickel and Manganese in the precursors was found out by using atomic absorption spectrometer AAS model PE3030. The percentage of Ni and Mn was found to be in the stoichiometric ratio as is there in $NiMn_2O_4$.

2. X-RAY Diffraction Studies:

2.1 Theory :

X-ray diffraction technique is a well established technique to study the crystal structure of the material. The XRD reveals the following information:

(i) confirm the completion of solid state reaction

(ii) Observe the impurity phases

(iii) determine the lattice constants, interplanar distances, octahedral and tetrahedral site radii and bond lengths etc.

The well known Bragg's law gives the relationship of diffracted x-rays from the (h k l) planes as follows:

$$2d_{hkl} \sin\theta = n\lambda \quad \text{---------- (1)}$$

Where d_{hkl} is the interplanar spacing of crystal planes of miller indices (h.k.l), θ is glancing angle, λ is the wavelength of x-ray radiation and n is the order of diffraction.

(in most of the cases, the first order diffraction where n=1 is used). Bragg's law applied to cubic crystal takes the following form

$$d_{hkl} = \frac{a}{(h^2 + k^2 + l^2)^{1/2}} \quad \text{---------- (2)}$$

Where a is the lattice constant.

From equations 1 and 2 the expression for the lattice parameter is given as

$$a = \frac{\lambda}{2 \sin \theta} (h^2 + k^2 + l^2)^{1/2} \quad \text{---------- (3)}$$

2.2 Experimental :

There are several methods of X-ray diffraction: Laue method; rotating crystal; powder. The powder method of X-ray diffraction is used in present studies. In this method the fine grained powder is filled in a capillary tube. The diffraction occurs simultaneously from the individual crystallites that happen to be oriented with planes having the same angle of incidence θ. At the outset, the wavelength is fixed and crystal is rotated. Recently counter diffractometers have been developed an arm carrying Geiger counter records the diffracted x-rays from the surface of the sample placed at the center. The XRD machine gives a complete diffraction pattern, by rotating the sample by an angle θ and the counter by 2θ.

The X-ray patterns of the decomposed TF, TS, TM, TO and TT were recorded on the fully computerised XRD unit PW1710 with Cu Kα radiation and nickel as a filter. The x-ray diffraction patterns were taken with 2θ values ranging from 20° to 80°.

Since the thermistor material used in present studies i.e. nickel manganite is a standard spinel, its lattice parameter (a) ranges between 8.33 A° to 8.39A°. The planes that diffract in cubic spinel systems are (111), (220), (331), (222), (400), (333), (533) etc. However, the plane (311) is the most intense one in spinels. The lattice parameter 'a' is calculated from observed d values of (311) plane. The observed d-values of all the samples were also compared with the standard ones reported in JCPDS file [189]. They are found to be in good agreement.

The interplanar distance (d) for each diffraction angle was calculated by using the equation 2. The tables 2 to 6 shows the values of observed and calculated d for carboxylate precursors. The d values for oxalic precursor decomposed at various temperatures are given in the tables from 7 to 9. The values of the lattice parameters calculated are in the range of 8.37 to 8.39. These values are in good agreement with the reported values of 8.37 to 8.41 for $NiMn_2O_4$.

Using the value of u = 0.383 A° reported in standard references [2, 81-83], the values of bond lengths (R_A and R_B) and site radii (r_A and r_B) were calculated using the following relations:

$$R_A = a\sqrt{3}\ (\delta + 1/\delta) \qquad \text{----------(4)}$$

$$R_B = a\sqrt{1/16 - \delta/2 + 3\delta^2} \qquad \text{----------(5)}$$

$$r_A = (u - \tfrac{1}{4})\, a\sqrt{3} - Ro \qquad \text{----------(6)}$$

$$r_B = (5/8 - u)\, a - Ro \qquad \text{----------(7)}$$

Where R_A = Distance of cations from oxygen in A site.

R_B = Distance of cations from oxygen in B site.

Ro = Radius of Oxygen ion = 1.35 A°.

r_A = Tetrahedral Site radius.

r_B = Octahedral site radius.

δ = deviation from oxygen parameter (u)

= $u - u_{ideal}$ [u_{ideal} = 0.375 A°]

The values of bond lengths (R_A and R_B) and site radii (r_A and r_B) are presented in table 6 . The bond length R_B is always greater than R_A. There is no remarkable change in the bond length and site radii of the samples.

XRD of the decomposed oxalic precursor at different temperature was studies as can be seen from the figure 1. It was found that the total decomposition of the precursor and formation of single phase $NiMn_2O_4$ takes place at 600°C.

3. Thermal Analysis:

Thermal analysis reveals the changes in physical and chemical properties of the materials with temperature. The thermal analysis techniques generally used and the respective parameter to be monitored is shown in the table 1.The thermal decomposition of carboxylates generally involves dehydration followed by decarboxylation to form oxides. In the present investigation, Thermogravimetric Analysis (TGA) and Differential Thermal Analysis (DTA) were carried out to find put the decompostion temperature of the precursor used.

Table 1: Different Methods of Thermal Analysis

Sr. No.	Thermal Analysis Technique	Parameter Measured
1.	Differential Thermal Analysis (DTA)	Temperature Difference
2.	Differential Scanning Calorimetery (DSC)	Heat Difference
3.	Thermogravimetric Analysis (TGA)	Mass
4.	Thermomechanical Analysis (TMA)	Dimension
5.	Synamic Mechanical Analysis (DMA)	Mechanical Stiffness and Damping
6.	Thermally Stimulated Current (TSC)	Dipole alignment and relaxation
7.	Dielectric Analysis (DEA)	Dielectric permitivity and loss factor
8.	Evolved Gas Analysis (EGA)	Gaseous decomposition products
9.	Thermo-optical Analysis (TOA)	Optical Properties

The thermo-gravimetric analysis of the precursor was done on STA 1500 instrument in air and oxygen atmosphere respectively. The heating rate employed was 10°C/min. The Differential thermal analysis was carried out with STA 1500 and TA SBT2960 instrument in air and oxygen

atmosphere with a heating rate 10°C/min. The TG/DTA characteristics for various carboxylate and oxalate precursors have been in the following order : TF; TT; TM; TA2; TA3; TA5; TA9; TA10; TA11.

It was found that the total decomposition of the different carboxylate precursor takes place between 325°C to 400°C forming $NiMn_2O_4$. Dehydraton of the carboxylate precursors takes place below 250°C. Similarly, in oxalic precursors, dehydration takes place below 200°C followed by total decomposition at 325°C.

Table 2: X-ray Diffraction Data of $NiMn_2O_4$ (TF)
Lattice Parameter a = 8.4040
Structure : cubic

Sr. No.	2 θ	hkl	d_{obs}	d_{cal}
1.	18.2850	111	4.8599	4.8519
2.	30.0950	220	2.9743	2.9713
3.	35.4700	311	2.5350	2.5339
4.	37.1500	222	2.4241	2.4260
5.	43.1400	400	2.1004	2.1010
6.	53.5600	422	1.7138	1.7155
7.	57.0600	333	1.6168	1.6173
8.	62.6800	440	1.4847	1.4856

Table 3: X-ray Diffraction Data of $NiMn_2O_4$ (TS)
Lattice Parameter a = 8.3687
Structure : cubic

Sr. No.	2 θ	hkl	d_{obs}	d_{cal}
1	18.3300	111	4.8361	4.8315
2	30.1650	220	2.9602	2.9588
3	35.5450	311	2.5235	2.5233
4	37.1750	222	2.4165	2.4158
5	43.2000	400	2.0924	2.0922
6	53.6150	422	1.7080	1.7082
7	57.1650	333	1.6100	1.6105
8	62.7800	440	1.4789	1.4794
9	75.3500	622	1.2603	1.2616

Table 4: X-ray Diffraction Data of $NiMn_2O_4$ (TO)
Lattice Parameter a = 8.3749
Structure : cubic

Sr. No.	2 θ	hkl	d_{obs}	d_{cal}
1	18.3650	111	4.8269	4.8351
2	30.1350	220	2.9631	2.9610
3	35.4950	311	2.5270	2.5251
4	37.1550	222	2.4178	2.4176
5	43.1450	400	2.0950	2.0937
6	53.5350	422	1.7103	1.7095
7	57.2300	333	1.6084	1.6117
8	62.6600	440	1.4814	1.4805
9	74.1500	533	1.2777	1.2772
10	75.1850	622	1.2627	1.2626

Table 5: X-ray Diffraction Data of $NiMn_2O_4$ (TT)
Lattice Parameter a = 8.3893
Structure : cubic

Sr. No.	2 θ	hkl	d_{obs}	d_{cal}
1	30.1500	220	2.9690	2.9661
2	35.5650	311	2.5284	2.5295
3	37.2350	222	2.4188	2.4218
4	43.2350	400	2.0960	2.0973
5	53.5000	422	1.7156	1.7125
6	57.0750	333	1.6164	1.6145
7	62.8750	440	1.4805	1.4830

Table 6: Data on Lattice Parameter, Bond Length (R_A and R_B) and Site radii (r_A and r_B)

Carboxylate Type	Lattice Parameter a	Bond Length		Site Radii	
		R_A-O	R_B-O	r_A	r_B
TF	8.4040	1.9360	2.0789	0.5860	0.6838
TS	8.3687	1.9278	2.0702	0.5778	0.6752
TM	8.3691	1.9233	2.0653	0.5733	0.6705
TO	8.3749	1.9293	2.0717	0.5793	0.6767
TT	8.3893	1.9326	2.0753	0.5826	0.6802

Table 7: X-ray Diffraction Data of $NiMn_2O_4$ synthesised by oxalic precursor route (TA1) Sintered at 450°C
Lattice Parameter a = 8.3911
Structure : cubic

Sr. No.	2 θ	hkl	d_{obs}	d_{cal}
1	30.2250	220.0000	2.9546	2.9667
2	35.5150	311.0000	2.5257	2.5300
3	37.3500	222.0000	2.4057	2.4223
4	43.2500	400.0000	2.0902	2.0978
5	53.2200	422.0000	1.7197	1.7128
6	57.1050	333.0000	1.6116	1.6149
7	72.8100	533.0000	1.2979	1.2796

Table 8: X-ray Diffraction Data of $NiMn_2O_4$ synthesised by oxalic precursor route (TA1) Sintered at 550°C
Lattice Parameter a = 8.3721
Structure : cubic

Sr. No.	2 θ	hkl	d_{obs}	d_{cal}
1	30.1800	220	2.9589	2.9600
2	35.5300	311	2.5246	2.5243
3	37.1400	222	2.4188	2.4168
4	43.1800	400	2.0934	2.0930
5	53.5850	422	1.7089	1.7089
6	57.1350	333	1.6109	1.6112
7	62.7650	440	1.4792	1.4800

Table 9: X-ray Diffraction Data of $NiMn_2O_4$ synthesised by oxalic precursor route (TA1) Sintered at 600°C
Lattice Parameter a = 8.3799
Structure : cubic

Sr. No.	2 θ	hkl	d_{obs}	d_{cal}
1	30.1450	220	2.9622	2.9628
2	35.5050	311	2.5264	2.5267
3	37.2250	222	2.4135	2.4191
4	43.1000	400	2.0971	2.0950
5	53.4850	422	1.7118	1.7105
6	57.0250	333	1.6137	1.6127
7	62.6500	440	1.4817	1.4814

Figure 1 : XRD Patterns of Decomposed $NiMn_2O_4$ at different temperatures

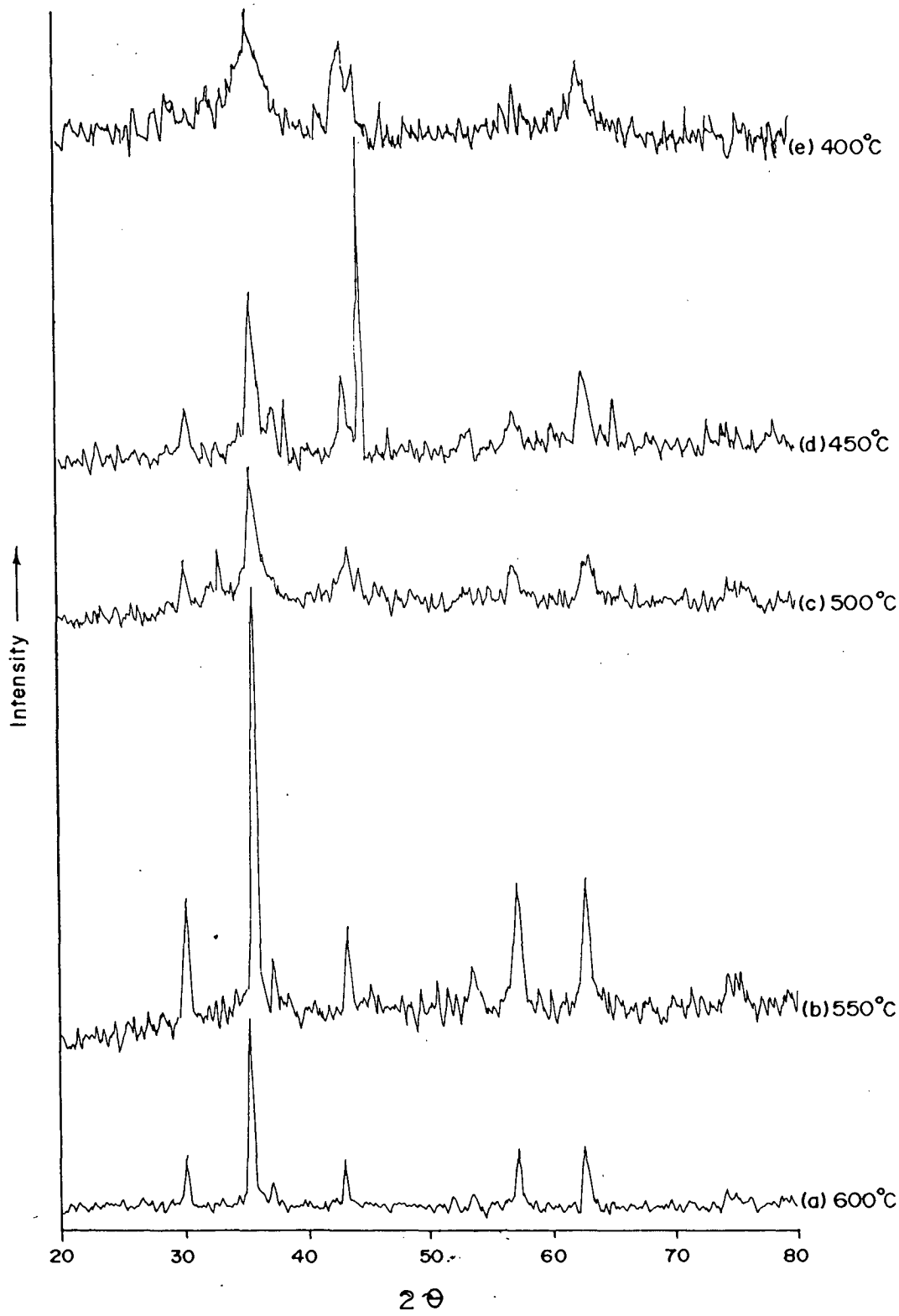

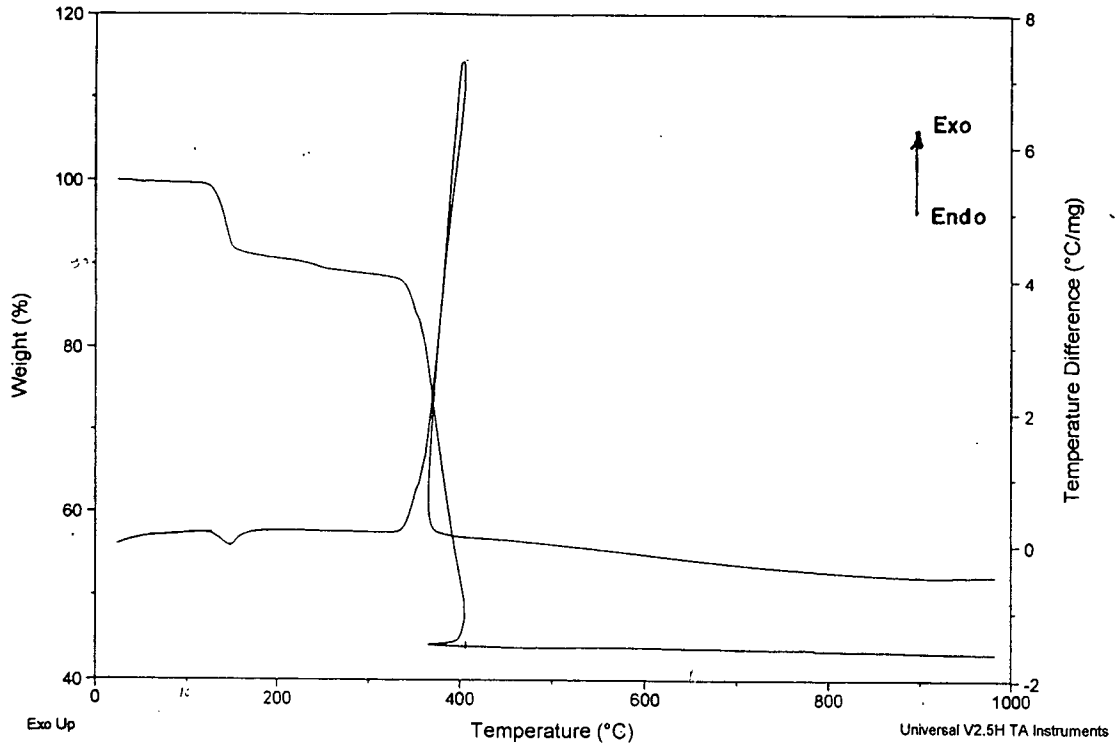

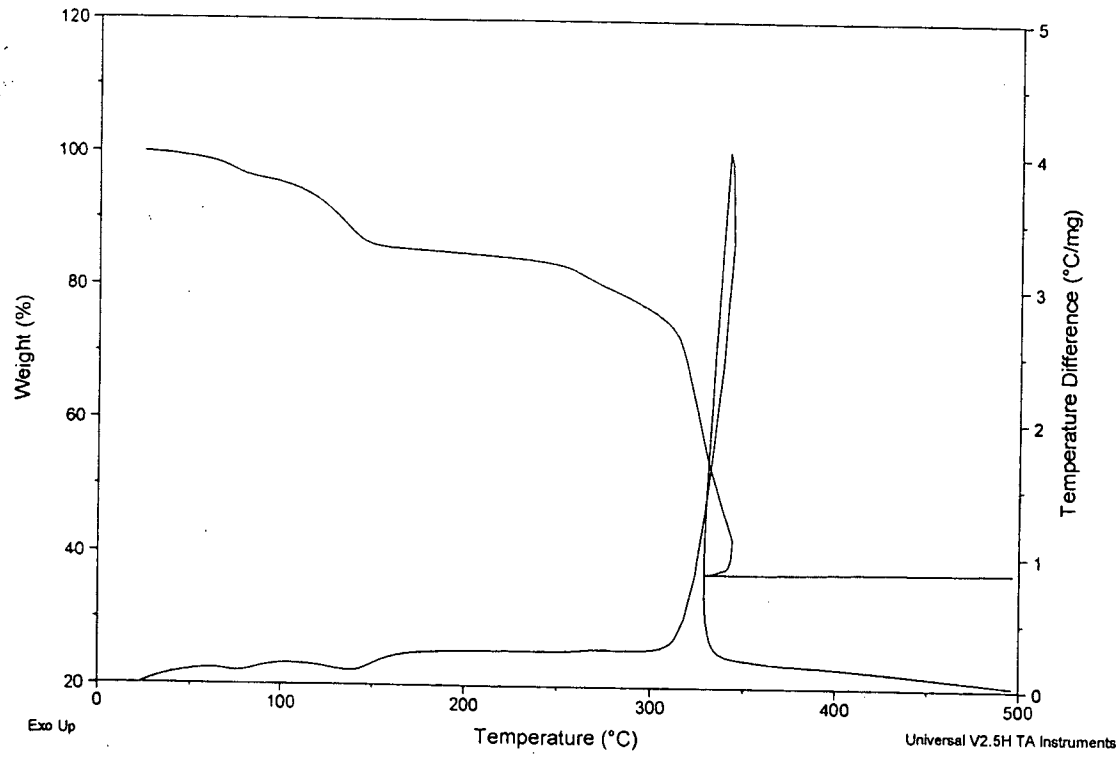

Figure 2 a.: TG/DTA Traces of TF and TT

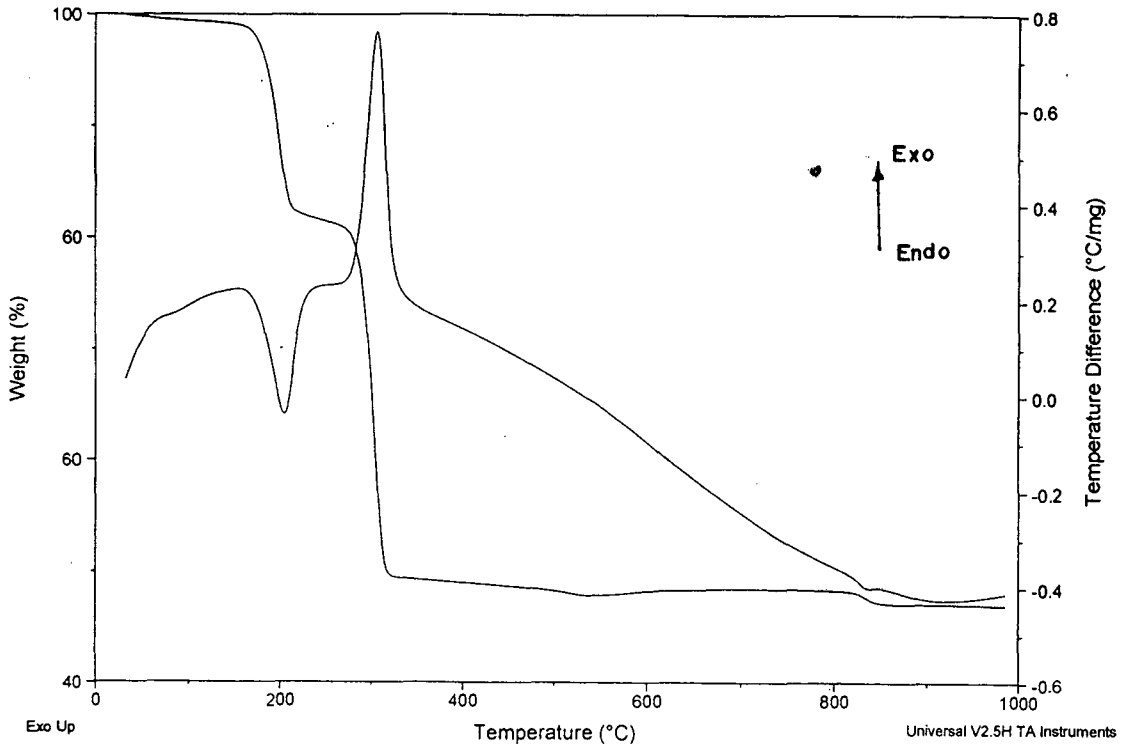

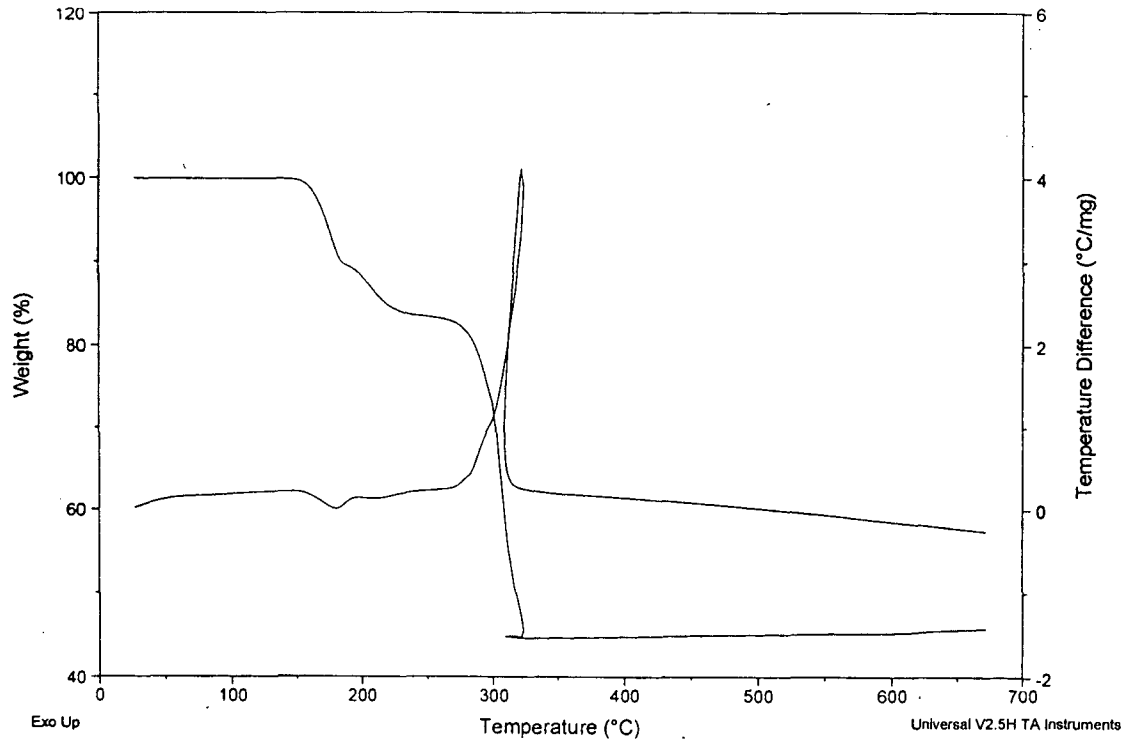

Figure 2 b.: TG/DTA Traces of TA2 & TM

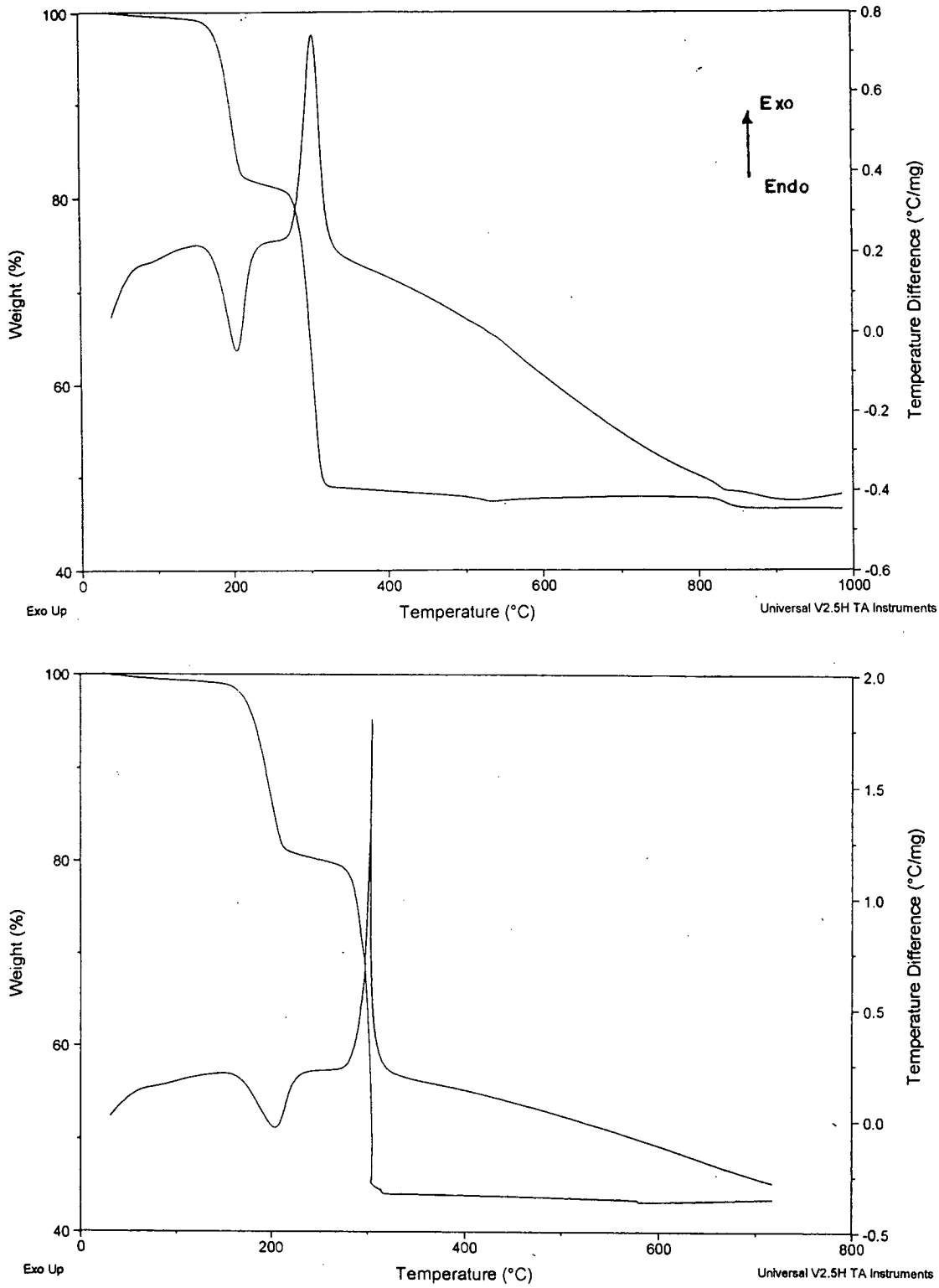

Figure 2 c.: TG/DTA Traces of TA3 and TA5

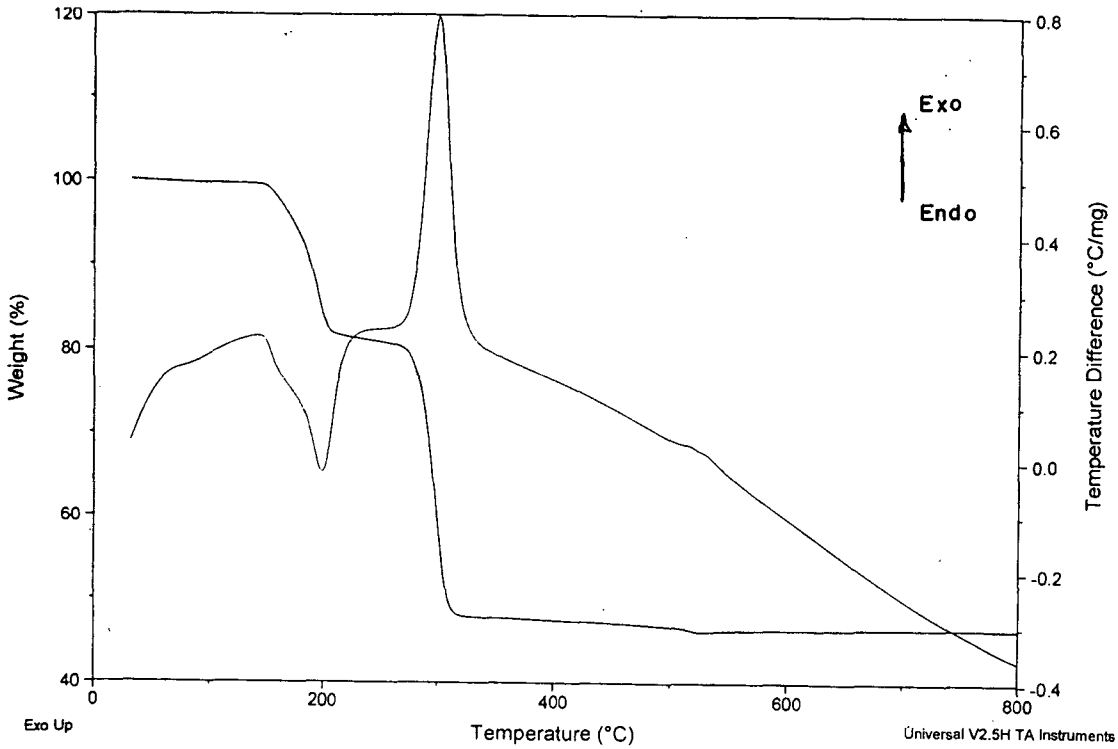

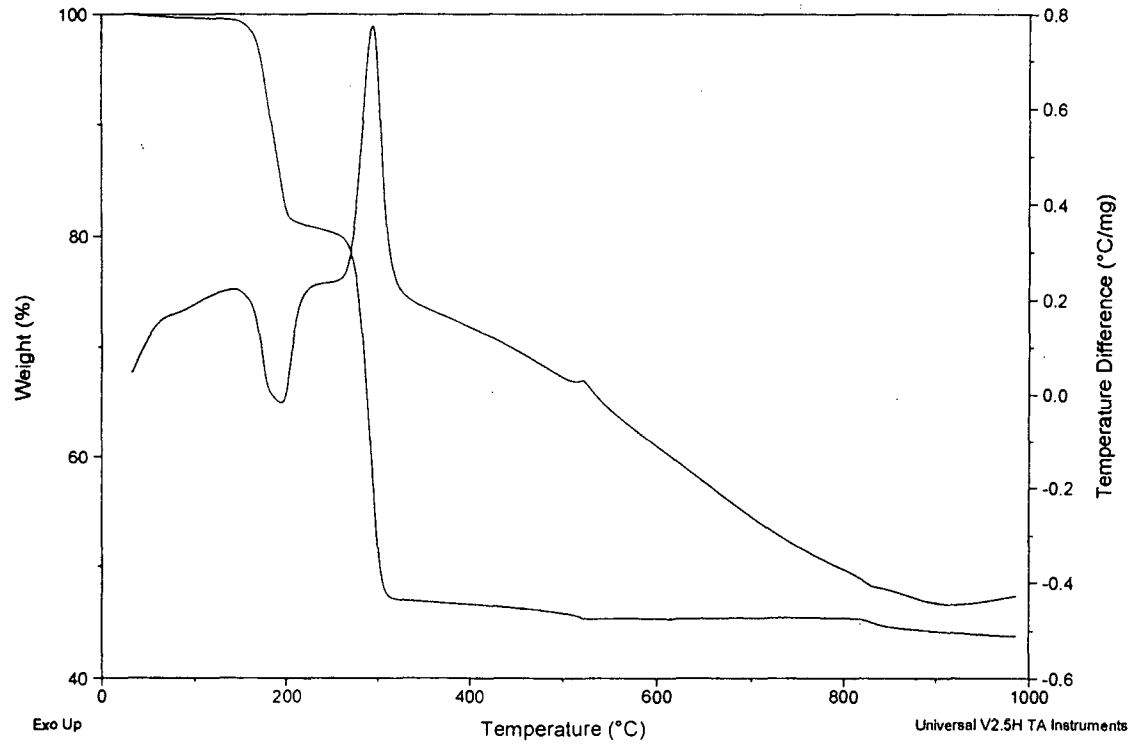

Figure 2d.: TG/DTA Traces of TA9, TA10.

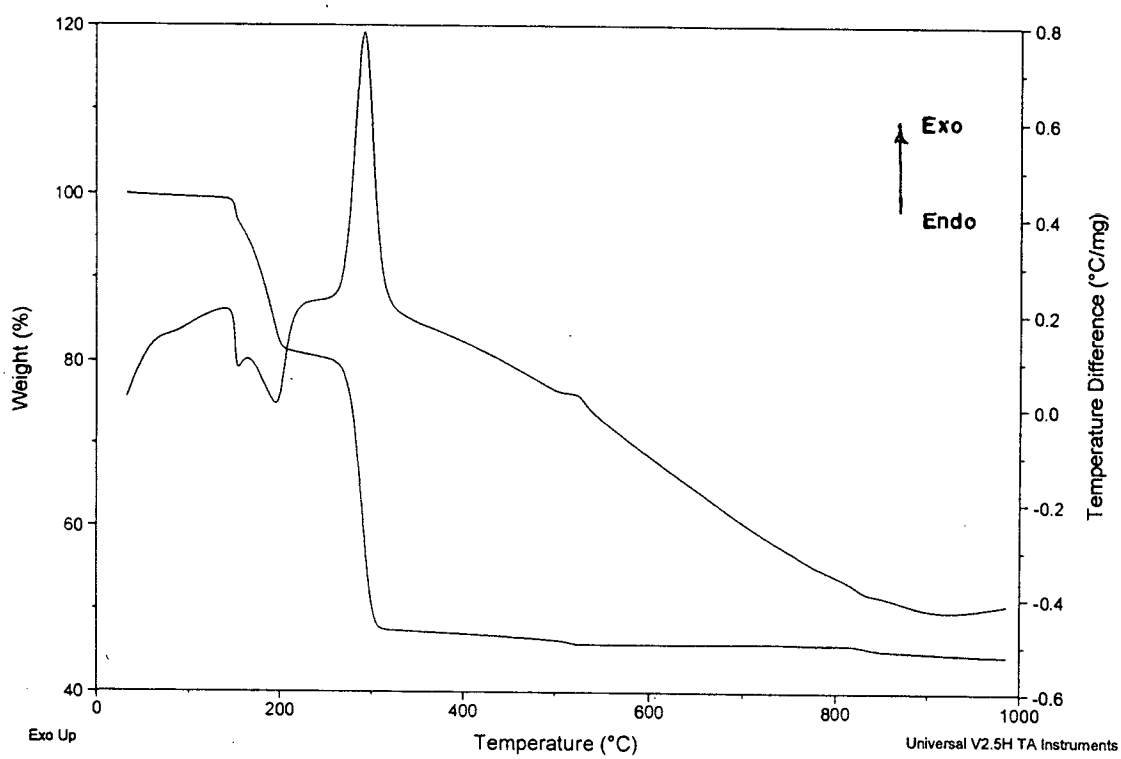

Figure 2e.: TG/DTA Trace of TA11

Explanation of TG/DTA traces:

The TG/DTA trace of hydrated Nickel Manganese Fumarate (figure 2a) shows the total decomposition of the complex at 400°C to form $NiMn_2O_4$. The observed total weight loss of 56.90% matches closely with the theoretically calculated weight loss of 57.40%. The complex remains almost stable upto 120°C as can be seen from the plateau in the TG curve from room temperature to 128°C. From 128°C to 150°C, TG shows a weight loss of 7% due to the loss of two water molecules. An endo peak in the DTA in the same region is an indication of dehydration. The dehydrated complex then remains stable upto 333°C. From 333°C to 400°C, TG shows a weight loss of 44.86% due to decarboxylation of the complex to form $NiMn_2O_4$. DTA shows a sharp exotherm in the same region due to decomposition of anhydrous nickel manganese fumarate complex to $NiMn_2O_4$. The large amount of heat generated during decarboxylation increases the temperature locally, which comes back to normal once decarboxylation is over, as can be seen in the TG curve which also reflects in the DTA with reverse loop in the exo peak. After 400°C, no change has been observed upto 1000°C, either in the TG or DTA curve, which indicates that final compound i.e. $NiMn_2O_4$ is formed at 400°C.

As regards to TG/DTA trace of hydrated nickel manganese malonate (figure 2b), the total decomposition of the complex to $NiMn_2O_4$ is attained at 323°C. The observed total weight loss in the TG (55.5%)

matches closely with the theoretically calculated total weight loss (55.9%). The nickel manganese malonate trihydrate complex remains stable upto 153°C after which it undergoes dehydration till 183°C with a weight loss of 10.5% which also reflects in DTA as endo peak. The unhydrated complex then undergoes decarboxylation from 200°C to 323°C as can be seen from the TG trace. The DTA shows the corresponding exo peak in the same region. The decarboxylation pattern is similar to fumarate complex.

The TG/DTA trace of hydrated nickel manganese tartarate complex is shown in figure 2a. The TG shows a continuous weight loss from 50°C to 343°C where total decomposition of the complex is attained. The initial weight loss upto 150°C is due to dehydration followed by decarboxylation to form $NiMn_2O_4$. The decarboxylation pattern here is similar to the other two complexes as can be seen from exotherm in DTA.

All the samples of hydrated $Ni_{1-x}Mn_{2+x}(C_2O_4)_3$ ($0 \leq x \leq 0.6$) series (figures 2b to 2e) show a similar two step decomposition pattern, first step due to dehydration followed by second step of decarboxylation with sharp endo and exo peaks, respectively, in the DTA. The TG trace of all the oxalate complexes show a minor weight loss of around 1.5% from RT to 150°C after which there is a sharp weight loss of 18.5% upto 215°C due to dehydration. There is a sharp endotherm in the corresponding region in DTA which confirms the dehydration. The decarboxylation starts at around 270°C and continues till 325°C, where the total decomposition of the compound takes place to form nickel manganites. The DTA shows a sharp exotherm between 270°C - 325°C due to decarboxylation in all these oxalate complexes.

APPENDIX II

LIST OF PUBLICATIONS

Journal Publications :

1. "Thermistor Based Conditional Output Sensor", R.K. Kamat, G.M. Naik and G.G. Tengshe, Circuit Cellar Ink, The Computer Applications Journal, USA, Volume 105, April 1999, pp. 28-31

2. "Synthesis and Characterisation of Nickel Manganese Carboxylate Precursors for Thermistor Applications", R.K. Kamat, G.M. Naik and V.M.S. Verenkar, Analog Application Journal of Texas Instrument Inc., USA, February 2001

3. "In Search of New Applications, Makers Cultivate Advance NTC Techniques", R.K. Kamat and G.M. Naik, Sensor Review: An International Journal of Sensors and Systems, Emerald, UK, Vol. 22, No. 4, November 2002, pp.334-340

4. "Thermistor based low power ASIC for bio-medical applications", R.K. Kamat and G.M. Naik, Accepted for Publication in the Proceedings of Society of Photo-Optical Instrumentation Engineers (SPIE), USA - 2003.

5. "Design and development of high performance NTC thermistors", R.K.Kamat, G.M. Naik and V.M.S. Verenkar, Abstract Published in the Proceedings of International Conference on Sensors by IEEE, USA, Full paper invited for publication in Special Issue of IEEE Sensors Journal.

6. "A PC based instrumentation set-up for determination of time constant of NTC thermistors", R.K.Kamat and G.M. Naik, Submitted to Journal of Measurement Science and Technology, UK

7. "A set-up for characterisation of effects of moisture on NTC thermistor", R.K.Kamat and G.M. Naik, Submitted Sensors and Actuators -A, UK

Full Papers Published in the proceedings of International and National Conferences:

1. "CMOS Implementation of Digital Thermometer", R.K. Kamat and G.M.Naik, .Published in the proceedings of International Conference on Smart Sensors and Systems, ISSS-2002 Organised by SPIE, Bangalore, India - 2002.

2. "Development and Optimization of Nickel-Manganese Oxide Thermistors Using Oxalic Precursors", R.K. Kamat, G.M. Naik and V.M.S. Verenkar, Proceedings of Sensors-9, Organised by IEEE Bombay Section, Institution of Engineers and Pune University, pp. C-3:1 - C-3:4, March - 2002

3. "Thermal Analysis of Nickel Manganese Carboxylate Precursors for Thermistor Applications", R.K. Kamat, G.M. Naik and V.M.S. Verenkar, Proceedings of Sensors-9, Organised by IEEE Bombay Section, Institution of Engineers and Pune University, pp. C-4:1 - C-4:4, March - 2002

4. "Novel Manufacturing Setup Improves Thermistor Specifications", R.K. Kamat, G.M. Naik and V.M.S. Verenkar, Proceedings of Sensors-9, Organised by IEEE Bombay Section, Institution of Engineers and Pune University, pp. C-5:1 - C-5:4, March - 2002

5. "Analogue to Digital Converter with Non-linear Transfer Function for Thermistor Applications", R.K. Kamat and G.M. Naik, Accepted, 4th International Conference on Advanced A/D and D/A Conversion Techniques and their Applications and 7th Europeian Workshop on ADC Modelling and Testing, Organised by IEE at CTU Prague, 2002

6. "A Fully Automated Test and Characterisation Setup for NTC Thermistors", R.K. Kamat and G.M. Naik, Proceedings of National Conference on Advanced Instrumentation, CSIO Chandigarh, January-2001

7. "Mathematical Modelling of NTC thermistors in Self Heated Region", R.K. Kamat and G.M. Naik, Proceedings of National Conference on Advanced Instrumentation, CSIO Chandigarh, January-2001

Papers Presented in Conferences:

1. "Synthesis of High Resolution NTC Thermistor", R.K. Kamat and G.M. Naik Presented at 24th National Symposium on Instrumentation, Goa February-2000

2. "Synthesis of NTC Thermistors using Oxalic Precursor Route", R.K. Kamat, G.M. Naik and V.M.S. Verenkar, Presented at Symposium on Inorganic Materials for New Millenium, IIT Madras, January 2001.

References:

1. "NTC Thennistor Update", Chris Faller, YSI Inc. Fred Arment, Artnent Associates,
   Sensors, June 1996, pp. 22-26

2. "Structural Properties of Nickel Manganite $Ni_xMn_{3-x},0_4$ with $0.5 \leq x \leq 1$", R. Legros, R. Metz, A. Rousset, Journal of Materials Science, 25 (1990), pp. 4410-4414

3. "Thermistor Sensor and Total Emittance Measurement", S.P. Varma and Joginder Singh, Rev. Sci. Instrum. 60 (10), October 1989, pp 3310-3315

4. "Ageing Study of NTC thermistors by thermo power measurements", P. Castelan, Bui Ai and A.Loublere, Sensors and Actuators A, 33 (1992), pp. 119-122.

5. "Doped Yttrium Iron Garnet for Thermistor Bolometers", A. S'Amico, A. Grilli, A. Paoletti and A. Tucciarone, Mat. Res. Bull., Vol. 19,1984, pp. 347-354

6. "Structural Electrical and Infrared Optical Properties of Vanadium Pentaoxide (V_20_5) thick Film Thermistors", P. Umadevi, C.L. Nagendra and G.K.N. Thutupalli, Sensors and Actuators A, 39 (1993), pp 59-69

7. "Improvement of thermal sensors based on Bi_2Tu_3, Sb_2Te_3 and $Bi_{0.1}Sb_{1.9}Te$ ", A. Mzerd, F. Tcheliebou, A. Sackda and A.Boyer, Sensors and Actuators A, 46-47, (1995), pp.387-390

8. "Complex Impedance Analysis of Nb-doped (Bao.6Sro.4)TiO3 PTC Thermistors", T. Yamamoto and S. Takao, Jp. J. Appl. Phys. Vol. 31 (1992) pp 3120-3123

9. "A widely Linear to Frequency Converter Using a Thermistor in a Pulse Generator", R.N. Sengupta, IEEE Transactions on Instrumentation and Measurement, Vol. 3 7, No. 1, March 1998. pp. 62-65

10. "Stable high Temperature (5OOoC) Thermistors", R.O. Carlson, Rev. Sci. Instrum. 55 (12) December 1984, pp 1999-2005

11. "A 20 mK temperature Sensor", N. wang, B. Sadoulet, T. Shutt, " IEEE Transactions on Nuclear Science, Vol. 35, No. 1, February-I 988, pp55-57

12. "Linear Composite Resistance Thermometers", Joseph M. Diamond, Transactions on Instrumentation and Measurements, Vol. M4-36, No.3, September-1987, pp 759-763

13. "The Preparation, Characterization and Electrical Properties of Copper Manganite Spinel, $Cu_xMn_{3-x}0_4$, $0 \leq X \leq 1$", R. Legros, R. Metz, A. Rousset, Journal of Materials Science, 24 (1989), pp 83-87

14. "Phase Change Materials for Thermal Stabilization of Composite Thermistors" Sheri A. Broduer, Wayne Huebner, James P. Runt and Robert E. Newnham, J.Mater. Res., vol 6 No. 1 . January 1991, pp 175-181.

15. "Ageing Study of Nickel-copper-managnite negative temperature coefficient thermistor by then,nopower measurements", P. Castelan, Bui Ai and A. Loubiere and R. Legos, J. Appl. Phys. 72 (10), 15 November 1990, pp 4705-4709

16. "Synthesis and Characterization and Catalytic CO oxidation studies over $Ni_{1-x}Cu_xMn_2O_4$" S.M. Gurav and A.V. Salker, Indian Journal of Chemistry, Vol. 38A, February 1999 pp. 130 135

17. "Physical properties and x-ray diffraction of a $NiMn_2O_4$ Single Crystal below and above the Ferrimagnetic transition at Tc=145K", S. Asbrink, A. Waskowska, M. Drozed and E. Talik, J. Phys. Chem. Solids Vol. 5 8, Number 5, pp. 725-729, 1997

18. "High Pressure Phase of the cubic Spinel $NiMn_20_4$", S. Asbrink, A. Waskowska, J. Staun Olsen, L.Gerward, Physical Review B, Vol 57, No. 9, 1 March 1998, pp. 4972-4974

19. "X-ray Photoelectron Spectroscopy of Nickel Manganese Oxide Thermistors" T. Hashemi and A.W. Bainkman, J. mater. Res., Vol 7, No. 5 May 1992 pp. 1278-1283

20. "A new type Semiconductor (Critical Temperature Resistor)", Hisao Futaki, Japanese Journal of Applied Physics, Vol 4, No. 1, January 1965, pp. 2 8-4 1.

21. "Effect of Cuo as an Impurity on the Electrical Properties of NiO-NM203 NTC Thermistor Materials", K. Singh, N.D. Pandit , C. Mande, Journal of Materials Science Letters 1 (I 982) pp. 99-102

22. "Investigation of Electrical Properties of Oxide Thermistors", M. A.K.L. Dissanayake and S.Ganansundaram, Physics Education, July-Sept 1991, pp. 102-107

23. "A high speed data acquisition and processing system for real time data analysis and control", JR. Ferron, Rev. Sci. Instrm, 63 (11) Nov. 1992, pp. 5464-5468

24. "A versatile computer controlled measuring system for recording voltage-current characteristics of various resistance sensors", D. Stankovic and M. Znatanovic, Sensors and Actuators A, 41-42 (1994) pp. 612-615

25. "Dynamic response of thermoresistive sensors", Gurudip S. Deep, IEEE Transactions on Instrumentation and Measurement, Vol 41 No.6, December 1992, pp. 815-819

26. "Noise in Senors", F. Bardoni, A. D'amico, Sensors and Actuators, A21-23 (1990), pp. 17-24

27. "Study of the reliability and accuracy of thermistors for temperature measurement using transportable mercury triple point cells", N I el-Sayed, F.M. Megahed and M M Ammar, Indian Journal of Engineering and Materials Science, Vol. 1, April 1994, pp. 107-1 10

28. "Self Calibration/Compensation Technique for Microcontroller based Sensor Arrays", Paul T. Kolen, IEEE Transactions on Instrumentation and Measurement, Vol.43, No.4, August 1994, pp. 620-623

29. "Linearised Thermistor thermometers using an analog multiplier" A.A. Khan, Mohammed A. Alturalgr, Adbul Rahm, M. Alamoud, IEEE Transactions on Instrumentation and Measurement, Vol. 37, No.2, June 1988, pp. 322-323

30. "Analogue-to-digital converter with digitally controlled transfer function", 1. Janiczek, Rev. Scl. Technol. 4 (1993),35-37

31. "Smart Sensor Interface with A/D Conversion and Programmable Calibration", P. Malcovati, C. Azeredo Leme, P. O'Leary, F. Maloberti and H. Baltes, IEEE Journal of Solid State Circuits, Vol. 29, No. 8, August 1994, 963-966

32. "Microcomputer system of parallel measuring structures for period/frequency monitoring", A. Krzywaznla, J. Ociepka and J. Pekala, Rev. Sci. Technolo. 7 (1996), pp. 1179-1181

33. "A Voltage controlled resistor for the remote control of monostable multivibrators", MichaelJ. Chudobiak, Rev. Sci. Instrum. 66(2) February 1995, pp. 1142-1145

34. "Silicon MicroMechanics" G.V. Ramaraju, U.P. Phadke, Electronics Information and Planning, August 1995, pp. 593-600

35. "Analogue and Mixed Signal IC Design", Rob Massara and Kevin Steptoe, IEE Review, February 1992, pp.75-79

36. "Microelectromechanical systems", Mehran Mehregany, Circuits and Devices, July 1993, pp. 14-22.

37. "Incorporating High Reliability into the design of Microprocessor - Based Instrumentation" I.A. Henderson, J.Mcghee, W. Szam'awski, E. Domaradzki, IEEE Proceedings A, Vol. 138, No. 2, March 1998, pp. 105-112.

38. "Designing ASICs with UABPL", S. M. Sait, M.S.T. Benten and A.M.T. Khan, IEEE Circuits and Devices, March 1995, pp. 15- 24

39. "A Modified Linearised Thermistor Thermometer using an Analog Multiplier" Sundarm Nataraj, IEE Transactions on Instrumentation and Measurements, Vol. 39, No. 2, 1990, pp. 440-441

40,"Error Evaluation of Thermistor Linearising Circuits" Daniel Slomovitz and Jose Joskowlcz, Rev. Sci. and Tech. 1 , 1990, pp. 1280-1284

41. "Hardware linearization of thertnistor response using series parallel resistors for temperature -to - time conversion", S. Kaliyugavaradan, P. Sankaran and V.G.K. Murti, Meas. Sci. Technol. 5(1994) pp. 786-788

42. "Using a free standing thermistor array to measure VUV emission from a tokamak plasma", S.F. Paul, R.J. Fonck, A.K. Macaulay, Rev. Sci. Instrum. 64 (9), September 1993, pp. 2423-2427

43. "A combined fuzzy and classical PID controller", D.P. Kwok, P.Wang, C.K. Li, Microprocessing and Microprogramming, 32 (1991) pp. 701-708

44."A low power multichannel sensor interface for use in digital telemetry", B. Puers, P. Wouters and M. De Cooman, Sensors and Actuators A, 37-38 (1993) pp. 260-266

45. "A microthennal diffusion sensor for non-invasive skin characterization", F. Arnaud, G. Delhomme, A. Dittmar, W.H. Newman, Sensors and Actuators A, 41-42 (1994) pp. 240-243

46. "A general circuit for resistive bridge sensors with bitstraem output", Luca G. Fasoli, Frank R. Riedijk and J.H. Huijsing, IEEE Transactions on Instrumentation and Measurements, Vol46, No. 4, August 1997, pp. 954-960

47. "Critical Study and applications of a self balancing bridge", M. Rehman, M.T. Ahmad and M. Arif, IEE Proceedings, Vol 137, January 1990, pp. 23-26

48. "Bridge -output - to - frequency converter for smart thermal air - flow sensors", Gert J. A. Van Dijk and Johan H. Huijsing, IEEE Transactions on Instrumentation and Measurement, Vol 44, No.4, August 1995, pp. 881-886

49. "High resolution thin film temperature sensor arrays for medical applications", G.Urban, A. Jachimowicz, M. Schonauer, Sensors and Actuators, A21-23 (1990) pp. 650-654

50. "Low cost high sensitivity integrated pressure and temperature sensors" P. Pons and G. Blasqez, Sensors and Actuators, A-41-42 (1995) pp. 398-401

51. "A Sensitive Differential thermometer", P.N. Murgatroyd and M Belloufi, Meas. Sci. Technol. I (I 990) pp. 9-12

52. "An improved way to use thermistors in temperature servomechanisms", DA Van Baak, Meas. Sci. Technol., 5, (1994), pp. 864-865

53. "Simulation of the thermal behavior of thermal flow sensors by equivalent electrical circuits", F. J. Auerbach, G. Meiendrs, R. Muller and Scheller, Sensors and Actuators A, 4144 (1994), pp. 275-278

54."A Method to reduce sensor bridge dependence on loading and excitation voltage ", P.J. Abatti, B. Schimeider Jr, Rev. Sci. Instrumentation, 65 (3) March 1994, pp. 756-757

55. "Temperature control in small water heated measuring cells" Maria Celia Lopez Iglesias and Maximo Baron, Rev. Sci. Instrumentation, 61 (8) August 1990, pp. 2245-2247

56. "A self heated thermistor flowmeter for small liquid flow in micro channels", C. Yang, M. Kummen and H. Sqeberg, Sensors and Actuators, 15 (1988) pp. 51-62

57. "Thermal Conductivity Measurements in Soil using an instrument based on the cylindrical probe method", J. Nicolos, P.H. Amdre, JF. Rivez and V. Debbaut, Rev. Sci. Instrum. 64, March 1993, pp. 774-781

58. " Thermistors as circuit elements in low frequency circuits", Kamil Kraus, The review of Scientific Instruments, Vol 39, No. 2, February 1968, pp. 216-221

59. "A simple a.c. bridge circuit for use in four terminal resistance thermometry", J.W. Ekin, D.K. Wagner, 1970 pp. 1108-1 1 11

60. "A Passive circuit for addition and subtraction for transducer signals with independent scaling", Darko Viroubal, IEEE Transactions On instrumentation and measurement, Vol. 40, No.6 December 1991, pp. 913-918

61. " A sensitive differential thermometer", P.N. Murgatroyd and M. Belloufi, Meas. Sci. Technol 1 (1990) pp. 9-12

62. "Discrete Transform technique for solving non-linear circuits and equations", S.Y.R. Hui, C.Christopoulos, IEE Proceedings A, Vol. 139, No. 6 Nov. 1992, pp. 321-328

63. "Linear Temperature to time period converter using standard thermistors", I.Y. Yankov, C.I. Gigov and E.A. Yankov, Meas. Sci. Techn. 1, (1990), pp. 118-1179

64. "A bridge circuit for temperature drift cancellation", M. Matsuno, S. Abachi, M. Nakayama and K. Watanabe, IEEE Transactions on Instrumentation and Measurements, Vol 42, No.4, August 1993, pp. 870-872

65. "The characterization and compensation through sensor array signal processing technique of drift and low frequency noise in thick film semiconductor sensors", J.K. Atkinson, R.P. Sion and E. Sizeland, Sensors and Actuators, A, 41-42 (1994), pp. 607-611

66. "Low frequency wave filters employing thermistors", Ribert A. Rasmussan, Review of Scientific Instruments, Vol. 3 1, No. 7, July 1960 pp. 747-751

67. " An inexpensive linear temperature-voltage converter", A.A.Khan and R. Senagupta, Indian J. of Pure and Appl. Phys. Vol. 20, Nov. 1982, pp. 914-915

68. "Indigenous commercial R &D in advanced ceramics -Retrospect and Prospects", V.C.S. Prasad, Current Science, Vol 68, No.6,25 March 1995, pp.593-598

69. "Hi-Tech Report: PTC Thermistors high Reliability Opens Doors for Application in Communication Equipment", Shuichi Sakagaki, TDK Corporation, JEE, August 1988, pp. 7l-73

70. Spotlighting: Sensors: "In Search of New Applications, Makers Cultivate Advanced PTC Techniques", Minoru Shimada, Murata Manufacturing Co., Ltd., JEE August 1992, pp. 57-59

71. "Electronics and Computers in thermal systems: Reviewing current trends", J. McGhee, I.A. Henderson and D. Sankowski, Trans Inst. MC, Vol. 13, No. 2, 199 1, pp.75-90

72. Spotlighting Sensors: "Trends Among Sensors Attract Attention" Editorial in JEE, February 1992, pp. 76-78

73. Spotlighting Sensors: "Technological Trends Focus on Temperature Sensors, Evolving Applications", Tetsuo Mura, Shibaura Electronics Co., Ltd., February 1992, pp. 79-81

74. "Temperature Measurement Thermistors Becoming Multi-functional Sensors", Soichiro Nakajima, JEE, June 1991, pp. 55-57

75. "Thermistors' Sensitivity Makes Them Desirable in Many Applications", Tetsuo Miura, Shibaura Electronics Co., Ltd., September 1990, pp. 86-89

76. "Temperature Sensors Play Important Roles in Industry, Society", Yoshiharu Tanaka, Ishizuka Electronics Corporation, JEE, August 1992, pp. 60-63

77. "Classical Taxonomy: An holistic perspective of temperature measuring systems and Instruments", I.A. Henderson and J. McGhee, IEE Proceedings-A, Vol. 140, No.4, July 1993, pp. 263-268

78. "Microprocessor Based Temperature Controller by Linearization of Thermistor Characteristics", B.P. Ladgaonkar, P.N. Vasambekar and A.S. Vaingankar, J. Instrmn. Soc. India 30(4) pp. 267-270

79. "Thick-film resistive temperature sensors", Andrze Dziedzic, Leszek J Golonka, Janusz Kozlowski, Benedykt W Licznerski and Karl Nitsch, Meas. Sci. Technol, 8 (1997), pp. 78-85

80. "Preparation and Characterization of NTC thermistors based on $Fe_{2+\delta}Mn_{1-x-\delta}Ni_xO_4$", M.L. Martinez Sarrion and M. Morales, Journal of Materials Science, 30, 1995, pp.2610-2615

81. "Resistivity and I-V measurements of tetragonal Mn_3O_4 and dependence of nickel manganite on Mn_3O_4 content of $NiO-Mn_3O_4$ mixture", S.K. Sarkar, M.L. Sharma and S.K. Lahiri, Journal of Materials Science Letters, 6, 1987, pp. 958-960

82. "Formation of Nickel-Manganese Oxide Thermistors Studied by XRD, SEM and Auger Spectroscopy", S. Azmi-Nam, F. Golestani-Fard and T. Hashemi, Journal of Electronic Materials, Vol. 16, No.2, 1987, pp. 133-137

83. "$NiMn_2O_4$ Revisited", Xiao-Yia Tang, A. Manthiram and J.B. Goodenough, Journal of LessCommon Metals, 156,1989, pp. 357-368

84. "Formulation of Silver loaded Manganite based thermistor paste and application of percolation theory for sudden transition in conductance", Nitya Vittal, R.C. Aiyer, C.R. Aiyer, M.S. Setty, S.D. Phadke and R.N. Karekar, J. Appl. Phys. 64 (10), 15 November 1988, pp.5244-5247

85. "Structural Properties of Nickel Manganite $Ni_xMn_{3-x}O_4$ with $0.5 \leq x \leq 1$", R. Legros, R. Metz and A. Rousset, Journal of Materials Science 25 (1990) pp. 4410-4414

86. "Preparation and Characterization of NTC Thermistors: Nickel Manganites Doped with Lithium" Maria Luisa Martinez Sarrion and Manuel Morales, Journal of the American Ceramic Society, Vol. 78, No. 4, April 1995, pp. 915-921

87. "Linear temperature-to-time period converters using standard thermistors", Ivan Y Yankov, Christo I Gigov and Evgeny A Yankov, Meas. Sci. Technol., 1, 1990, pp. 1168-1171

88. "A Novel Wide Range Linearisation Approach for thermistor Thermometer', AA Khan, MA Al-Tour and AR M. Alameda, Transactions on Instrumentation and Measurement, Vol. IM-36, No. 3, September 1987, pp.763-769

89. "Calibration and Linearization Method for Microcontroller Based Sensor Systems", Gert van deer Ohm, Child Leah and Johan Huijsing, Measurement + Control, Volume 29, November 1996, pp. 270-273

90. "A New Compensation Scheme for Thermistors and its Implementation for Response Linearization Over a Wide temperature Range", S. Kaliyugavardan, P. Sankaran and V.G.K. Murti, IEEE Transactions on Instrumentation and Measurement, Vol. 42, No.5, October 1993, pp.952-956

91. "Linearisation of transducers through a generalized software technique", D. Ghosh and D. Patranabis, Meas. Sci. Technol. 2, (199 1), pp. 102-105

92. "Software based Linearisation of thermistor and nonlinearity", D. Ghosh and D. Patranabis, IEE Proceedings-G, Vol. 139, No. 3, June 1992, pp.339-342

93. "Useful procedure in least squares, and tests of some equations for thermistors", Harold J. Hoge, Rev. Sci. Instrum., 59 (6), June 1988, pp.975-979

94. "The future of Sensors, Materials Science or Software Engineering?", Peter Kleinschmidt and Wolfgang Hanrider, Sensors and Actuators A, 33, 1992, pp. 5-17

95. "The new Current Loop: An Instrumentation and Measurement Circuit Topology", Karl F. Anderson, IEEE Transactions on Instrumentation and Measurement, Vol. 46, No.5, October 1997

96. "A Novel BIN40S Signal Processor for Pt 100 Temperature Sensors with Microcontroller Interfacing", Gerard C.M. Meijer and Cor H. Voorwinden, Sensors and Actuators A, 25-27, 1991, pp. 613-620

97. "High Sensitivity and Detectivity Radiation Thermopiles made by Mulit-layer Technology", F. Volklein and A. Wiegand, Sensors and Actuators A, 24, 1990, pp. 14

98. "A Linearisation and compensation method for integrated sensors", Peter Hille, Rainer Hohler and Hans Strack, Sensors and Actuators A, 44, 1994, pp. 95-102

99. "Introduction to Sensors Compatible with Microprocessors", A.W. Van Herwaarden and R.F. Wolffenbuttel, Microprocessors and Microsystems, September 1989, pp. 74-82

100. "Problems associated with bringing a sensor technology to the market place", A.J. Collins, Sensors and Actuators A, 31, 1992, pp. 77-80

101. " A smart balanced thermal pyranometer using a sigma-delta A-to-D converter for direct communication with microcontrollers", F.R. Riedijk and J.H. Huijsing, Sensors and Actuators A, 37-38, 1993, pp. 16-25

102. "Considerations for the utilization of smart sensors", Gerry Smith and Mark Bowen, Sensors and Actuators A, 46-47, 1995, pp. 521-524

103. "A programmable Temperature Monitoring Device for Tagging Small Fish: A Prototype Chip Development", Godi Fischer, James C. Daly, Conrad W. Recksiek and Kevin D. Friedland, IEEE Transactions on Very Large Scale Integration (VLSI) Systems, Vol. 5, No.4, December 1997, pp. 401407

104. "Design of integrated thermal flow sensors using thermal sigma-delta modulation", HuibertJ an Verhoeven and Johan H. Huijising, Sensors and Actuators A 52, 1996, pp. 198-202

105. "Hierarchy of Structures of intelligent transducers", Janusz Kwasniewski Sensors and Actuators A, 41-42, 1994, pp. 604-606

106. "Considerations for the design of smart sensors", Mark Bowen and Gerry Smith, Sensors and Actuators A, 46-47, 1995, pp. 516-520

107. "Microcropower CMOS Temperature Sensor with Digital Output", Anton Bakker and Johan H. Huijising, IEEE Journal of Solid-State Circuits, Vol. 31, No. 7, July 1996, pp. 933-937

108. "Aspects of Intelligent Sensor reconfiguration", A.H. Taner and J.E. Brignell, Sensors and Actuators A, 46-47, 1995, pp. 525-529

109. "CMOS Sensor Systems", Bedrich J. Hosticka, Sensors and Actuators A, 66, 1998, pp. 335341

110. "Dynamic Calibration of Sensors using EEPROMS", P.P.L. Regtien and P.J. Trimp, Sensors and Actuator A2 I -A23, 1990, pp. 615-618

111. "Multisensor Data fusion", PK. Varshney, Electronics and Communication Engineering Journal, December 1997, pp.245-252

112. "Microminiaturized Thermistor Arrays for Temperature Gradient, Flow and Perfusion Measurements", H. Kuttner, G. Urban, A. Jachimowicz, F. Kohl, F. Olcaytug and P. Goiser, Sensors and Actuators A, 25-27, 199 1, pp.641-645

113. "A Neural Network Controller for a Temperature Control System", Marzuki Child and Sigeru Omatu, IEEE Control Systems, June 1992, pp. 58-64

114. "Measuring Temperature using Thermistors", Jonathan Valvano, Circuit Cellar Ink, The computer Applications Journal, August 2000.

115. "The design and application of Honeywell's laser-trimmed temperature sensors", H. Hencke, Measurement + Control, Volume 22, October 1989, pp. 233-236

116. "A temperature Sensor with single Resistor Set-point Programming", A. Paul Brokaw, IEEE Journal of Solid State Circuits, Vol. 3 1, No. 12, December 1998, pp. 1908-1915

117. "A new Method for in-situ dynamic calibration of temperature sensors", R. Budwig, Rev. Sci. Instrmn, 60 (12), December 1989, pp. 3717-3719

118. "Temperature Measurement in Thermogravimetry", Emanuel P. Manche and Benjamin Carroll, The Review of Scientific Instruments, Vol. 35, Number II, November 1964, pp.1486-1488

119. "Thermistors, Varistors Enjoy Rising Demand, Fight Falling Prices", JEE, June 1990, pp.59-61.

120. "Technological Trends and Uses of Thermistors", Souichiro Nakajima, JEE, November 1982, pp. 90-93.

121. "Thermistors. Part 1. Static Characteristics", Otto J.M. Smith, The Review of Scientific Instruments, Volume 2 1, Number 4, April 1950

122. "Makers Add Value to Temperature, Humidity Sensors", JEE August 1992, pp.54-55

123. "Preparation, temperature and composition dependence of some physical and electrical properties of mixtures within the Nio-Mn3O4 system", S.K. Sarkar, M.L. Sharma, H.L, Bhaskar and K. C. Nagpal, Journal of Materials Science, 1, 1984, pp. 541-551.

124. "A New Method for Fabrication of Stable and Reproducible Yttria-based thermistors", Ayan Banerjee and Sheikh A. Akbar, thesis submitted to Ohio StateUniversity,December-1999 http://www.mse.eng.ohio-state.edu/-akbar/newmethod.htm

125. Verilog-AMS Sample Library.

126. Manual by Open Verilog International.

127. Intrusoft NewsLetter, Personal computer Circuit Design Tools, July 1988

128. "Electronic Thermometer" US patent number US4838707, Ozawa Masaki, Hasaka Toshiyuki and Yoshizaa Masayuki, 1997.

129. Catalogue of Agilent 34401Aamplicon LiveLine Limited, UK (http://www.amplicon.co.uk)

130. White Paper on "Stability of glass-encapsulated disc-type thermistors", J.A. Wise, National Institute of Standards and Technology, Gaithersburg.

131. "Reliability of Sensor Applications in Industrial Environment", T. Bandopadhyay and R. Sengupta, Proceedings of the 5th National Seminar on Physics and Technology of Sensors, February 2-4, 1998, pp. C 56-1.

132. http://www.amplicon.co.uk : Agilent Application Manual.

133. "Thermistors", P. Sankaran, S. Kaliyugavardan, V.G.K. Murty, Unpublished Article.

134. http://www.temperatures.com/index.html : The site is an interactive repository and guide to temperature sensors which includes theoretical details of almost all the sensors, the major vendors and their product specifications and contact information, application stories, training courses and calibration services.

135. http://www.iijnet.or.jp/murata/products/english/design/thermis/ : Since 1994, Murata Manufacturing Co., Ltd. Is working in the field of Ceramics especially thermistors. The website gives information regarding the company products especially resin coated radial lead type and surface mounted chip type NTC thermistors. Application notes charging control of Ni-Cd batteries, stabilisation of LCD display using thermistors are worth reading.

136. http://www.alphasensors.com/twhatsnew.html : Alpha Sensors Inc. has been in business for nearly 23 years, offering a complete line of precision NTC thermistors and custom temperature sensors for use in HVAC systems, consumer electronics, computers, communications, medical and many other applications. The website gives information about their new line of glass encapsulated thermistors with improved stability and accuracy over a broader temperature range than is possible with epoxy or plastic encapsulated sensors.

137. http://www.mmea.com/new.htm : Home page of Mitsubishi Materials Corporation, producer of the smallest chip thermistor (Dimensions: 0.6 x 0.3 x 0.3 mm) in the world.

138. http://www.tdk.co.jp/teaah01/aah04000.htm: Manufacturer of 1.0 x 0.5mm Multilayer Chip NTC Thermistor the smallest one in industry for compensation of oscillation frequency fluctuations and temperature in crystal oscillator elements used in portable cellular phones.

139. http://www.vishay.com/news/releases/011120/thermistor/011120thermistor.html : Information about New Vishay Dale NTC Thermistor Assemblies that offers wide range of standard and custom configurations.

140. http://www.hk-microtech.com/component/shiba.htm : Information about chip, disk and glass encapsulated NTC thermistors.

141. http://www.temperatures.com/thermivendors.html : On this webpage links are provided which takes you to the websites of several vendors. Almost all the thermistor vendors around the globe are listed on this page. The links are as follows: Alpha Thermistor, Ametherm, BetaTHERM Corp, Cera-Mite Corporation, Comeau Technique Ltd., Cornerstone Sensors, Inc., Cox Recorders Probe, Custom Design Solutions, Elmwood Sensors, Elscott Corp., Fenwall Electronics Group, Division of Invesys Sensor Systems (USA), Hanna Instruments' products, Kalglo Products, Kele & Associates, LYNX Technical Data, MMC Electronics America Inc., Nichicon USA, Nomadics Thermistor products, NIC Components Corp., .Picotech, Precision Engineering Ltd(UK), Precision Measurement Engineering, recision Thermistors and Probes, Quality Thermistor, Inc. (USA)Boise, RTI and Katema Thermistors, Sensor Scientific, Inc.(USA) Fairfield, New Jersey, Smith Systems Inc (USA) Brevard, North Carolina, SMTnet Electronic Component Manufacturers Directory, Solar Powered Industrial Thermometers, STOLAB - Accurate Industrial Thermometers (USA), Tech Instrumentation(USA), Temperature probes, probes, temperature probes, Elscott Corp. - thermistor, Therm O-Disc NTC and PTC Thermistors(USA), Thermometrics, Inc. (USA), Therm-X, Thermalogic Temperature and Process Controllers and Sensors(USA),

U.S. Sensor Corp. (USA), Victory Engineering Corporation(USA), Western Electric-Australia-Thermistors, Western Electronic Component Corp (USA), Wuntronic GmbH(Germany), YPco Electronics, YSI-(VECO-Springfield, NJ) (USA), YSI-(Yellow Springs Instruments, Ohio) (USA) Precision Thermistors and medical instruments.

142. http://www.iijnet.or.jp/murata/products/english/design/thermis/ Thermistor FAQ, Applications, Note on charging Control of NiCd batteries by muRata Inc.

143. http://www.ilxlightwave.com :"Thermistor Calibration and the Steinhart-Hart Equation", Application Note No.4, ILX LightWave Corporation, Test and Measurement Instrumentation, Bozeman, MT.

144. http://www.betatherm.com or http://www.betatherm-usa.com : Bellcore White Paper, Betatherm Reliability Model.

145. http://www.thermometrics.com : Webpage of Thermometrics Inc., A thermistor manufacturing company.

146. http://ww.circuitcellar.com/online: "Measuring Temperature using Thermistors", Jonathan Valvano, August 2002, Crcuit Cellar Online, USA.

147. http://www.mse.eng.ohio-state.edu/~akbar : Ceramic Sensors for Industrial Applications, Sheikh A. Akbar and Prabir K. Dutta, NSF Center for Industrial Sensors and Measurements (CISM), The Ohio State University (OSU), Columbus, Ohio 43210, USA

148. http://mineral.galleries.com/minerals/oxides/spinel.htm: Mineral Gallery of Spinel Group

149. http://www.uvm.edu/~swgordon/13101/131web/santinabrohen/home.html : Santina Brohen's Chemistry 131 Final Project.

150. "R &D Work of Sensor in our country", Singh R.P., Proc. 4th National Seminar on Physics and Technology of Sensors, pp. I1-1, February 3-5, 1997.

151. http://www.tmworld.com "Make a Strip Chart Recorder in Excel" by Werner Haussmann, Agilent Technologies, Loveland, CO Test and Measurement World Online, January 2001

152. http://www.tmworld.com : "Errors Abound When Switching Temperature Sensors", Maurizio Basso, National Instruments, Italy; Michel Haddad, National Instruments, USA, CO Test and Measurement World Online, 2000.

153. http://www.national.com/thermist : "Four Wire Resistance Measurement for NTC thermistors, Application Note by National Instruments Inc.

154. http://www.tmworld.com : "Thermistor and DMM Measure Temperature", Werner Haussmann, Hewlett-Packard, Loveland, CO -- Test & Measurement World, 10/1/1999

155. http://www.cahners.com : "Putting the New Breed of Linear Thermistors to Work", Javed Khan, Vishay Intertechnology, Inc. , Cahners Business Information Special Report 04/01/2001,Reed Elseiver Inc.

156. http://www.edn.com : "Design A High-Resolution- ADC Using An 8-Bit Microcontroller : A simple integrating amplifier is combined with an MCU's analog peripherals to realize a 10-bit analog-to-digital converter", Bonnie C. Baker, Microchip Technology Inc. , Electronic Design, July 24, 2000.

157. http://www.edn.com : "Maintaining Signal Integrity Enhances ADC Circuit Performance : Careful use of the driving amplifier optimizes high-speed ADC input circuitry and minimizes noise and distortion", Nicholas Gray, National Semiconductor Corp., Electronic Design, May 1, 2000.

158. http://www/globalspec.com : "New releases in Japan targeted at telecom applications", Sourcing Report, Posted: September 21, 2001, by Global Sources

159. http://www.sensorsmag.com/resources/businessdigest/sbd0700.shtml.: "Sensor Companies Must Leverage Their Competencies into New Markets", Sensor Business Digest, SENSOR INDUSTRY DEVELOPMENTS AND TRENDS, Edited by Peter Adrian and puplished monthly by Vital Information Publication, Inc., 754 Caravel Lane, Foster City, CA 94404; July 2000

160. http://www.temperatures.com/TSN_1101.html : "TemperatureSensorNews: Helping people better understand and use temperature sensors", November 30, 2001 Third PREVIEW Edition.

161. http://www.ysi.com : "What is a Thermistor" Web Report by YSI Inc.

162. http://www.ametherm.com/ntc_thermistors/ntc_desription.htm :Webpage of Ametherm Inc., Manufacturers of Circuit Protection Thermistors.

163. http://www.hitekelec.com/uppermostcatalog.htm : Webpage of Hi-Tek Electronics Inc., MA., A Thermistor manufacturing company.

164. "Predictive temperature measurement system", United States Patent Application, 020003832, Kind Code A1, Siefert, Robert J. January 10, 2002

165. http://www.sensormag.com : "A New PC Card Solution" Colin Cumming, Nomadics, Inc., Sensors Magazine, August 1999.

166. http://www.sensycon.de : "A comparison of Platinum Temperature Sensors versus Thermistors"

167. http://www.maxim-ic.com : "MAX:6961 Four Channel Thermistor Temperature- to Pulse Width Converter"

168. http://www.andovercontrols.com : "Smart Sensor LED/LCD Display Temperature Sensors" AndOverControls Inc.

169. http://www.maxim-ic.com : "Maximicro: Using Maxim's Smart ADC to Compensate Sensors" December 2001.

170. http://www.sensorsmag.com/articles/0899/39/index.htm :Garvey, Doris, "So, What Is an RTD?," Sensors, August 1999, p.39.

171. http://www.sensorsonline.com or http://www.sensorsmag.com : "How to Select and Use the Right Temperature Sensor", Ron Desmarais and Jim Breuer, Airpax, Sensors, January 2001.

172. http://www.pel-ltd.co.uk/english/homepage.htm : Webpage of Precision Engineering Ltd. U.K. ,A Thermistor manufacturing Company.

173. http://www.chipcenter.com : "Measuring Temperatures Twice for Accuracy", Bonnie C. Baker, Staff Engineer, Microchip Technology, Inc. 2002

174. http://www.todmcpg.com/measure/measure.html: "Thermistor, Application Information" by Therm-O-Disc, A thermistor Manufacturing company.

175. "A study of folding and interpolating ADC", Yun Chiu and Dejan Markovic, EECS 247, Midterm Report, Fall 2000.

176. Catalogue on "Temperature Smart Sensor", by Applied Microsystems Limited, Canada 2002.

177. Applicaton Note AN-276 : "Analog to Digital Converter using Voltage to Frequency Conversion", Paul Klonowski, Analog devices.

178. Report On "Temperature Measurement Using an EEPROM Lookup Table", By Peter H. Anderson, Morgan State University, Baltimore, December 1996.

179. Report On "Calculation Considerations in PIC Applications", By Peter H. Anderson, Morgan State University, Baltimore, July 1997.

180. Report On " Design of A Very Low Power Astable Multivibrator" by Dave Johnson

181. "Technical Information of Thermistors", Catalogue of DEC Electronics Co. Ltd. Korea - 2002

182. Report on "Annotated C Programs", INTEC Automation Inc. -2002

183. Nondestructive Evaluation: Overview, "Microstructural Characterisation of Sensors based on electronic Ceramic Materials", P.I. Gouma, S.A> Akbar amd M.J. Mills, JOM-e, Vol. 50, No.11, November 1998.

184. "Novel Cobalt Ruthenate Thermistors", J. Hormaddy, The Institute for Applied Research, Ben Gurion University of Negav, Israel, pending U.S. Patent.

185. "Studies on Field Quenched Non-Stoichiometric Nickel Ferrites", M.Phil. Dissertation by N.D. Chaudhari, 1995

186. N.D. Chaudhari, Ph.D. Thesis, 1999

187. "Studies on High Permeability Cu-Mg-Zn Ferrites" Ph.D. Thesis by D.N. Bhosale, 2000

188. "Beneficiation of Goan Ore rejects to get pure iron oxide and utilisation of the iron oxide to synthesize ferrites, hich-tech magnetic materials" Ph.D. Thesis by V.M.S. Verenkar

189. JCPDS, Powder diffraction file, Int. Centre for diffraction data, Swarthmor, P.A. no. 1-1110.

190. "Ceramic Fabrication Process", Murray P., Livey D.T. and Williams J., W.D. Kingley (Ed.), Wiley, New York, pp. 147, 1948.

191. "Oxide Magnetic Materials", Standley K.J., Oxford University Press, London (1962), pp. 64

192. "Handbook of Ceramics and Composites", K.C. Patil, S. Sunder Manoharan and D. Gajapath, Marcel Dekkar Inc., New York p.649

193. Swallow D., Rodrigues G.P., J. Appl. Phys, 29 (1958), p.105

194. "Synthesis of high permeability Cu-Mg-Zn ferrites using oxalate precursors", D.N. Bhosale, N.D. Chaudhari and S.R. Sawant, IEEE Transactions on Magnetics, March 1998, Vol. 341, No.2, p.535

195. "Negative Temperature Coefficient Thermistors Part I: Characteristics, materials and Configurations", Greg Lavenuta, Cornerstone Sensors Inc., Sensors-online, May 1997.

196. Thermistor Catalogue of Shibaura Electronics Co. Ltd., Japan

197. http://www.ceramicindustry.com : Ceramic Industry Magazine.

198. Sinter Process Optimisation - Si_3N_4 : Report by NETZSCH-Gerätebau GmbH, 02/28/01

199. Burnout of Polymeric Binder : Report by NETZSCH-Gerätebau GmbH, 09/28/00

200. "Variable Capacitance signal transduction and the comparison with other transduction schemes" S.Y. Lee, Setra Systems Inc., Natick, Mass

201. Catalogue of Setra Systems Inc., Natick, Mass

202. "Greater Precision for noncontact sensors", Mach. Des., p. 117, Dec. 6, 1979; Lion Precision Corp., Newton, Mass

203. "A Course in Electrical and Electronics Measurement and Instrumentation", A.K. Sawhney, Dhanpatrai & Co. (Pvt.) Ltd., 1998, pp. 913-1089

204. "SPICE3 Version 3f3 User's Manual", T. Quarles, A.R. Newton, D.O. Pederson and A. Sangiovanni-Vincentelli, University of Californa, Berkely, 1993.

205. "Centre for advancement of sensors - a means to achieve self sufficiency", V.N. Krishnamurthy, DRDO-ISRO Cell for Sensors, Proc., NSPTS, 2000.

206. Report on: "Technology Vision 2020", Technology Information forecasting and Assessment Control (TIFAC), Department of Science and Technology, India - 2000.

207. "Crystallisation of bulk Tl-Ge-Se glasses under high pressure", **G.M. Naik** et al., J. Mater. Sci. Lett., 4, pp. 1017, 1985

208. "Electric transport and thermal studies on bulk Tl_xSe_{100-x} glasses", **G.M. Naik** et.al. J. Mater. Sci. Letters.

209. "Infrared Absorption Spectra of Ti^{4+} and Zr^{4+} Substituted Ni-Zn Ferrites", R.S. Patil, S.V. Kakatkar, S.R. Sawant, **R..K. Kamat** and S.S. Suryavanshi, Indian Journal of Pure and Applied Physics, Vol. 32, 1994 pp. 193-194

210. "Relaxation time studies on $Ni_{0.7}Zn_{0.3}Al_xFe_{2-x}O_4$ and $Ni_{0.7}Zn_{0.3}Cr_xFe_{2-x}O_4$", A.M. Sankpal, S.V. Kakatkar, **R.K. Kamat**, S.S. Suryavanshi and S.R. Sawant, Materials Chemistry and Physics, Vol.53, 1998 pp.77-79

211. "Synthesis and Initial Susceptibility Studies of Mn Substituted Ni-Zn Ferrites", **R.K. Kamat**, N.D. Choudhary, S.S. Suryavanshi and S.R. Sawant, Journal of International Academy of Physics Sciences, November 1997

212. "Microprocessor based system to monitor curie temperature of Ferrites", **R.K. Kamat** and S.R. Sawant, Proceedings of 5th National Conference on Physics and Technology of Sensors", February 1997

[213]

[1] "Flip-Flop Sensor - an Offer for Increased Function of the Smart Sensors", Martin Collar, Sensors & Transducers e-Digest (S&TD), No. 9, September 2002.

[2] "NMOS flip-flop sensors: a multipurpose digital-output sensor technique"

French, P.J.; Lian, W.; Middelhoek, S. ,Control Theory and Applications,

IEE Proceedings, Volume: 135, Issue: 5, Jul 1988, pp. 359-363

[3] "Formula for the calculation of the equivalent voltage of the flip-flop sensor", Martin Kollár, Electronics Letters.com, ISSN 1213-161X, paper #1/10/2002